

**HIGH PRESSURE STRUCTURAL INVESTIGATIONS OF SOLIDS
USING X-RAY AND SYNCHROTRON RADIATION**

A thesis presented for the degree of
Doctor of Philosophy in the Faculty of Science

by

ANDREW EDMUND HEATH

University of Leicester 1989

UMI Number: U497454

All rights reserved

INFORMATION TO ALL USERS

The quality of this reproduction is dependent upon the quality of the copy submitted.

In the unlikely event that the author did not send a complete manuscript and there are missing pages, these will be noted. Also, if material had to be removed, a note will indicate the deletion.



UMI U497454

Published by ProQuest LLC 2015. Copyright in the Dissertation held by the Author.
Microform Edition © ProQuest LLC.

All rights reserved. This work is protected against
unauthorized copying under Title 17, United States Code.



ProQuest LLC
789 East Eisenhower Parkway
P.O. Box 1346
Ann Arbor, MI 48106-1346



8178740057

x 75159404x

Statement:

The work presented in this thesis is original unless acknowledged in the text or by reference, and was carried out by the author in the Department of Chemistry of the University of Leicester and Daresbury Laboratory between October 1985 and October 1988. This work has not been, nor will be, presented for any other degree.

A handwritten signature in black ink, appearing to read 'A. E. Heath', with a stylized flourish at the end.

A. E. Heath
University of Leicester
1989

ABSTRACT

HIGH PRESSURE STRUCTURAL INVESTIGATIONS OF SOLIDS USING X-RAY AND SYNCHROTRON RADIATION

A. E. HEATH

X-ray diffraction has been used to investigate the structure and structural behaviour of several inorganic solids under variable pressure and temperature conditions. A brief description of the diamond anvil cell (d.a.c.) and its applications to the high-pressure investigations is given. A spectroscopic system built for pressure calibration is discussed, plus an account of powder diffraction data analysis including a detailed description of a software package engineered for the specific reduction of powder data obtained under variable pressure.

Potassium nitrate (KNO_3) has seven polymorphs in the pressure range 0.0-4.0 GPa. This material has been studied with energy dispersive powder diffraction (EDXRD) to 9.3 GPa. The structure of the non-ambient phase IV refined by neutron diffraction at 0.36 GPa has been confirmed, the compressibility of the high-pressure phase measured and found to be anisotropic with axial compression ratios $a:b:c = 1.0:0.64:0.50$.

The valence induced structural transition at 0.8 GPa in EuPd_2Si_2 has been studied using EDXRD and uni-axial compressibilities calculated. A basic explanation of the electronic theory which accompanies the subtle shortening of the a lattice parameter in the tetragonal asymmetric unit is also given.

The structures of two compounds CH_3HgX ($X = \text{I}, \text{Cl}$) have been investigated using single crystal and angle-dispersive powder techniques respectively. The crystal structure of methyl mercuric iodide is reported. CH_3HgCl has been observed above and below the temperature induced I/II phase boundary at 162.5 K. A hypothesis detailing the iso-structural nature of CH_3HgCl low temperature phase II and the ambient phase I of the analogous methyl mercuric bromide is also tested.

ACKNOWLEDGEMENTS

I would like to thank the following people, without whose assistance this work would not have been possible:

My supervisor, David Adams, for his ideas and encouragement throughout.

David Russell for the benefit of his experience, support, humour and several computer programs used in Chapter 6.

The Technical Staff of both the Department of Chemistry, in particular Phil Acton, and Alf Nield at Daresbury Laboratory whose patience and sense of humour finally succeeded in getting the experiments to work. Special thanks to Ann Crane for producing most of the diagrams. Also, Pete Hatton of Edinburgh University for sharing his ideas and beer.

The members of the High Pressure research group, past and present, in particular Simon Leonard for assistance during the late Daresbury years and Andrew Norman for his help in Perth!

All the friends who made me get on with writing this thesis, especially Andy, and in particular Ashley for being there when the going got tough.

The staff of Leicester University Computer Centre, especially Pam Gibson and Daniel Pead. Thanks also to the staff of the Biological NMR Centre, in particular Gordon Roberts for being patient.

I would also like to acknowledge the receipt of a maintenance grant from the Science and Engineering Research Council and thank the Council for providing the funding which enabled attendance at the XIVth International Union of Crystallography, Perth, Australia.

I dedicate this thesis to my mother,
and my father who would have loved to have seen it.

*Quia ars tanta est, numquam perficere
potest deserere tantum.*

(after Adams, D.M.; translation Scott, R.S.F.)

CONTENTS

| | | |
|-------------------|--|----|
| CHAPTER 1 | Introduction: Aims and Techniques | 1 |
| CHAPTER 2 | A Software Package for Data Acquisition and Analysis: Application to a Ruby R-line Spectroscopic System | 13 |
| CHAPTER 3 | Analysis of Powder Diffraction Data | 21 |
| CHAPTER 4 | High Pressure X-ray Diffraction Measurements on Potassium Nitrate (KNO_3) | 31 |
| CHAPTER 5 | A High Pressure Study of a Valence Transition in EuPd_2Si_2 | 37 |
| CHAPTER 6 | Structural Investigations of the Methyl Mercuric Halides CH_3HgX ($\text{X} = \text{Cl}, \text{Br}, \text{I}$) | 43 |
| APPENDIX 1 | Source code listing of program VARVEC | |
| APPENDIX 2 | Source code listings for BBC micro-computer programs | |

CHAPTER 1

INTRODUCTION: AIMS AND TECHNIQUES

CHAPTER 1

Introduction: Aims and Techniques

1.1 Introduction

Diffraction-based techniques for obtaining structural information on solids have, over many years, grown more specialised to cope with particular problems. The x-ray determination of structure from single crystals remains the most popular method, but has many limitations when applied to systems under non-standard conditions. Extreme temperatures or pressures can lead to some form of phase transition. Volumetric, thermodynamic and spectroscopic based techniques have been used to characterise the behaviour of these systems. However, to interpret these data it is often necessary to know the accompanying structural changes. Consequently, there has been considerable world-wide research into developing high-pressure diffraction-based techniques [1]. The major part of the work presented in this thesis is devoted to developing synchrotron-radiation-based techniques for high-pressure studies and associated methods of pressure calibration and data processing.

1.2 Aims

The overall aim of this work was to use x-ray diffraction to elucidate structural information in both known and unknown phases in the solid-state. Following from this, a description of the mechanisms involved in these transformations can often be attempted. The physical methods employed in this work have been refined, especially those concerned with pressure calibration and data-processing.

Although recent advances in techniques [2] and especially in gasket designs [3] have allowed collection of high-pressure x-ray diffraction data from single crystals, the geometry of diamond anvil cells (d.a.c.s) restricts the range of reciprocal space over which allowed reflection intensities can be measured. Moreover, the use of beryllium backings limits the accessible pressure range to approx. 8 GPa. In phase transition studies, the use of single crystal diffraction is further restricted as many structural transitions involve a volume collapse, often causing single crystals to shatter.

For neutron diffraction, the small scattering cross-section (*i.e.* scattering factors) requires a sample volume of several mm³, resulting in relatively massive pressure cells. This leads to severe restrictions on the scattering geometry and the large amount of

sample limits the readily available pressure range to less than 2.5 GPa. The use of spallation neutron sources relaxes some of the geometrical limitations, but is not expected to increase the attainable pressure range to that currently available using x-rays. However, the enforced larger sample size required for neutron techniques does allow for meaningful intensity measurements and hence the possibility of applying Rietveld refinement on a proposed high-pressure model to derive atomic parameters providing such a model is known or can be deduced.

Rapid developments in the use of synchrotron radiation (SR) have made energy dispersive x-ray diffraction (EDXRD) the primary investigative tool for high-pressure studies of solids. The location of Bragg peak positions in the EDXRD spectrum may be used to identify the Bravais lattice, the unit cell parameters and, in favourable cases, elements of symmetry pertaining to the associated space group. Advances in Rietveld techniques with SR have improved the use of angle-dispersive powder diffraction. Little success has yet been achieved at high-pressure with this method, since the intensity of the monochromated incident beam is several orders of magnitude lower than that used in the corresponding energy-dispersive experiment, presenting problems when the method is used with the d.a.c.s used to obtain high pressure. The small amount of scattering material coupled with this low incident x-ray intensity gives a weak diffraction signal; which would lead to very long scan times and poor signal/noise ratios. However, the improved resolution of Bragg peaks would allow for study of lower symmetry high-pressure phases than current methods allow. The increased number of measurable reflections could be used for indexing patterns with more success. Small molecule crystallography remains the most popular method for solving ambient phase systems. However, some systems exhibit peculiarities under ambient conditions which render this method impossible for structure solution. The sample required must be a single crystal of a certain size with few (preferably no) imperfections. In cases where such a crystal cannot be formed recourse to powder-based techniques can attempt to provide an acceptable answer. The section 2 of Chapter 6 details such a dilemma.

Extended X-ray Absorption Fine Structure (or EXAFS) has been used increasingly over the past twenty years as a qualitative tool for structural investigation. The interference pattern observed in an EXAFS experiment reflects directly the net phaseshift of an electron wave backscattered from atoms neighbouring the parent atom of the wave. This electron wave comprises the product of the electron wavevector and the distance travelled, but also includes contributions from the scattering process and from the passage of the photoelectron out and back through the potential of the emitting atom. The amplitude of the resulting oscillations depends on the number and electron cross-

section of the scattering atoms. Consequently, the distance of, type and number of nearest neighbours of the excited atom can be derived from analysis of the measured EXAFS.

This x-ray based spectroscopic technique offers great potential when applied to measurement of bond length variations as a function of pressure, particularly when a structural phase transition is involved, but to date published work in this field is very limited. Although the tunability and high flux of SR can be employed experimental problems are again encountered due to the low intensity of the transmitted monochromatic radiation through a diamond anvil cell. The d.a.c. also introduces a significant problem into the data analysis because of Bragg diffraction of the incident x-rays by the single crystal diamond anvils. These diffraction data are convoluted with the observed interference pattern. It is essential that these features are removed, although careful treatment of the data by way of mathematical deconvolution can achieve this. The X-ray Absorption Near Edge Structure (XANES) region [4] utilises only a narrow energy range in the incident beam which enables Bragg reflections to be readily avoided. As a result, some high-pressure d.a.c.-based studies have been attempted making use of this region [5,6].

1.3 High-pressure Techniques

The main design features of the diamond anvil cells (d.a.c.) used for the high-pressure work here are shown in Figure 1.1. This design of d.a.c. was pioneered in the late 1950's and since has undergone various design modifications. However, all have retained the essential feature of compressing a sample between the parallel faces of two opposed diamond anvils [7-11]. The cells used for all work presented here have been developed within this laboratory [12]; the Mark III cell currently in use is produced in two models, the Diacell and Dynocell. The former is rated for a working maximum pressure of up to 15 GPa, the latter up to 100 GPa (*i.e.* a megabar) [13]. When the cell is assembled, force is generated either hydraulically or by compressing Belleville spring washers by a simple screw mechanism, and is transmitted to the moving anvil holder via the lever arms and presser plate. The light ports beneath each diamond permit the passage of electromagnetic radiation through the diamonds and sample, Figure 1.2. Diamond is transparent to laser light. No diffraction spots are observed from the diamond (single crystals) during x-ray experiments due to the one dimensional nature of powder work and small diffraction detection area.

The sample can be held in a hydrostatic environment when under pressure by introducing it and a pressure transmitting medium into a gasket centered between the anvil faces. This ensures that qualitative measurements can be made at high pressure

Figure 1.1

Schematic diagram to show main design features of the diamond anvil cell (the diacell: plan and side elevation)

Parts labelled are:

1. Cell body
2. Central insert
3. Fixed anvil holder
4. Moving anvil holder
5. Presser plate
6. Lever arms
7. Internal hydraulic ram
8. Knurled backing screw
9. Piston plate
10. Central pivot
11. Piston screw
12. Oil feed for hydraulic ram

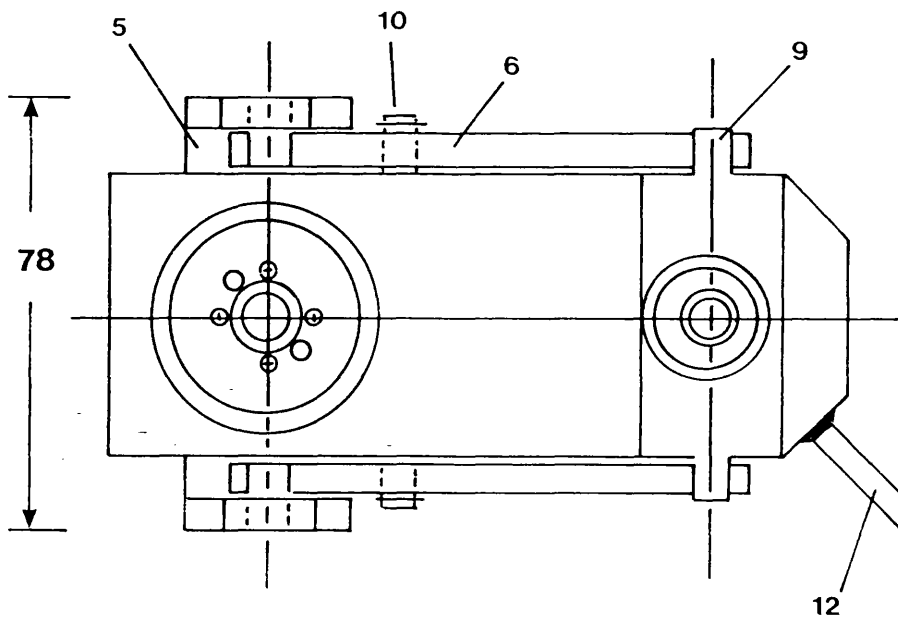
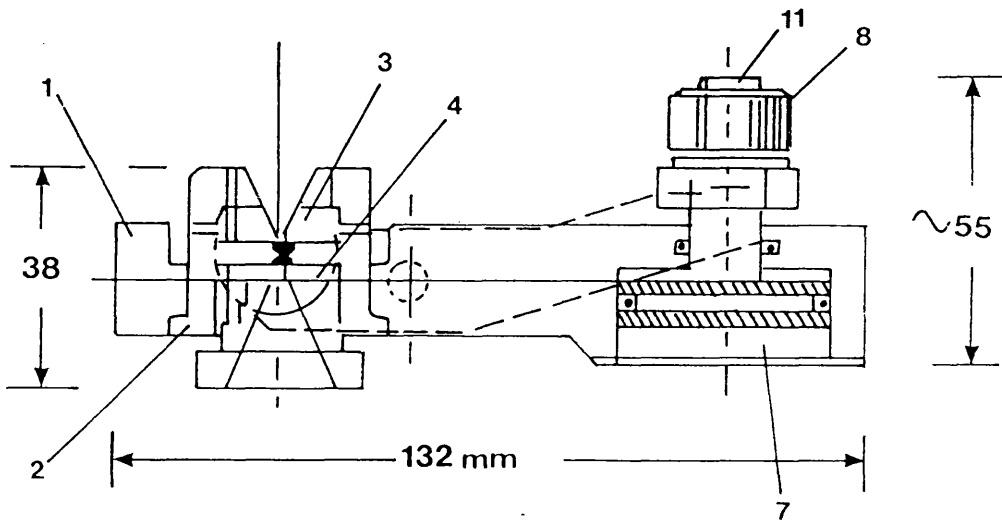
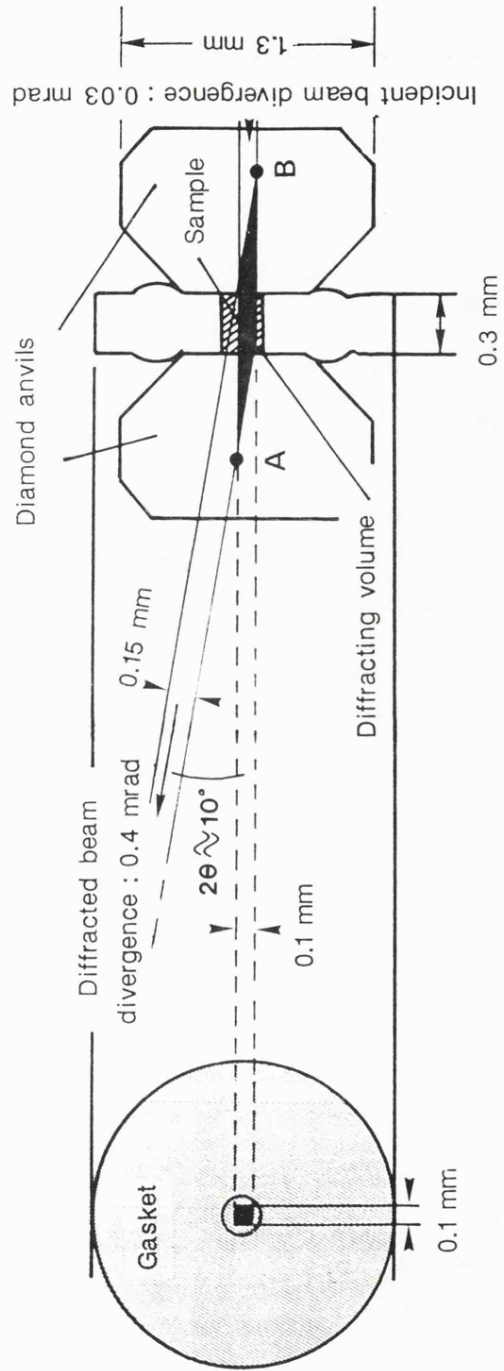


Figure 1.2

X-ray path through a d.a.c.
showing gasket, diamonds
and sample



single pressure. The gasket is a piece of thin metal sheet through which a hole is drilled (or spark-eroded) usually of diameter 0.1-0.4 mm. Gasket materials vary but the most commonly used here is Inconel (a Ni/Cr/Fe alloy), stainless steel and molybdenum also being employed. This choice of gasket materials is occasionally necessary if a sample under investigation is found to react with a certain material. The pressure transmitting medium usually employed is a 4:1 mixture of methanol/ethanol. Other mediums include some inert gases (*e.g.* argon and neon), also glycerine is useful with pressures below 2 GPa (glycerine crystallises at pressures greater than 2 GPa). Techniques of diamond selection, gasket preparation and sample loading are explained in detail elsewhere [14,15].

In experiments where the sample is held at high static pressures within a d.a.c., it is necessary to routinely examine pressure quickly and accurately. There are two versatile methods which can be used to achieve this in powder diffraction work; the ruby fluorescence technique and the use of internal calibrants. The former method is based on monitoring the frequency shift of the R_1 and R_2 fluorescence lines of ruby, which result from trace amounts of Cr^{3+} incorporated in the Al_2O_3 lattice. The shift ($7.6 \times 10^{-2} cm^{-1} GPa^{-1}$) is nearly linear to pressures above 1 Mbar and can be measured with an accuracy of $5 \times 10^{-2} GPa$ or better [16-19]. A laser is used to excite the fluorescence from a small chip of ruby embodied within the sample compartment on loading. This technique has been employed in the high pressure work outlined in this thesis and required the design and construction of a spectroscopic system to be used on site at the Daresbury Synchrotron Facility. Full details of this system and the associated computer interfacing are given in Chapter 2.

The use of internal x-ray pressure calibrants such as some rare gases (*e.g.* argon or neon) offer an attractive alternative for *in situ* pressure determination. These rare gases act as pressure transmitting media, they are highly compressible with unit-cell lengths which can be measured to one part in 10^4 . The equation-of-state for these elements under pressure are known and hence, pressures can be calibrated which are sensitive to 5 bars at 5 GPa. However, their presence further complicates a powder diffraction pattern and can, occasionally, obscure vital information because of Bragg peak overlap of sample and calibrant diffraction lines. The ruby fluorescence technique has been favoured in this work since pressures can be calibrated prior to x-ray exposure and hence any necessary adjustments made, also vital information relating to the hydrostatic state of the sample can be gained from the separation and shape of the R_1 and R_2 fluorescence lines [20] (see Chapter 2).

1.4 Phase Transitions

The terms *first* and *second* order phase transitions used in this thesis require definition. A detailed discussion of the thermodynamic and symmetry related properties of structural solid-solid phase transitions would be out of place here; the following is intended to introduce the concepts involved. However, several treatments which approach the subject in depth using different arguments are available [21-23].

A solid-state phase change is stimulated when a particular phase of that solid becomes unstable with respect to a given set of thermodynamic criteria. The choice between types of transition as first or second order arises from the order of partial differentiation required in the Gibbs equation to produce a term which becomes discontinuous at the phase change [24]. The Gibbs free energy expression can be expressed as:

$$dG = dE + PdV + VdP - TdS - SdT$$

$$\therefore dG = VdP - SdT \text{ (since } dE = TdS - PdV)$$

The first and second order partial derivatives of this equation can be written as:

$$\left(\frac{\partial G}{\partial P}\right)_T = V \qquad \left(\frac{\partial G}{\partial T}\right)_P = -S$$

$$\left(\frac{\partial^2 G}{\partial P^2}\right)_T = \left(\frac{\partial V}{\partial P}\right)_T = -V\beta$$

$$\left(\frac{\partial^2 G}{\partial T^2}\right)_P = \left(\frac{\partial S}{\partial T}\right)_P = -\frac{C_P}{T}$$

$$\left(\frac{\partial^2 G}{\partial P \partial T}\right) = \left(\frac{\partial V}{\partial T}\right)_P = -V\alpha$$

where:

C_P = heat capacity, α = volume thermal expansivity, β = isothermal compressibility

Thus, first order transitions are characterised by discontinuity in volume change (if pressure induced) and latent heat (if temperature induced). Any symmetry relationship between the space groups of the parent and daughter phases is not generally obvious since commonly the two phases have very different structures (Chapter 4 shows both phases to have the same space group). Attempts can be made to correlate the two groups [25], but this requires knowledge of the crystal structures in both phases; that of the daughter phase is not usually available.

Using diffraction-based techniques a first order transition is often observed as a radical change in the powder pattern. Large volume decrease means reformation of the asymmetric unit with different lattice parameters (and commonly symmetry) which alters the observed d_{hkl} in both intensity and position. Hysteresis is also common in first order systems and is observed as a difference in the critical temperature/pressure involved in the change when approached from either the forward or reverse direction [26,27].

The second order partial derivatives of the Gibbs equation show entropy and volume remain continuous whilst α , β and C_p undergo discontinuous change. The second order transition is generally characterised by some form of disordering process in which the symmetry of the two phases is related in some way. The symmetry of the asymmetric unit in one phase is generally higher than that in the other. In most cases, the higher symmetry phase is found at lower pressure (higher temperature) and the lower symmetry at higher pressure (low temperature). Although the first and second order definitions are useful for comparison, in general most transitions display discontinuity in parameters from both sets of thermodynamic criteria and hence show mixed order.

1.5 Synchrotron Radiation

Synchrotron radiation (SR) is emitted by electrons in circular motion with velocities close to that of light. The Daresbury Synchrotron Radiation Source (SRS) typically holds a beam of electrons with an energy of 2.0 GeV and current of approx. 200 mA or greater (see Figure 1.3). The circular orbit of the beam is sustained by bending magnets located strategically around the ring. The characteristics of synchrotron radiation are well documented elsewhere [28]. The radiation produced is a continuous spectrum (so-called 'white' radiation) ranging from the infrared to the far x-ray region. SR is emitted tangentially to the beam orbit with a very small angular divergence in the plane perpendicular to its orbital plane (Figure 1.4). The resulting radiation is very intense and highly collimated. By applying a stronger magnetic field locally the radius of curvature of the beam becomes smaller and the emitted photons attain a higher (momentum) energy, *i.e.* there is a shift to shorter wavelengths and harder x-rays are produced. This effect is accomplished by a so-called 'wiggler' which is a combination of high-field (2.5 and 5 Tesla) supercooled magnets. The properties outlined above make SR an ideal source of x-rays for diffraction-based investigations. The continuous nature of this x-ray source is very useful indeed; tunability of incident radiation with a monochromator is straightforward, this being especially important in EXAFS experiments and angle-dispersive powder diffraction. White radiation is vital for any energy-dispersive technique (*vide infra*). The relatively high intensity of incident x-rays in comparison to conventional sources allows the beam to be reduced dramatically in cross-section for

Figure 1.3

The Daresbury Synchrotron facility showing
beam lines and location of experimental hutches
and wiggler magnet

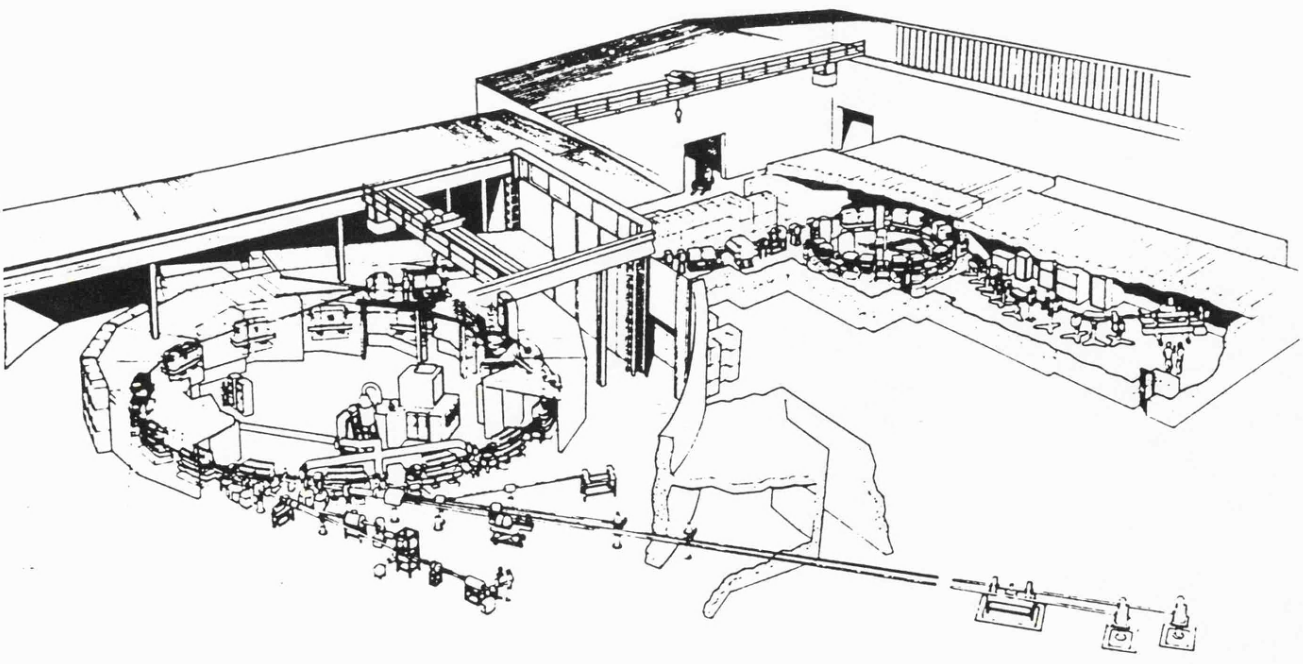
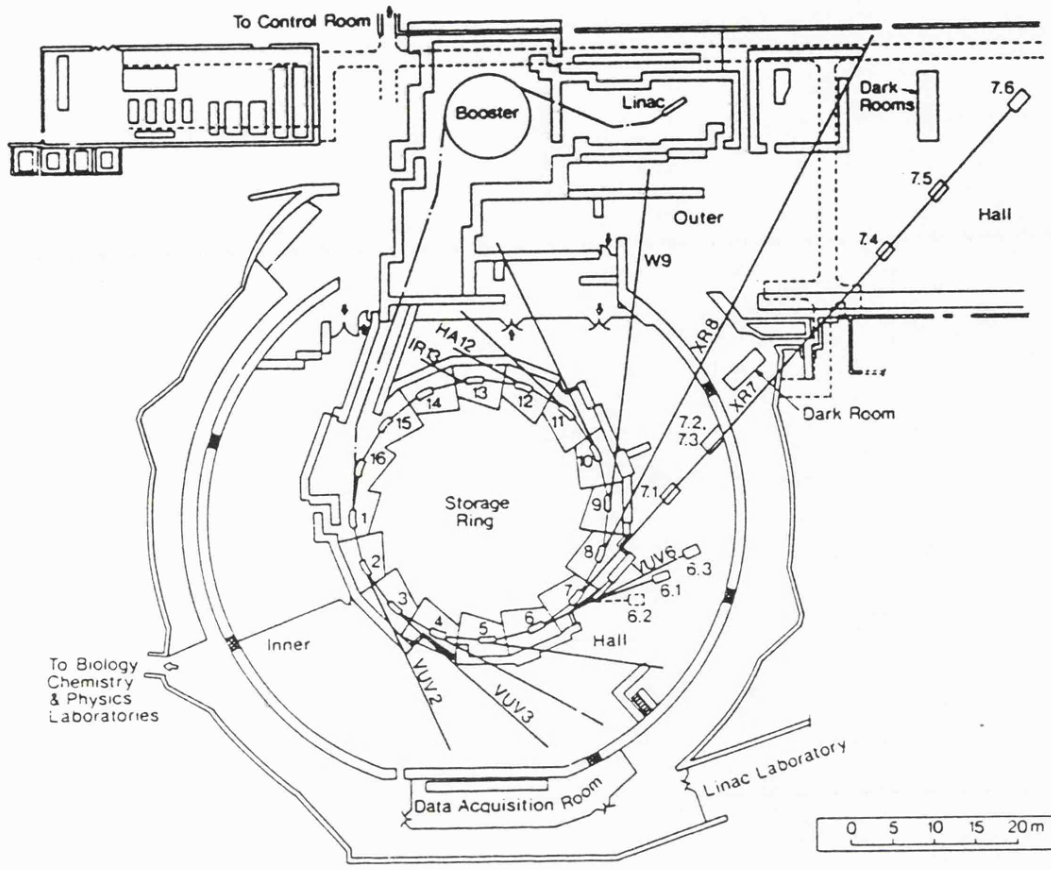


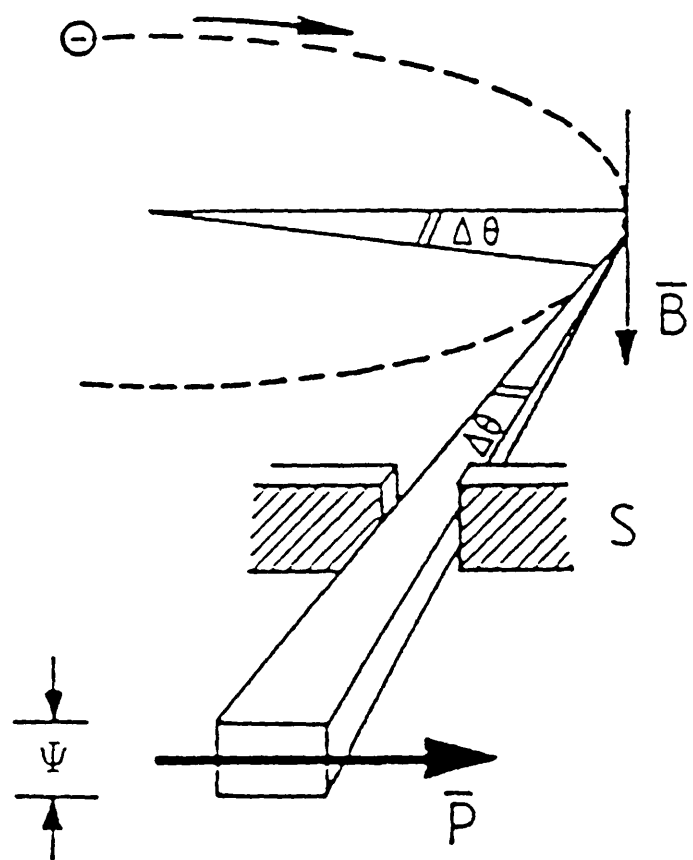
Figure 1.4

Geometry of emission of Synchrotron radiation by electrons in circular motion. Velocity close to c .

i) $\Psi = 0.25 \text{ mrad} = 52''$ (for 2 GeV).

ii) \mathbf{B} - bending magnetic field \perp to electron orbit.

(iii) \mathbf{P} - direction of polarisation



precision micro-collimation (*e.g.* during high-pressure d.a.c. experiments) whilst still producing satisfactory diffraction intensity from the sample. Although a rotating anode can produce the above effects it is generally agreed that SR is superior [29].

There are, however, a number of disadvantages which have been encountered while using the Daresbury SRS as an experimental source. Daresbury Laboratory is a central facility which should be operational 24 hours per day, 7 days per week and large numbers of users are scheduled to make use of the facility. Unfortunately, due to various machine faults the Daresbury SRS had a record of enforced shutdowns over the period of time when the work presented here was carried out. The wiggler magnet was not generally reliable and has caused shutdowns of all experimental stations on the wiggler-line many times. The large number of users means that allocated beam-time lost from a schedule is very difficult to make up; all users can possibly suffer the same fate and one simply hopes all will be well during one's allocated experimental time.

1.5 Energy Dispersive X-ray Powder Diffraction

1.5.1 Introduction

The energy dispersive x-ray diffraction (EDXRD) technique was developed by Giessen and Gordon [30] in 1968. During the past two decades EDXRD has been applied to single crystals, powders, amorphous solids and liquids for measurements of lattice parameters, structure, temperature, absorption factors, preferred orientation, stress and particle size effects. An extensive literature survey was published by Buras in 1980 [31].

Energy dispersive powder diffraction is a technique related to the conventional angular dispersive method as the Laue method is to the Bragg method. The latter employs monochromatic incident radiation and the reflections appear at angles determined by the lattice spacings d as shown by the Bragg equation:

$$d\sin\theta = \lambda/2 = \text{constant}$$

In the energy dispersive method the reflections are generated from continuous x-radiation at a selected angle 2θ . Combining the well-known relationship of wavelength as a function of its energy E with the equation above the resulting expression given by Cole [32] is:

$$Ed\sin\theta = hc/2 \text{ (where } h \text{ is Planck's constant)}$$

If E is expressed in keV and d in Å this equation becomes:

$$Ed\sin\theta \approx 6.19926 = \text{constant}$$

Therefore, when a white (polychromatic) beam of x-rays is incident on the powder sample, the above equation shows for a fixed value of 2θ , discrete values of d will produce reflections in an energy spectrum collected by an energy sensitive detector. This is the principle of EDXRD.

The main characteristics and advantages of this method as compared with the angular scan method can therefore be summarised as follows:

- i) White, high intensity primary beam
- ii) θ fixed during experiments but can be optimised for a particular experiment
- iii) All Bragg reflections recorded simultaneously

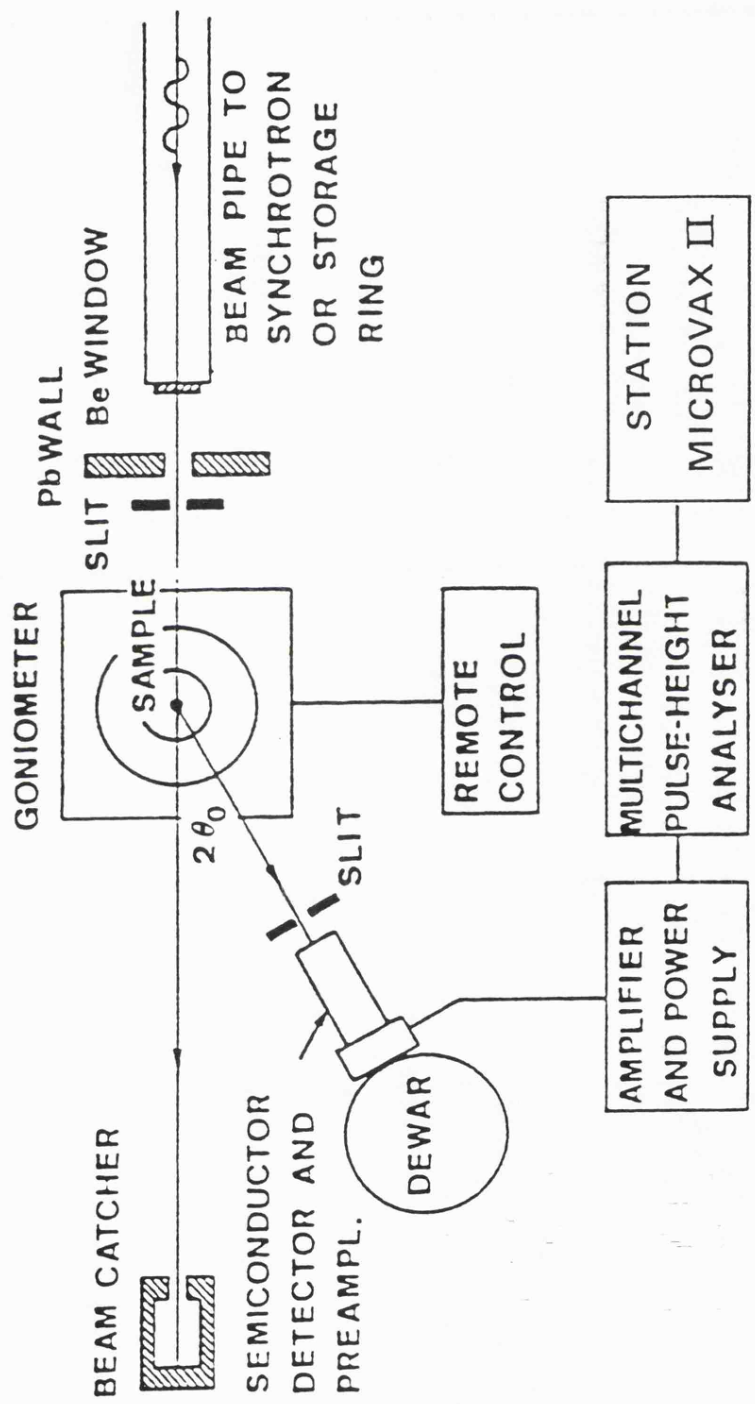
1.5.2 Experimental

The use of d.a.c.s for high-pressure work favours Debye-Scherrer scattering geometry, because of the small sample size, gasket thickness and geometric constraints on the x-ray paths due to the piston and cylinder design (see Figure 1.2). Some ambient patterns were generated using a $\theta:2\theta$ setting of the specimen and detector with the sample mounted on a flat plate. The angle θ is taken between the incident beam and the specimen surface, and 2θ is the angle between the primary and diffracted beams.

A schematic representation of the high-pressure experimental setup is shown in Figure 1.5. An ORTEC nitrogen cooled Ge semi-conductor detector was used for the high-pressure scans. The resolution of measured reflections is dependent on the detector system and the collimation of diffracted radiation (see Chapter 3.1). The maximum resolution achieved was 165 eV at 5.9 keV. The d.a.c. was mounted on a remotely controlled XYZ-translation stage, the DC stepping motors allowed the precise movement necessary for alignment of the small sample compartment. The d.a.c. was positioned on precision machined pegs on the mounting stage to allow for accurate replacement following pressure adjustment. The cross-section of the primary synchrotron radiation was reduced to a circle of $\sim 50 \mu\text{m}$ in diameter by a set of evacuated slits and pinholes. Because of the simultaneous recording of reflections and the highly intense primary beam, the counting time used in this experiment is relatively short compared with other powder methods. Further decrease of counting time is limited by the present maximum count-rate of semi-conductor detectors ($\sim 10^5$ counts/sec). In the high-pressure experiment counting times are increased because of the reduced primary beam cross-section. In our experiments 20-30 minutes was found to be optimum. This counting time was also found to be dependent on the crystallinity of the sample and the scattering cross-sections of the atomic constituents.

Figure 1.5

Schematic diagram to show the set-up
used in the EDXRD experiment



The detector system comprised of the Ge (solid state) detector, from which a signal was amplified to a multi-channel analyser (MCA). The amplifier was optimised for each scan if a specific section of the pattern required intensive data collection. Therefore, careful calibration between the detector and MCA was required after any adjustment of amplifier 'gain'. The well documented fluorescence energies (K_{α} , K_{β} , etc) of several elements (*e.g.* copper, molybdenum, silver, *etc*) excited by a radioactive dial source was used to form the correlation between channel number and energy (keV). A least squares fit of energy to channel number always found a linear relationship (Figure 1.6). The experiments demanded absolute values for the lattice spacings and thus, the diffraction angle θ was required. This can be derived from the relative energy displacements of a Bragg peak as the 2θ diffractometer is moved (so-called differential measurements, see Chapter 3.1) or calculation of the angle from an ambient EDXRD spectrum of a standard (*e.g.* silicon) where the d-spacings are known to high precision and indexing the pattern is trivial.

1.5.3 Information obtainable from EDXRD

The data derived from EDXRD patterns can be used to establish the Bravais lattice type, cell parameters and, in favourable cases, the space group. If the structure of the high-pressure phase is known then pattern indexing is elementary and indexed reflections can be followed as they move with pressure. During a phase transition a combination of phases (especially if hysteresis is suspected in the system) can result in a very complex but informative pattern. Observation of Bragg peaks which have split can provide valuable information to the identity of this next phase. When the high-pressure phase is unknown indexing can be difficult (in some cases impossible) to carry out unambiguously. Most numeric algorithms require at least twenty resolved reflections before any possible conclusion can be drawn about the dimensions and shape of the asymmetric unit.

Information concerning the atomic positional parameters within the unit cell is contained within the intensity of the observed Bragg peaks. However, the integrated intensities obtained from the very small samples used in d.a.c.s are generally unreliable. Such a sample contains a very small number of crystallites which, together with the high collimation of the synchrotron radiation, leads to a small number of crystallographic planes in the diffracting position. Thus, the measured integrated intensities depend rather accidentally on the spacial orientation of a very limited number of crystallites. This statistical problem means that refinement of energy-dispersive profiles generated under high-pressure conditions with Reitveld-type techniques is not generally feasible. A solution to this dilemma is to use a larger quantity of sample, however, this would

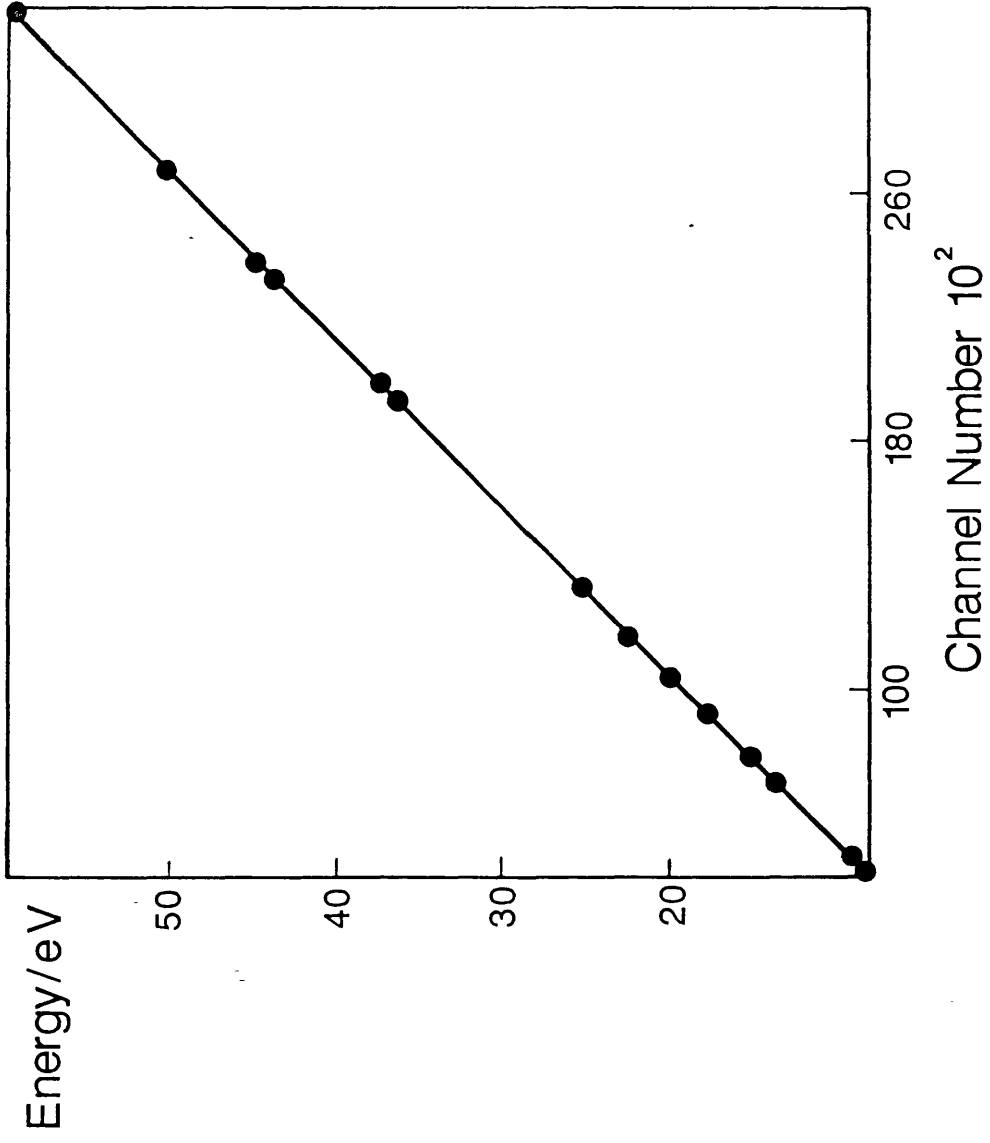
Figure 1.6

Typical linear least squares fit of
channel number to energy (keV).

$$\text{Fitting } E(\text{keV}) = aX + b$$

(X = channel number)

MCA Calibration Curve



severely limit the accessible pressure range. Rotation of the sample around the axis of the primary beam would improve counting statistics but this presents practical difficulties with the d.a.c.s used here. High-pressure EDXRD is also prone to high background counts from Compton (elastic) scattering by the diamonds surrounding the sample compartment.

In conclusion, EDXRD is a powerful tool for high-pressure structural investigation despite the limitations described above. Phase transitions are readily observed making suspected changes simple to verify both quickly and accurately. The other methods available for high-pressure x-ray solid-state studies have been briefly discussed and all have their merits and disadvantages. A combination of techniques would allow conclusions to be drawn more confidently regarding new structural phases and the mechanisms of their formation.

References

1. Adams D.M. and Martin J., 1981, *High Temp, High Pres.*, **13**, 361
2. Hazen R.M. and Finger L.W., 1982, "Comparative Crystal Chemistry", Wiley, New York.
3. Katrusiak A, and Nelmes R.J., 1986, *J. Appl. Cryst.*, **19**, 73
4. Belli M., *et al*, 1980, *Solid State Comm.*, **35**, 355
5. Ingalls R., Tranquada J.M., Whitmore J.E. and Crozier E.P., 1983, "EXAFS and Near Edge Structures", Proceedings of the International Conference, Frascati, Italy, 1982; **154**, Springer-Verlag, Berlin.
6. Röhler J., Krill G., Kappler J.P. and Ravet M.F., 1983, "EXAFS and Near Edge Structures", Proceedings of the International Conference, Frascati, Italy, 1982; **213**, Springer-Verlag, Berlin.
7. Piermarini G.J. and Block S., 1975, *Rev. Sci. Instrum.*, **46**, 973
8. Bassett W.A., Takahashi T. and Stook P.W., 1976, *Rev. Sci. Instrum.*, **38**, 37
9. Mao H.K. and Bell P.M., 1978, *Carnegie Inst. Washington Year Book*, **77**, 904
10. Huber G., Syassen K. and Holzapfel W.B., 1974, *Rev. Sci. Instrum.*, **45**, 290
11. Merrill L. and Bassett W.A., 1974, *Rev. Sci. Instrum.*, **45**, 290
12. Appleby R., 1977, *Ph.D. Thesis*, University of Leicester.
13. Diacell Products Limited, 54 Ashtree Road, Oadby, Leics.
14. Williams A.D., 1980, *Ph.D. Thesis*, University of Leicester.
15. Adams D.M. and Payne S.J., 1974, *J. Chem. Soc. Farad. Trans. II*, **70**, 1959
16. Mao H.K. and Bell P.M., 1979, *Carnegie Inst. Washington Year Book*, **78**, 665
17. Barnett J.D., Block S. and Piermarini G.J., 1973, *Rev. Sci. Instrum.*, **44**, 1
18. Bell P.M. and Mao H.K., 1975, *Carnegie Inst. Washington Year Book*, **74**, 399
19. King H.E. and Prewitt C.T., 1980, *Rev. Sci. Instrum.*, **51**, 1037
20. Adams D.M., Appleby R. and Sharma S.K., 1976, *J. Phys. E*, **9**, 1140
21. Iqbal Z. and Owens F.J., eds., 1984, "Vibrational Spectroscopy of Phase Transitions", Academic Press, London.
22. Rao C.N.R. and Rao K.J., 1968, "Phase Transitions in Solids - An Approach to the study of Chemistry and Physics of Solids", McGraw-Hill, New York.
23. Kochinski J., 1983, "Theory of Symmetry Changes at Continuous Phase Transitions", Phase Transition Phenomena Vol. 2, Elsevier, Amsterdam.
24. Ehrenfest P., 1933, *Proc. Amsterdam Acad.*, **36**, 153

25. Boyle L.L., unpublished work.
26. Bridgman P.W., 1932, *Rec. Trav. Chem.*, **51**, 627
27. Dornell A.J. and McCollum W.A., 1970, *High Temp. Sci.*, **2**, 331
28. Winick H. and Doniach S., eds., 1980, "Synchrotron Radiation Research", Plenum, New York.
29. Buras B., 1979, *Proceedings of Symposium on Accuracy in Powder Diffraction*, NBS Special Publication 567
30. Giessen B.C. and Gordan G.E., 1968, *Science*, **159**, 973
31. Buras B., 1980, NBS Spec. Pub. 567, "Proceedings of Symposium on Accuracy in Powder Diffraction", NBS, Gaithersburg, MD.
32. Cole H., 1970, *J. Appl. Cryst.*, **3**, 405

CHAPTER 2

A SOFTWARE PACKAGE FOR DATA ACQUISITION AND ANALYSIS: APPLICATION TO A RUBY R-LINE SPECTROSCOPIC SYSTEM

CHAPTER 2

A Software Package for Data Acquisition and Analysis: Application to a Ruby R-line Spectroscopic System

2.1 Introduction

There are many different types of high pressure spectroscopic device [1] but the attainment of very high static pressures in the solid state is simplest with Bridgman opposed anvil cells. Of these, the diamond anvil cell (d.a.c.) is the most versatile [2,3]. It has been used to generate pressures of up to 5.5 Mbar [4], thus overlapping with the lower end of the pressure range accessible by dynamic (shock wave) methods.

Accurate measurement of the hydrostatic pressure exerted on a sample by the anvils is crucial to any such experiment. The most widely used secondary pressure standard involves use of the ruby R_1 and R_2 fluorescence lines [5,6]. Their shift with pressure is linear ($7.6 \times 10^{-2} \text{ cm}^{-1}$ per GPa) up to at least 20 GPa. The general form of the shift is represented by Equation 2.1 which has been shown to be valid to at least 2 Mbar [7].

$$P(\text{Mbar}) = 3.808 \{ [1 + (\Delta\lambda/\lambda)]^5 - 1 \} \quad (2.1)$$

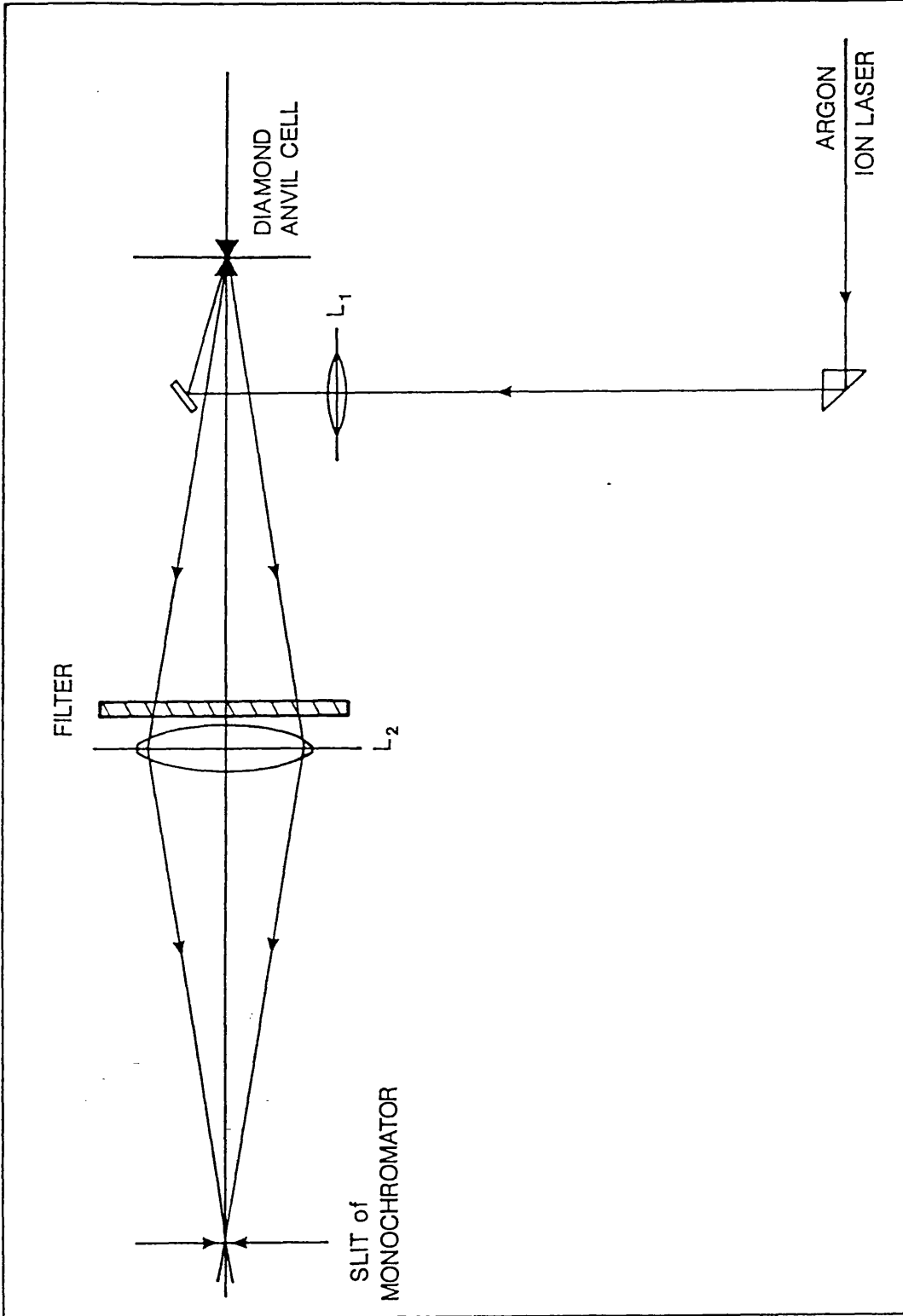
In the course of high-pressure work with energy dispersive x-ray powder diffraction using synchrotron radiation at the Daresbury SRS facility, d.a.c.'s were used to obtain the high-pressure powder spectra, and the sample pressure was calibrated using the ruby R-line method. This calibration necessitated the construction of a spectroscopic system which was interfaced to microcomputer for ease of data acquisition and analysis. This chapter details the methodology of the real-time software designed to work with this system and a brief outline of the system itself. Suggestions are also made for the application of the software to other experimental tasks and other compatible micro-computers.

2.2 The Spectroscopic System

The optical system is shown in Figure 2.1. A focussed laser beam was used for stimulation of the fluorescence and a monochromator (Jobin-Yvon HR-320) coupled to a

Figure 2.1

R-line spectroscopic optical system



photomultiplier tube was used for detection. A large proportion of the high-pressure systems studied by users are opaque to laser light and hence a back-scatter geometry was adopted: this works equally well with laser-transparent samples.

The start position, rate of scan and scan range of the collected spectrum were controlled by a scan controller (Jobin-Yvon). This controller, together with the photomultiplier voltage (PMV) amplifier was interfaced to the micro-computer (an Acorn BBC model B) to allow real-time data acquisition.

2.3 Software

2.3.1 Introduction

The system is used by many different experimenters, and knowledge of the operating system of the BBC model B cannot be assumed. The software was designed to be as user-friendly as possible, not least as users are frequently tired since the synchrotron facility is in 24hr/day operation. The system makes use of both colour and sound to help the user calibrate a pressure as quickly and precisely as possible. All programs were designed to be driven from a main-menu which can be activated with a <SHIFT/BREAK> from the keyboard. Three programs are driven from the main-menu. They are:

1. A 'peaking up' program to assist optimisation of the ruby fluorescence signal from the d.a.c.. The cell is aligned in the laser beam using an XZ-stage operated manually. As this is a simple operation, automation of the stage, although easy in terms of both hardware and software, was considered cost-ineffective.
2. An acquisition and analysis program for data from ruby at ambient pressure.
3. An analogous program for high-pressure scans and calculation of pressure.

BBC BASIC was used throughout in conjunction with 6502 Assembler language. The flexibility of BASIC coupled with the power of Assembler made the code easy to read and understand, whilst giving the speed of execution required in real-time computing.

2.3.2 Peaking Program

A schematic 'flow' diagram of the logic structure of this program is shown in Figure 2.2. This program makes use of one of the four built-in analogue to digital converters (ADC's) of the BBC model B.

The function of this program is to display a representation of the fluorescence signal strength from the sample. Several screens are employed, representing different sensitivity levels, a lower level applying to a stronger signal (*cf* use of GAIN on a chart recorder). A marker is used to show the maximum attained at any one time.

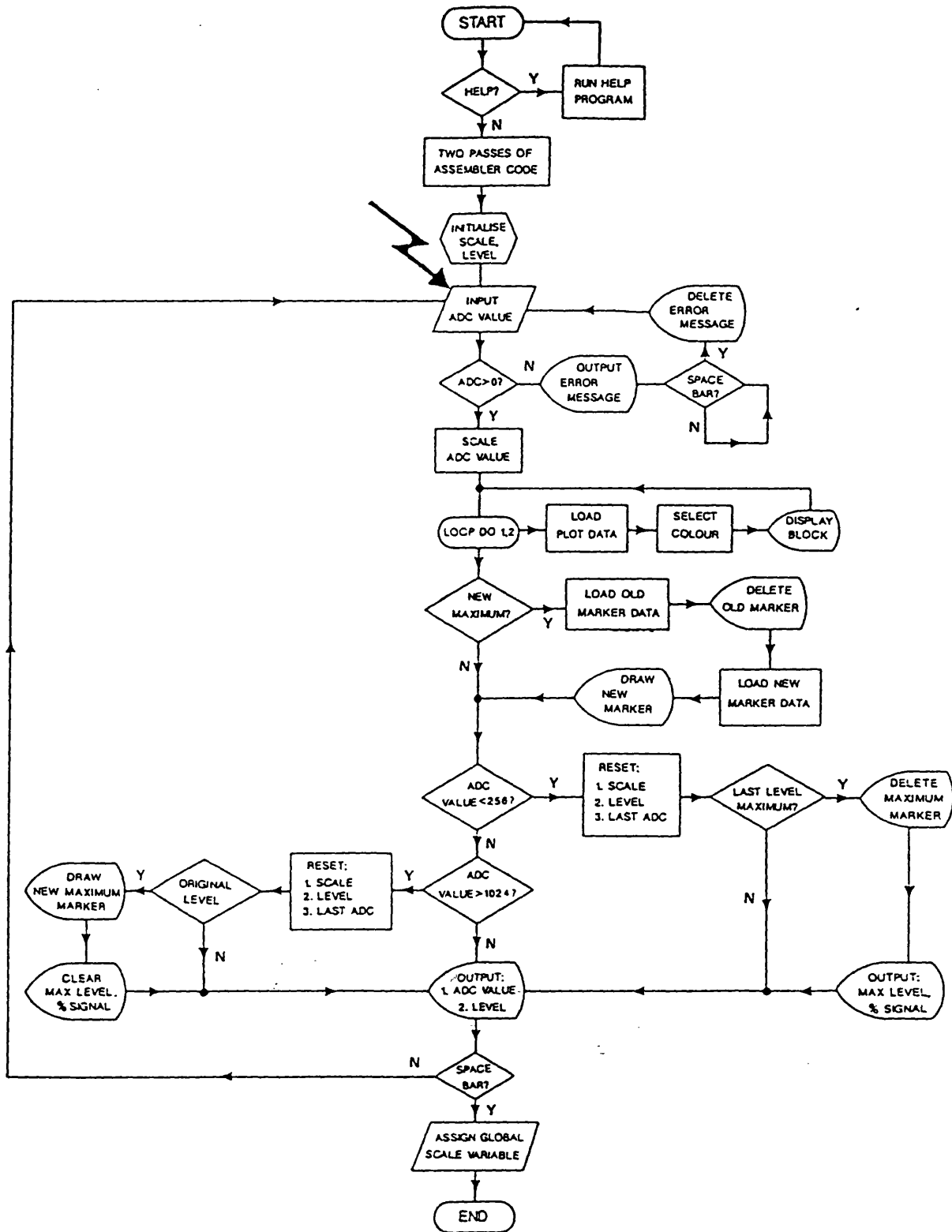
The program is executed from the main-menu. The user is given the option of help - this includes a brief explanation of the software system and attached hardware. On execution two passes of the Assembler code are made to compile this into machine code in random access memory (RAM). Two passes are required since forward referencing is used in the Assembler code. This code is split into modules, each module serving a specific function (*e.g.* calculation of vector positions, line drawing, etc).

The ADC is stimulated and a value read. The ADC is capable of interpreting analogue signals from the amplifier in the range 0-1.8 volts and converting these to digital values between 0 and 65536. An error is flagged and the program temporarily terminated if the ADC receives zero input. If the value is positive this is divided by a scale factor in an attempt to scale the result to a magnitude comparable with the vertical plot coordinates of the BBC screen (*i.e.* 0-1024). Initially the value of the scale factor is two but this is automatically reset (if necessary) as described below.

The main section of the program is a loop which serves the purpose of drawing a histogramic type block, the height of which is proportional to the scaled ADC value and hence the analogue signal input. A loop is required since the display is animated by being drawn twice using the same plot data; firstly in a colour to show up on the background and then in the same colour as the background *i.e.* the block is deleted immediately after it is drawn. The ADC signal is then compared with the previously attained maximum. If the old maximum has been exceeded the marker is deleted (by being redrawn in the background colour) and a new marker drawn in the appropriate place. The magnitude of the vertical plot is then checked to see if it can still be represented on the screen (*i.e.* vertical plot coordinates between 256 and 1024). If this is not the case the screen is refreshed into another sensitivity level. If the signal becomes weaker a higher sensitivity level is selected and the scaling factor halved. This results in a more sensitive observation of the signal strength since as much of the screen as possible is utilised in drawing the

Figure 2.2

Flow diagram for peaking program



histogram. The marker is redrawn in the appropriate place on the new screen. This change of level is flagged; if the previous level contained the maximum signal strength yet obtained, a message is written informing the user of the percentage signal strength and the number of the previous level (levels range between 1 and 8, level 1 representing the strongest signal) enabling more accurate re-peaking.

If the signal is stronger than the previous maximum level, the sensitivity level is dropped, the screen refreshed, and the flag checked to see if the maximum level has been reattained. If so the message informing of the former maximum is deleted and the marker redrawn to indicate the position of the old maximum. Thus, the main program is animated by employing an endless loop; updating the histogramic block, marker and if necessary the screen up to five times per second.

When the ruby signal has been maximised, the program is exited by pressing the space-bar. The keyboard buffer is tested during each cycle of the main program to check if the space bar has been pressed. If it has, a global variable is assigned for use by later programs containing the scaling factor for the screen co-ordinates. The program terminates and returns the user to the main-menu.

2.3.3 Acquisition and Analysis Programs

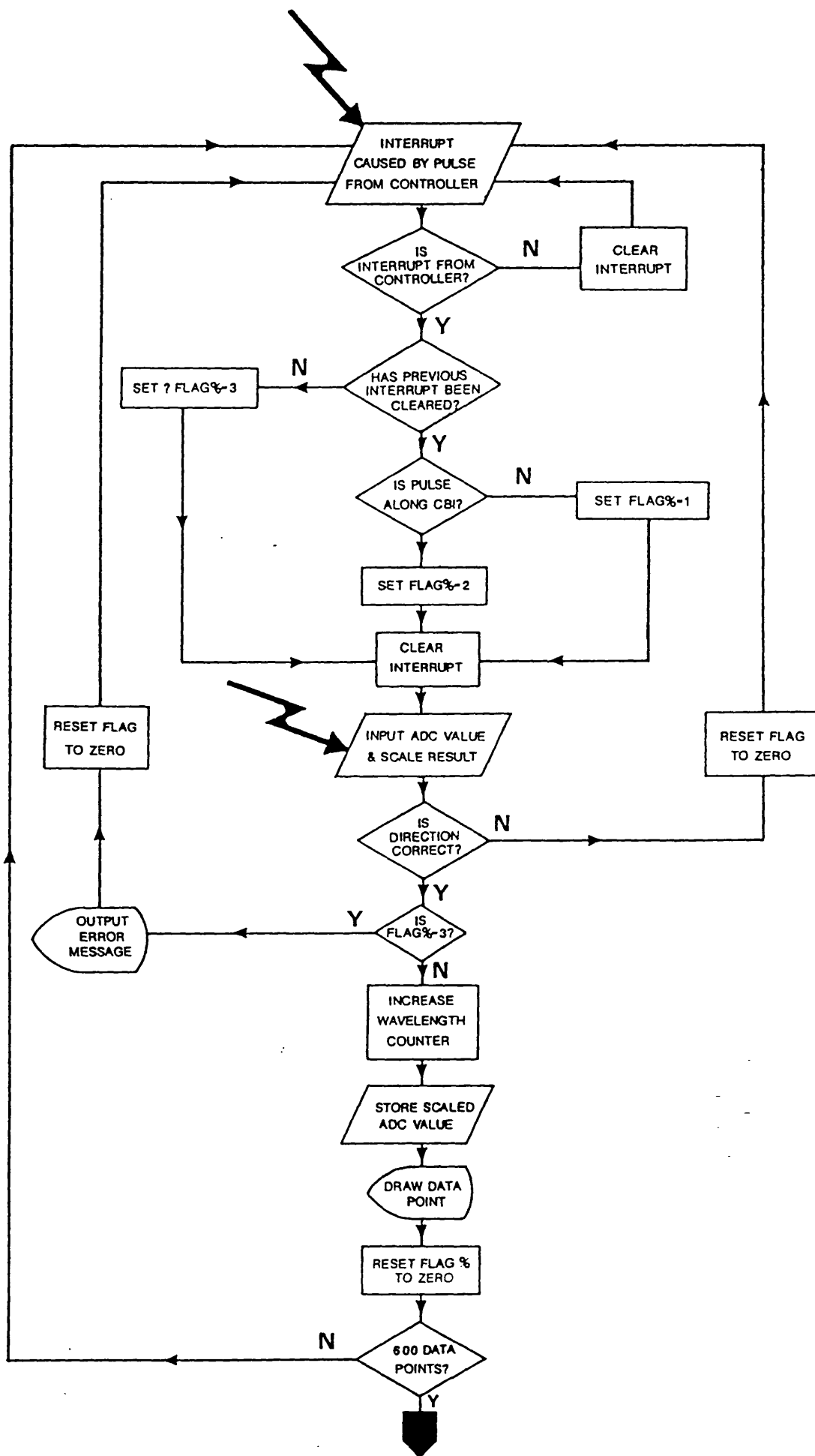
The data-acquisition parts of these two programs are identical. The schematic flow diagram is shown in Figure 2.3. The analysis sections differ from each other and are outlined later. The function of these two programs is to plot, in real-time, a ruby fluorescence spectrum and analyse the collected data for the R-line peak positions. The high-pressure option is used to calculate the pressure exerted on a ruby chip from the shifts of both the R_1 and R_2 peaks relative to the ambient positions. The programs also give the R_1 and R_2 frequency difference as this parameter is a useful indicator of any departure from hydrostatic conditions.

These programs are entered from the main-menu. Two passes of the Assembler code are made to compile the 6502 code. This code is written in modules to perform specific functions, such as 'enabling' user interrupts, or directing these interrupts away from the normal operating system handling procedures.

The program begins by inquiring the start position and direction the scan is to take. Six hundred data points are collected over a 60 nm range. The screen is then cleared and X-Y axes drawn (with appropriate intervals marked) for the subsequent spectrum.

Figure 2.3

Flow diagram of software common
to acquisition programs



Several compiled Assembler (*i.e.* machine code) routines are called as one module. The user Versatile Interface Adapter (VIA) is used to connect the scan controller to the computer. The VIA is a socket and a 6522 microchip which is programmed by a machine code routine each time the program is executed. The VIA receives pulses along one of two cables from the scan controller every 0.1 nm; the cables correspond to either forward or reverse direction dictated by the controller. The VIA chip is programmed to register these pulses as interrupts and to enable their detection by the 6502 central processor unit (CPU) chip. Another routine redirects the action taken by the CPU when its operations are interrupted to a polling routine (also written in Assembler code); this polling routine simply assigns a value to a memory location as described below.

The program then executes a continuous loop checking the contents of a memory location addressed by a variable (Flag%). An addressing method is used here since this is the most efficient way of assigning a variable which is passed between machine code and BASIC. The content of this variable is set when an interrupt occurs from the VIA. The value of the content of Flag% is given by the response of the polling routine to the pulse from the scan controller. The content code is defined by:

- 1 = 'Forward' pulse
- 2 = 'Reverse' pulse
- 3 = 'Overflow'

When the content of Flag% is set the interrupt which has caused the polling routine to be called is cleared in the hardware and the continuous loop escaped. The content code is tested against the user-defined scan direction; if these are inconsistent the loop is re-entered and the next interrupt awaited. If the content of Flag% is 3 then Flag% has not been cleared from the previous interrupt operation and hence the scan rate is too rapid for the computer. In this case an error is displayed to the user and the scan would be restarted with altered parameters.

The ADC is sampled and the value read scaled by a factor held in a global variable from the previous peaking program. If the direction condition is met the data point counter is monotonically incremented and the scaled ADC value stored in an array for post-processing. The screen co-ordinates of the data point are calculated and the point plotted on the screen. The content of Flag% is reset to zero and the number of collected data points checked for the end-of-scan condition. If this is not met control returns to the continuous loop in preparation for the next interrupt from the scan controller.

On satisfying the end-of-scan condition (*i.e.* 600 data points collected) the computer's reaction to user-defined interrupts is reset to the default operating system polling procedures. The spectral data are then smoothed and peak-searched with a

standard Savitsky-Golay algorithm [8]. From this point the two programs differ in operation and will be summarised separately.

2.3.3 (i) Ambient data analysis

The peak positions of the R_1 and R_2 fluorescence peaks are written to the screen. A schematic flow diagram is shown in Figure 2.4(i). The user is prompted for the date and time when the ambient spectrum was taken. A data file (on disk) is opened, the date, time and peak positions are written to it, and the file closed. The name of this data file is always the same; the old version is automatically deleted by being overwritten. The program ends returning control to the main-menu.

2.3.3 (ii) High pressure data analysis

Under pressure the fluorescence peaks not only shift, but may also deteriorate relative to their initial condition. If non-hydrostatic components develop, the shape of the peaks changes and they may even merge. Weak fluorescence output results in noisy spectra and, in bad cases, it is possible for the search algorithm to find more than two peaks in the high-pressure spectrum. The Savitsky-Golay algorithm operates first by smoothing the stored data with a 9-point running average. Following this the numerical first derivative in the data-set at each point is calculated and all possible peaks located. The second derivative spectrum is then calculated around these peak positions - information gained regarding the width of the peak can be used as criteria for 'noise' (a narrow weak signal) and this rejected. If the search has found more than two possible fluorescence signals these peaks are defined by vertical graticules drawn from the wavelength axis to their origin. The user is prompted to pick the two peaks which best represent the fluorescence maxima by entering the appropriate graticule numbers (counted from the left).

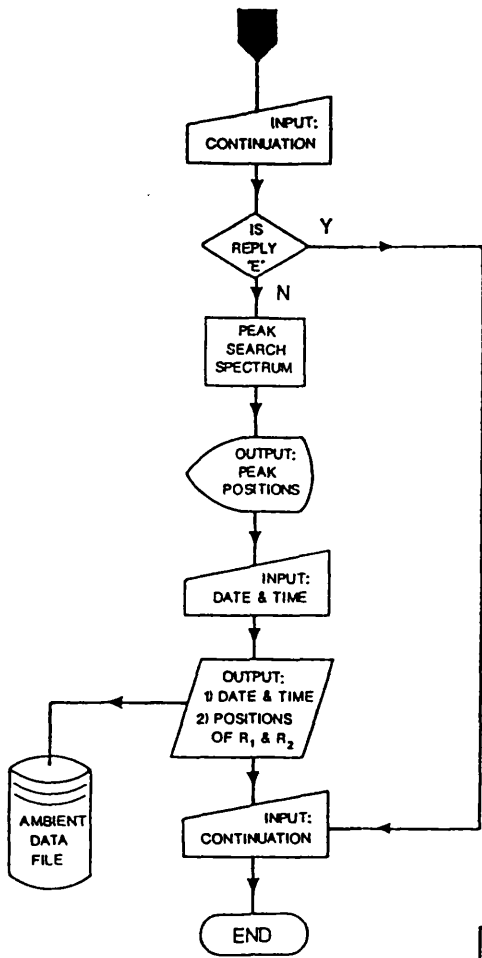
The pressure-shifted peak positions of R_1 and R_2 are written to the screen along with the R_1/R_2 peak separation calculated in wavenumbers. A peak separation of 29 ± 1 cm^{-1} implies the ruby inside the gasket is under hydrostatic conditions [6], if both peaks are well-defined and their separation deviates strongly from the ideal value the experiment should be repeated using a fresh sample loading. The flow diagram for this part of the program is shown in Figure 2.4(ii). The ambient data file is opened and the date, time and band positions of the last ambient spectrum are read in and displayed. The pressure (Equation 2.1) is calculated for each peak and displayed along with the averaged value. On pressing the space bar the program ends and control returns to the main-menu.

Figure 2.4

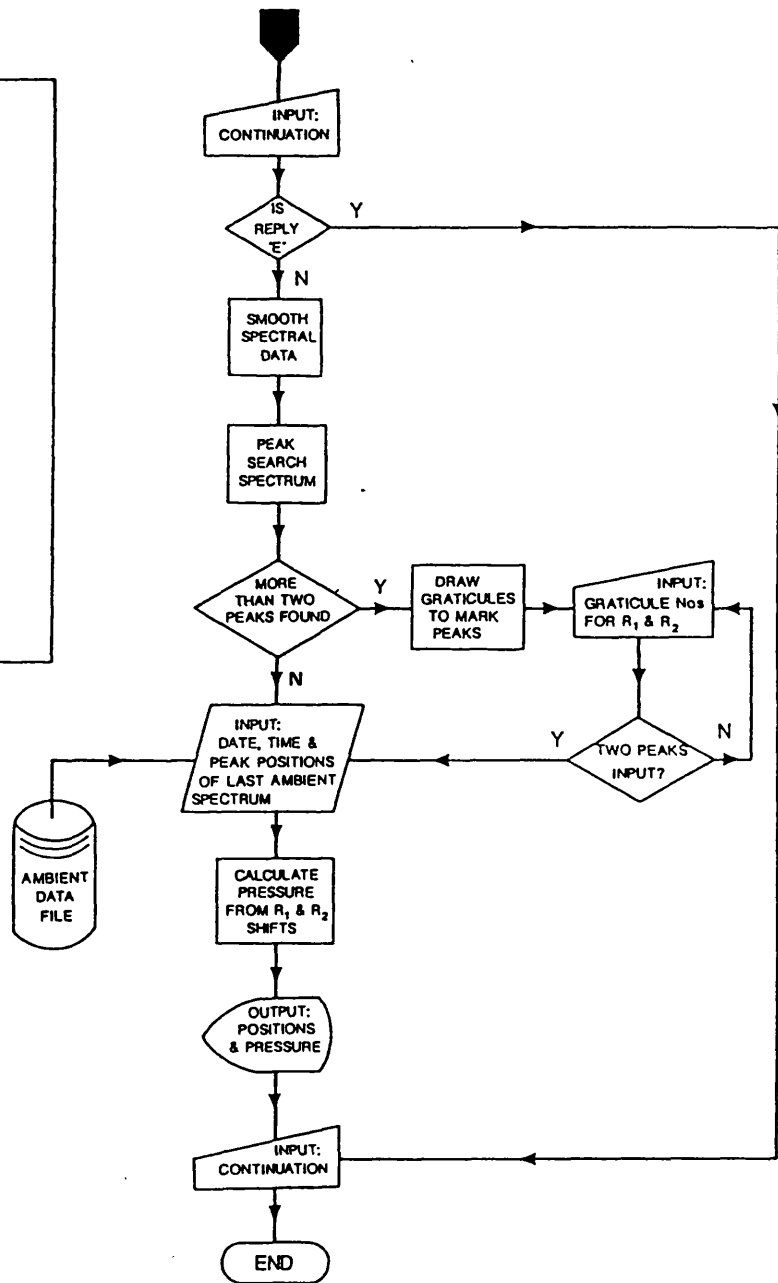
Flow diagrams of remaining software for

(i) ambient data

(ii) high-pressure data



(i)



(ii)

2.4 Development and Implementation

The spectroscopic system and software have been very successful for calibrating pressures within d.a.c.'s. However, the software could be applied to a number of similar problems which require sampling of an analogue signal at regular intervals. The system is best suited to spectroscopic tasks but is not limited to this type of experiment. A simple alteration of array dimensions (RAM permitting) would allow the collection of much larger spectra. All 32 kilobytes of RAM can be utilised in the BBC model B if a so-called shadow board is installed; this board provides memory mapping for the screen hence freeing a substantial amount of RAM space. The fluorescence spectrum of ruby is relatively simple to analyse for peak positions. The effects of pressure and noise on the spectra were taken into account (smoothing, calculation of second derivative spectrum) but the analysis algorithm could be extended by a user for more exacting sets of data. For instance, provision could be made for intensity calculation, background subtraction and interactive peak-picking. The physical interfacing of hardware is trivial, the only requirement of the software being a systematic pulse to the user port of the micro when a sampling of the ADC is required.

The software will run on any Acorn machine which is of a specification of the BBC model B or higher. The only alteration required would be the addressing parameters used for the operating system routines called by the various programs. Colour codes may also differ for those users with monochrome monitors. The software is publicly available and has been used at Daresbury Laboratory by several research groups involved in high-pressure work. The Physics department at Leicester University have mounted the programs on a BBC Master machine and use them in conjunction with their d.a.c. based research.

References

1. Sherman W.F. and Stadmuller A.A., 1987, "Experimental Techniques in High-Pressure Research", Wiley, Chichester
2. Jayaraman A., 1983, *Rev. Mod. Phys.*, **55**, 65-108
3. Jayaraman A., 1986, *Rev. Sci. Instrum.*, **57**, 1013-1031
4. Xu J.A., Mao H.K. and Bell P.M., 1986, *Science*, **232**, 1404-1406
5. Piermarini G.J., Block S., Barnett J.D. and Forman R.A., 1975, *J. Appl. Phys.*, **46**, 2774-2780
6. Adams D.M., Appleby R. and Sharma S.K., 1976, *J. Phys. E:Sci. Instru.*, **9**, 1140-1144
7. Bell P.M., Ji-an Xu and Mao H.K., 1986, "Shock Waves in Condensed Matter", Plenum Publishing Corporation, New York
8. Savitzky A. and Golay M.J.E., 1964, *Anal. Chem.*, **36**, No. 8
9. Bray A.C., Dickens A.C. and Holmes M.A., 1983, "The Advanced User Guide (for the BBC microcomputer)", Cambridge Microcomputer Centre

CHAPTER 3

ANALYSIS OF POWDER DIFFRACTION DATA

CHAPTER 3

Analysis of Powder Diffraction Data

Introduction

EDXRD is intrinsically a low resolution technique for measuring lattice parameters. Buschert [1] first used a triple axis spectrometer in 1965 for high-precision lattice constant comparisons with an accuracy of 1 part in 10^7 . Hart [2] discussed the advantages of using such pseudo-non-dispersive techniques and obtained an accuracy of 1 part in 10^7 when comparing the lattice parameters of two silicon wafers using a double crystal arrangement. By the 1980s new techniques had been developed giving accuracies which varied from a few parts in 10^8 to 1 part in 10^9 ; all these methods were reviewed by Hart [3] in a comprehensive survey in 1981.

Most high resolution techniques to date have required two or three detectors, one or two x-ray sources and two or three crystals. Further, many of these experimental arrangements required specially built equipment and commonly many man hours of specialist labour.

This chapter outlines some of the possible errors found in powder diffraction measurements with synchrotron radiation and details the principles involved in analysis of collected data. A description is also given of a computer program, VARVEC, written to automate the major parts of the analysis for any currently examined crystal system.

3.1 Theory of powder measurements

3.1.1 Principle of precision measurements

Angle dispersive powder diffraction analysis for lattice parameters is based on the original Bragg equation:

$$2d\sin\theta = n\lambda \quad (3.1)$$

where d is the distance between the planes reflecting the x-rays with wavelength λ at the diffracting angle θ . If all reflections are given general indices hkl then $n=1$. Differentiating equation 3.1 with respect to its three variables gives:

$$\frac{\delta d}{d} = \frac{\delta \lambda}{\lambda} - \cot \theta \delta \theta \quad (3.2)$$

which theoretically means the final accuracy in d should only be limited by the precision with which θ and λ are known. In practice λ is known to a very high degree of accuracy when using (the angle dispersive) station 9.1 of the SRS since a triple axis Si crystal is used as an incident beam monochromator. Extensive discussions of all possible errors have been published by Hart [2,3]. Corrections to these type of measurements usually include one for refraction which causes a shift of the Bragg peak position from that calculated in equation 3.1 to higher angles. Absorption causes the Bragg peak to be further displaced and distorted by dispersion, since it has a finite width, and added to this is further dispersion caused by the finite width of the x-ray line itself. In EDXRD the Bragg equation is rewritten in terms of energy:

$$Ed \sin \theta = hc/2 = 6.19926 \text{ (keV.Å)} \quad (3.3)$$

where h is Planck's constant and E measured in keV. The accuracy of absolute lattice spacing measurements is given in principle by the expression:

$$\frac{\delta d}{d} = -\frac{\delta E}{E} - \cot \theta \delta \theta \quad (3.4)$$

derived from partial differentiation of equation 3.3 with respect to its three variables. The final relative error $\delta E/E$ associated with the measurements of energy E of a reflection is made up again of two main contributory factors. The contribution from the linearity of the detector system was determined from the energy calibration as being ~ 5 in 10^4 . Calculation of the peak centroids in an EDXRD pattern leads to an inaccuracy of ~ 3 in 10^4 . The theoretical full width at half maximum (FWHM) of an EDXRD peak given by Buras *et al* (E_T) [4] is:

$$\Delta E_T = [(\Delta E_D)^2 + (\Delta E_G)^2]^{1/2} \quad (3.5)$$

where ΔE_D is the broadening due to the detector and ΔE_G that from geometric effects. Electronic noise, the energy required to create an electron-pair hole in the Ge crystal and the statistical nature with which a photon deposits energy within the crystal all contribute to detector effect. A detailed treatment of theory behind resolution of solid state detectors has been given by England [5]. By differentiating equation 3.3 (keeping d constant) we get:

$$\frac{\delta E}{E} = -\cot\theta\delta\theta$$

hence:

$$|\Delta E_G| = \cot\theta\delta\theta.E$$

which shows the geometric effect of broadening of the diffracted beam will be greater when θ is small. Equation 3.5 represents the FWHM fully if there are no other contributions, either from the asymmetric effects of geometric and physical aberrations [6] or broadening due to the sample [7]. The accuracy of the angular contribution to the expression in equation 3.4 is dependent on the extent to which the absolute value of the angle of diffraction is known. Using differential measurements the absolute values of d and E are not required. Hence, a standard (*e.g.* silicon) can be exposed to diffraction at several diffracting angles θ and the differences in the relative Bragg energies used to calculate the value of 2θ (*i.e.* the diffractometer circle setting).

3.1.2 Compressibility measurements

In Chapters 4 and 5 EDXRD was used to measure the change in d - spacings of poly-crystalline samples subjected to pressure. If the pressure P is established by some independent means, such as the ruby R-line technique, then the compressibility B_1 can be calculated. B_1 was given by Hazen and Finger [8] to be:

$$B_1 = -\frac{1}{d} \frac{(\Delta d)}{(\Delta P)} \quad (3.6)$$

If sufficient information is obtained from d -spacing measurements and the asymmetric unit is known, changes in volume can be established and hence, the volume compressibility B_v given by:

$$B_v = -\frac{1}{V} \frac{(\Delta V)}{(\Delta P)} \quad (3.7)$$

Equation 3.6 shows linear compressibility measurements are differential in type. They are concerned with the relative change in the lattice spacings of the sample with pressure from their values at zero pressure. In EDXRD the beam geometry is static and involves only the observation of changes in the positions of the reflections on the energy scale. The relevant equation is:

$$\frac{\Delta d}{d} = -\frac{\Delta E}{E} \quad (3.8)$$

from equation 3.4 which shows the scattering angle does not have to be known.

However, the measurement of volume compressibility and uni-axial compression for non-high symmetry problems demands knowledge of lattice constant variation with pressure. These lattice constants are calculated from absolute (indexed) d-spacings and thus, the absolute diffraction angle must be known. Chapters 4 and 5 show examples of both volume and uni-axial compressibility measurements.

3.2 VARVEC: Program for analysis of high-pressure Bragg data

3.2.1 Introduction

The analysis of information present in a set of EDXRD patterns taken from a sample subjected to varying pressure (or temperature) can be divided into five main parts:

- i) Detector calibration and calculation of diffraction angle θ
- ii) Measurement of peak centroids and conversion to lattice (d) spacings
- iii) Indexing of Bragg reflections
- iv) Calculation of lattice parameters
- v) Calculation of uni-axial and volume compressibilities

Both (i) and (ii) above have been described in Chapter 1. If the crystal structure of the sample is known (or at least the space group and lattice constants), a prediction of the expected EDXRD spectrum can be generated with a computer program (*e.g.* DRAGON [10] or EDPREDIC [11]). Peak-position matching between this and the observed spectrum allows indexing of peaks originating from diffraction by the sample. Any other peaks found in the pattern can usually be attributed to fluorescence from constituent elements or so-called escape peaks generated by the solid state detection system. These escape peaks are normally found to be 11.3 keV lower in energy than their parent (Bragg) signal with ~10% the intensity and arise from a photo electron effect in the Ge single crystal. Spectral deconvolution can often be attempted if these intensities overlap suspected reflections. Impure sample or multi-phase systems can also complicate a pattern. Very intense contributions to the spectra can arise if the gasket material used in a high-pressure device coincides with the incident x-ray beam. Careful use of slits, pin-holes and gasket size in the experiment usually serves to remove these features from the data.

The observed d_{hkl} can be used to generate lattice parameters. In simple crystal systems such as cubic this procedure is trivial but many of the data from lower symmetry Bravais lattices contain information relating to more than one lattice constant. For

instance, the value of a d_{hkl} ($h \neq 0, k \neq 0, l \neq 0$) reflection originating from orthorhombic lattice symmetry includes contributions from the three lattice parameters a, b and c . The solution to this dilemma is to fit a set of calculated d_{hkl} based on the known unit cell via a non-linear least squares method to the observed d_{hkl} using the lattice constants (*i.e.* $a, b, c, \alpha, \beta, \gamma$) as fitting parameters. A brief description of the non-linear least squares method is given below, followed by the application of this method to the powder-based problem outlined above. The program VARVEC encompasses sections (iv) and (v) of the data analysis and also includes calculation of estimated standard deviations (e.s.d.s) on all solutions, error checking and re-calculation of ideal observed values to help with future input data selection.

3.2.2 Non-linear least squares method

We define a function to be minimised as Δ :

$$\Delta = f_{\text{obs}} - f_{\text{calc}} \quad (3.9)$$

As f_{calc} approaches f_{obs} then: $\sum_i \Delta_i^2 \rightarrow \text{minimum}$

where the summation is over all i observations. If f_{calc} is expressed as a function of j parameters, u , then

$$f_{\text{calc}} = f(u_1, u_2, u_3, \dots, u_j)$$

and Δ will be minimised when

$$\frac{\partial (\sum \Delta^2)}{\partial u_i} = 0 \quad (3.10)$$

Differentiating equation 3.10 gives

$$\sum_i \omega_i \Delta_i \frac{\partial \Delta_i}{\partial u_j} = 0$$

where ω is a weight applied to observation i . The partial derivatives of Δ may not be linear, the Taylor series is therefore used to expand this expression to give:

$$\sum_i \sum_j (\frac{\partial \Delta_i}{\partial u_j} \frac{\partial \Delta_i}{\partial u_j} \omega_i) \epsilon_j = \sum_i \Delta_i \frac{\partial \Delta_i}{\partial u_j} \omega_i \quad (3.11)$$

where ϵ_j represents the error in parameter j and ω_i is the weight corresponding to observation i . Equation 3.11 can be expressed more simply in matrix form:

$$A \cdot \epsilon = B \quad (3.12)$$

the solution of equation 3.12 yields the error vector ϵ . The set of fitting parameters is added to this vector and the process repeated. This repetition represents an iterative cycle which will continue until the function Δ is deemed minimised. This decision is based on the ratio (over the last two cycles at any point in the iteration) of the so-called G (goodness-of-fit) factor calculated for both the penultimate and final cycle. This G factor is characterised by:

$$G = 100\% \times \left[\frac{\sum \omega \cdot \Delta^2}{m-n} \right]^{1/2} \quad (3.13)$$

with m equal to the number of data available and ω is the weight applied to each piece of data. A value is decided for the G factor ratio below which the function is considered minimised and iteration ceases. The initial parameter set has been successively updated in each cycle and now represent the best fit set which successfully minimised the function Δ .

3.2.3 Application of the Least Squares method to powder data

Application of the above theory to the variation of lattice constants with pressure is commonly only successful if the Bravais lattice type is known. D-spacings are generated from lattice parameters via the general expression used to represent inter-planar distances for any crystal system:

$$d^{*2}(hkl) = h^2a^{*2} + k^2b^{*2} + l^2c^{*2} + 2klb^*c^*\cos\alpha^* + 2lhc^*a^*\cos\beta^* + 2hka^*b^*\cos\gamma^* \quad (3.14)$$

(*indicates reciprocal space)

and the minimum function Δ is expressed as:

$$\Delta = d^{*2}(\text{obs}) - d^{*2}(\text{calc}) \quad (3.15)$$

An initial set of parameters (starting values) for the lattice constants is required. If the lattice had orthogonal vectors (tetragonal or orthorhombic symmetry) it was found that this starting set can be random and refinement was still successful within a small number of iterations. The partial derivatives shown in equation 3.11 are calculated by differentiation of equation 3.14 with respect to each variable (*i.e.* parameter to be minimised). These partials are calculated and summed over all observations as expressed by equation 3.11 to give the $n \times n$ square matrix (A) in equation 3.12. The resulting matrix equation is solved and the error vector calculated. The initial parameters are updated and iterations continue until the G-factor ratio between two cycles falls below 10^{-6} .

3.2.4 Description of algorithms

The program requires an input file of indexed d-spacings produced from a sample which has undergone diffraction at various pressures (Figure 3.1). Also required is a set of initial lattice constants, the Bravais lattice type and greatest number of reflections recorded at any pressure.

The starting values given for the lattice variables are reformed into suitable fitting parameters depending on the crystal system chosen. This simplifies the algebra involved in partial differentiation (and hence the final algorithms), reduces the total number of calculations and increases the speed and efficiency of solution. Each data set (or data record) represents indexed d-spacings measured at one pressure. Due to preferred orientation, fluorescence and/or sample deterioration under pressure it is possible that some reflections were not measurable at certain pressures. Any piece of data which previously could be measured but at higher pressure can not is expressed by a zero-value in that column of the data file. The input routine sorts and compresses the data before each pressure record is used in calculation.

For each d-spacing in a pressure record the minimum function Δ (equations 3.15 and 3.14), partial derivatives and weighting factor are calculated. The weighting scheme used here was proportional to d^2 ; the solid state detector resolution was maximum at low energies and convolution of peaks at high energy (*i.e.* low d) complicated peak centroid measurement.

The set of linear equations used to invert the matrix A are solved by the Gauss-Jordan (elimination) method. Iteration continues until the value of G-factor ratioed against its previous value falls below 10^{-6} . The original parameter conversion is reversed and the best-fit set of variables is reformed to a set of real lattice constants. The volume of the unit cell is calculated. The standard deviations of these solutions are estimated from the diagonal elements of the inverted matrix produced in the final iterative cycle. Combination of the e.s.d.s from the lattice constants gives a measure of deviation which can be ascribed to the cell volume. The best-fit cell constants are used to calculate a set of d-spacings matching the original observed set for that pressure. Hence, the user can compare these lists for possible errors in the input file generated when indexing the Bragg data or mis-interpretation of the original pattern. Finally, a reliability factor for the refinement is calculated based on the well-known crystallographic weighted R-factor [12].

Figure 3.1

Typical input file to VARVEC

note:

- i) Title record
- ii) Miller indices record
- iii) Pressure records - format: P, d_{hkl} , d_{hkl} , ...

KNO3 PHASE IV

0 1 1 2 0 0 0 0 2 2 0 1 2 1 0 0 2 0 1 1 2

| | | | | | | | |
|------|--------|--------|--------|--------|--------|--------|--------|
| 0.83 | 4.2971 | 3.7434 | 3.3814 | 3.2751 | 3.1060 | 2.7824 | 2.6959 |
| 1.6 | 4.2216 | 3.6999 | 3.3495 | 3.2410 | 3.0633 | 2.7590 | 2.6713 |
| 2.0 | 4.1918 | 3.6698 | 3.3292 | 3.2127 | 3.0373 | 2.7362 | 2.6532 |
| 2.58 | 0.0000 | 3.6588 | 0.0000 | 3.1911 | 3.0286 | 2.7244 | 2.6499 |
| 3.0 | 0.0000 | 3.6544 | 3.3212 | 3.1857 | 3.0210 | 2.7205 | 2.6485 |
| 4.58 | 0.0000 | 3.6251 | 0.0000 | 0.0000 | 2.9882 | 2.7031 | 2.6332 |
| 5.1 | 0.0000 | 3.5981 | 0.0000 | 0.0000 | 2.9702 | 2.6751 | 2.6183 |
| 7.36 | 0.0000 | 3.5683 | 0.0000 | 0.0000 | 2.9300 | 2.6479 | 2.5971 |
| 9.3 | 0.0000 | 3.4708 | 3.2257 | 0.0000 | 0.0000 | 2.6170 | 2.5603 |

3.2.5 Program implementation

The program VARVEC was written in FORTRAN-77 and consists of a main module of approximately 100 statements and 21 subroutines. Input of the initial set of lattice constants, data-file name and Bravais code are managed by a main-menu which also serves to control the execution of calculations. The main module is responsible for input/output management, control of flow to the main-menu, calls to the subroutine responsible for a certain Bravais lattice type and the sorting and initial processing of observed data from the input data file. The program also allows all main-menu options to be saved for future processing of data from the same sample. All output files from the program have the same name as the original input file but with different filename extensions. A typical output file (extension ``.OUT``) from the program is shown in Figure 3.2. Another output file bearing a ``.GRF`` extension is produced as input to several graphics packages to plot the solutions.

Some of the 21 subroutines perform specific functions which can be summarised as follows:

| | |
|--------|--|
| CALCON | Calculation of weighting factor, goodness-of-fit and R-factor. |
| CHARCK | Check input for possible internal conversion errors. |
| CHECK | Check initial lattice parameters with respect to specified lattice type. |
| DCALC | Calculation of d-spacings corresponding to indexed observables. |
| ERROR | Output of (any) errors found by CHECK |
| HELP | Output of information concerning program usage and definition of crystal system codes employed. |
| INTSUM | Initialisation of variables to be summed |
| LOTOUP | Lower to uppercase conversion |
| MENOUT | Dump menu options to file for possible later recall. |
| MENU | Main-menu routine which handles all input. HELP option and initiates processing of data. |
| OUTPUT | Writes all output to specified files. Output consists of refined lattice parameters, cell volume, standard deviations, R & G factors, final iteration matrix equation and indexed obs/calc d-spacings for each pressure observed. Creates file for graphics post-processing. |
| SETMAT | Creates sets of linear equations. |
| SOLVE | Inverts derivative matrix and solves linear equations. |

Figure 3.2

Typical page of output file from VARVEC

note:

- i) Observed data printed out
- ii) Matrix equation and final inverted matrix printed
- iii) Table of d_{obs}/d_{calc}

KNO3 HIGH PRESSURE DATA

Pressure = 1.60 GPa Number of obs. = 7 R = 3.69% G = 0.0290

Obs. hkl: 0 1 1 2 0 0 0 0 2 2 0 1 2 1 0 0 2 0 1 1 2
 Obs. d: 4.2216 3.6999 3.3495 3.2410 3.0633 2.7590 2.6713

| | | | |
|--------|-------|---------------|------------------------|
| Param. | Value | Standard Dev. | Cell vol. = 273.081 |
| ----- | ----- | ----- | s.d. vol. = 9.2961E-01 |
| a | 7.391 | 1.5673E-02 | |
| b | 5.513 | 9.6358E-03 | |
| c | 6.701 | 1.3465E-02 | |

Minimised matrix equation:

| | | | | |
|----------|-------|----------|----------------|----------------|
| (14.859 | 1.680 | 2.732) | (-1.163E-19) | (-5.794E-19) |
| (| | | (| (|
| (1.680 | 6.737 | 1.734) | (3.487E-19) | (2.511E-18) |
| (| | | (| (|
| (2.732 | 1.734 | 11.312) | (2.058E-19) | (2.616E-18) |

Number of iterations performed in refinement = 7

Inverted matrix derived from final Iteration:

| | | | |
|-------------|------------|--------------|--------------------------|
| (7.167E-02 | -1.397E-02 | -1.516E-02) | Element(1,1) = 7.167E-02 |
| (| | |) |
| (-1.397E-02 | 1.573E-01 | -2.074E-02) | Element(2,2) = 1.573E-01 |
| (| | |) |
| (-1.516E-02 | -2.074E-02 | 9.524E-02) | Element(3,3) = 9.524E-02 |

Data correlation

| h k l | Observed | Calculated |
|-------|----------|------------|
| 0 1 1 | 4.2216 | 4.2576 |
| 2 0 0 | 3.6999 | 3.6956 |
| 0 0 2 | 3.3495 | 3.3506 |
| 2 0 1 | 3.2410 | 3.2361 |
| 2 1 0 | 3.0633 | 3.0698 |
| 0 2 0 | 2.7590 | 2.7567 |
| 1 1 2 | 2.6713 | 2.6700 |

MONO, ORTHO, RHOMB, TETRA & HEXA:

Creation of fitting parameters and calculation of minimum function, partial derivatives and standard deviations of refined parameters and cell volume for specified crystal system.

VARVEC was originally written to cope with the specific reduction of high-pressure EDXRD data. Other programs have since become available (*e.g.* in the powder diffraction program library, Daresbury Laboratory) which have similar functions. Chapter 6 details a situation in which VARVEC, prediction and indexing programs, and other cell refinement codes are used together to obtain maximum information from angle-dispersive powder data.

References

1. Buschert R.C., 1965, *Bull. Am. Phys. Soc.*, **10**, 125-133
2. Hart M., 1969, *Proc. Roy. Soc.*, **309**, 281-296
3. Hart M. 1981, *Journal of Crystal Growth*, **55**, 409-427
4. Buras B., Niimura N. and Staun Olsen J., 1978, *J. Appl. Cryst.*, **11**, 137-140
5. England J.B., 1974, "Techniques in Nuclear Structure Physics". Part 1, Macmillan
6. Wilson A.J.C., 1973, *J. Appl. Cryst.*, **6**, 230-237
7. Gerward L., Moldrup S. and Topsoe H., 1976, *J. of Appl. Phys.*, **47**, 822-825
8. Hazen and Finger, 1982, "Comparative Crystal Chemistry". John Wiley and Sons
9. Murray A., 1987, *Powder Diffraction Program Library*, Daresbury Laboratory
10. Heath A.E. and Russell D.R., 1986, *EDPREDIC: Program for simulation of powder EDXRD peak positions*, University of Leicester.
11. "International Tables of Crystallography". Vol. II
12. Lipson H. and Steeple H., 1968. "Interpretation of X-ray Powder Diffraction Patterns", Macmillan

CHAPTER 4

HIGH PRESSURE X-RAY DIFFRACTION MEASUREMENTS ON POTASSIUM NITRATE (KNO₃)

CHAPTER 4

High Pressure X-ray Diffraction Measurements on Potassium Nitrate (KNO₃)

4.1 Introduction

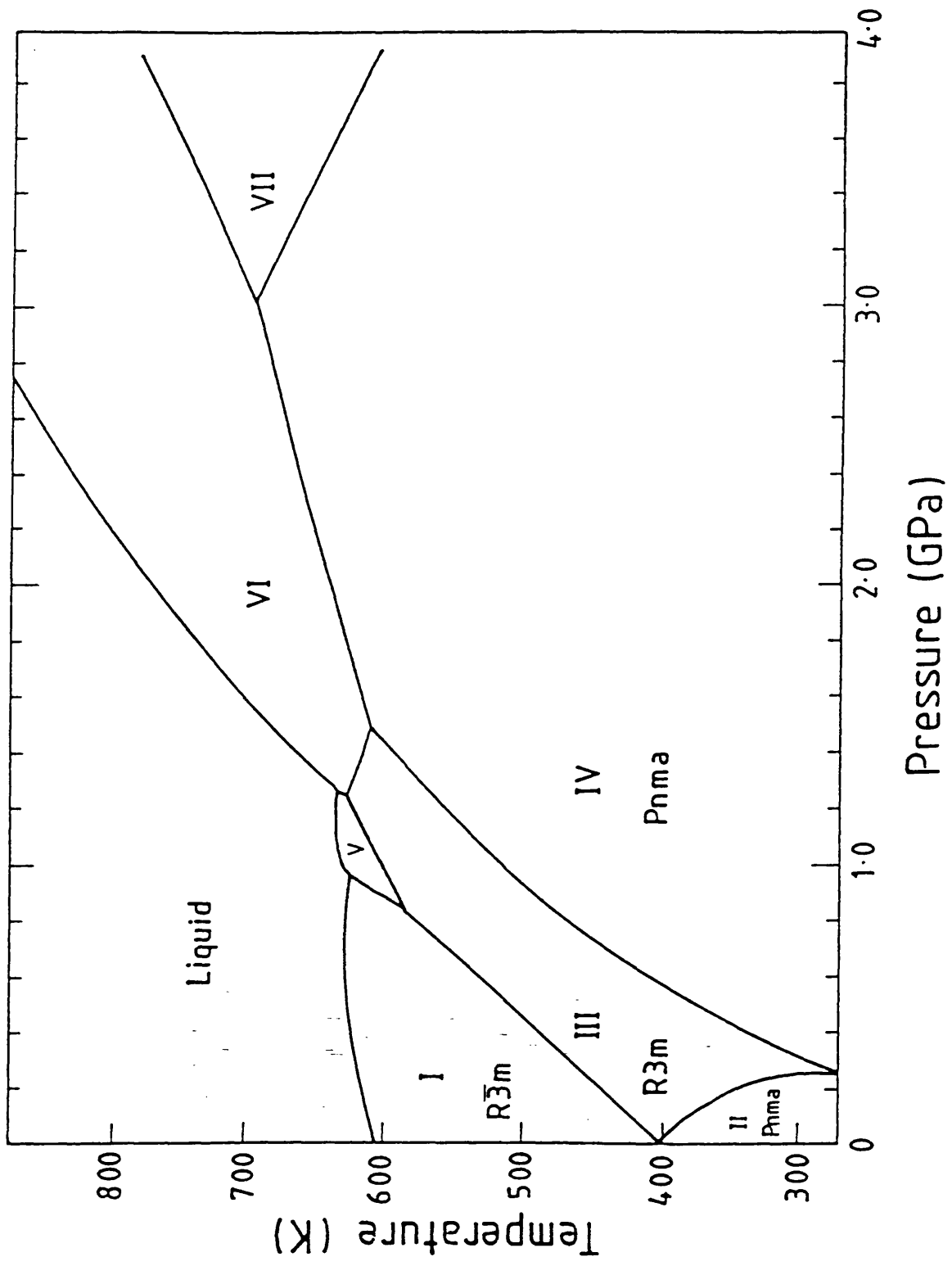
Potassium nitrate displays complex polymorphism with many reversible phase transitions as a function of both temperature and pressure. Three solid phases are accessible by temperature variation alone at ambient pressure (see Figure 4.1) with phase I occurring at temperatures in excess of approx. 400 K. This phase is rhombohedral with a calcite (CaCO₃) type structure [1]. Phase III has only limited temperature stability at ambient pressure (although rapidly increasing temperature stability with increasing pressure) and is rhombohedral and ferroelectric [1,2]. Phase II, which occurs under ambient conditions, is an antiferroelectric material with orthorhombic symmetry $Pnma$, $Z = 4$ [3,4].

Increase of pressure beyond the II-III-IV triple point at 0.3 GPa, 294.3 K yields KNO₃ IV. Since discovery of this phase by Bridgman [5] a number of attempts have been made to solve its structure. Early x-ray-based experiments were unsuccessful. Jamieson studied KNO₃ IV using powder diffraction and proposed a rhombohedral cell with $Z = 18$ [6]. The material was re-examined by Davis and Adams [7] who proposed an orthorhombic space group ($Pmn2_1$) with $Z = 10$. In view of these uncertainties Weir *et al* [8] used single crystals grown under pressure from aqueous solution. They concluded that the crystal was orthorhombic with a tetramolecular cell and $a = 5.58$, $b = 7.52$ and $c = 6.58$ Å. Systematic absences were consistent with space groups $P2_1nb$ or $Pmnb$. In addition, further phases found only at high temperatures and pressures have been reported on the basis of differential thermal analysis to 4.0 GPa [9]. No structural information concerning these phases exists. In this chapter EDXRD measurements (using synchrotron radiation) have been used for accurately determining the lattice parameters of KNO₃ IV as a function of pressure. This exercise has also extended the search for further phases to higher pressures.

During the study a Rietveld refinement of KNO₃ IV at 0.36 GPa using time-of-flight neutron powder diffraction was published by Worlton *et al* [10]. This structure was reported as orthorhombic $Pnma$ with $a = 7.4867$, $b = 5.5648$ and $c = 6.762$ Å and $Z = 4$, the atomic co-ordinates were different from those found in phase II. Worlton *et al*'s study therefore confirmed the unit cell of Weir *et al* [8].

Figure 4.1

The phase diagram of KNO_3
(Pistorius, 1976)



4.2 Experimental

The finely powdered material was placed in an inconel gasket with a hole initially of 200 μm diameter, centered in a d.a.c.. A 4:1 mixture of methanol:ethanol was used as the pressure transmitting medium, thus ensuring hydrostaticity. Pressure was determined by the ruby R-line method, measured using back-scattering from an Ar^+ ion laser (see Chapter 2). Diffraction from the gasket was avoided by reducing the incident beam cross section to approx. 40 μm^2 using tantalum slits. The diffraction angle used in all patterns 10.04° (2 θ).

A large distance between the detector and the sample together with fine detector slits ensured the highest possible resolution and signal/background ratio. A pure germanium solid state detector with an energy resolution of 165 eV (FWHM) at 5.9 keV was used. Exposure times were typically 1000 seconds. Diffraction patterns were obtained as a function of increasing pressure.

4.3 Data analysis and results

Figures 4.2, 4.3 and 4.4 show examples of EDXRD spectra recorded as a function of pressure. For each indexed (hkl) diffraction peak the interplanar spacing d_{hkl} can be calculated from the Bragg equation, written in terms of the corresponding photon energy E_{hkl} :

$$E_{hkl}d_{hkl}\sin\theta = hc/2 = 6.199 \text{ keV}\cdot\text{\AA} \quad (4.1)$$

The peak positions (E_{hkl}) were accurately determined by fitting Gaussians to the observable peaks using the GENIE data analysis package [11]. The observed peaks were shown to have excellent Gaussian symmetry. The calculated values for d_{hkl} were fitted via a non-linear least squares method to the observed d_{hkl} (obtained from equation 4.1) based on an orthorhombic unit cell using the locally written computer program VARVEC (see Chapter 3.2). The lattice vectors a , b and c as fitting parameters. The function to be minimised, Δ , was defined thus:

$$\Delta = d_{\text{obs}}^*2 - d_{\text{calc}}^*2 = d_{\text{obs}}^*2 - h^2a^*2 - k^2b^*2 - l^2c^*2 \quad (4.2)$$

(*indicates reciprocal space)

Excellent agreement was obtained, as illustrated by the 2.0 GPa data, Table 4.1.

Figure 4.2

EDXRD indexed pattern of
 KNO_3 II at ambient pressure.
(e = escape peak of detector).

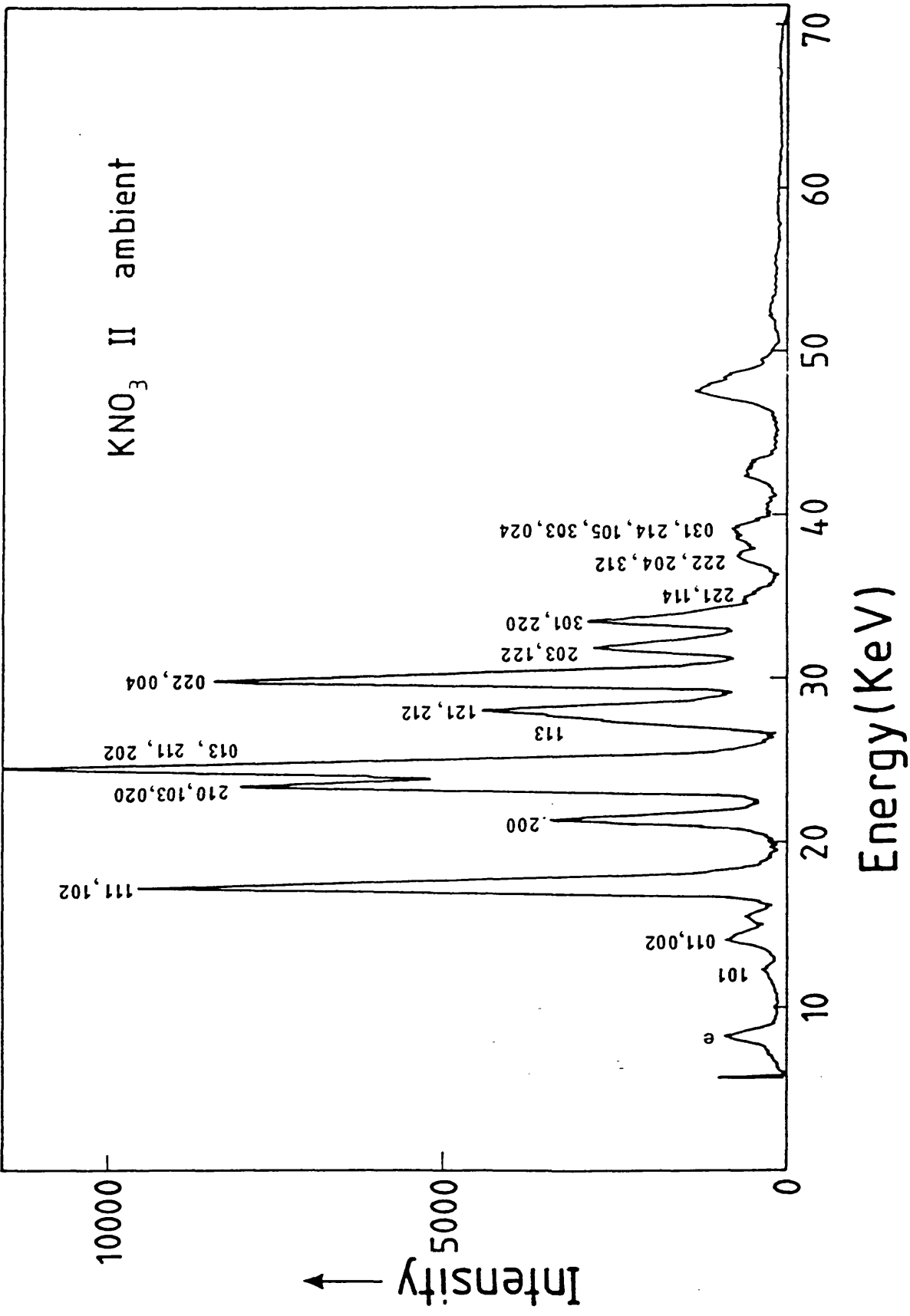


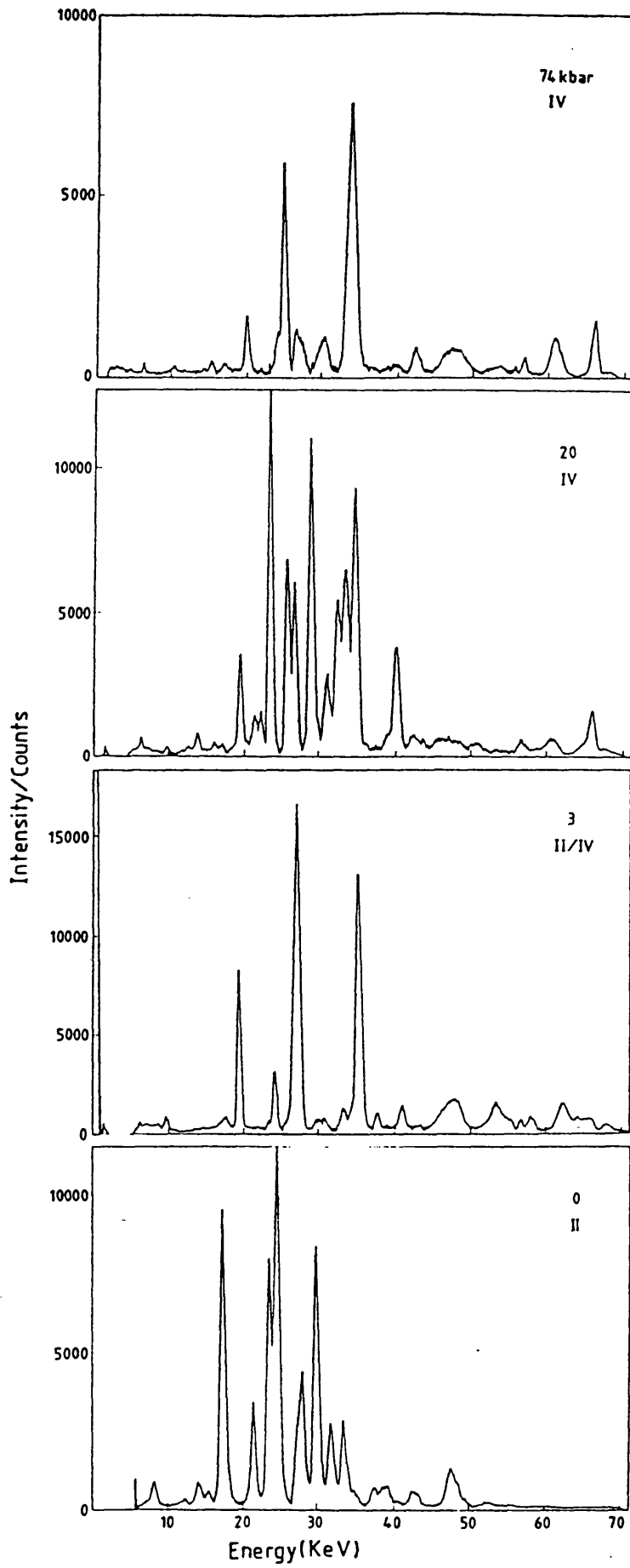
Figure 4.3

EDXRD indexed spectrum of
KNO₃ IV at 2.0 GPa
(e = escape peak of detector).

Figure 4.4

The EDXRD patterns of KNO_3 at various pressures (GPa).

KNO_3 II/IV



The refined unit cell vectors are given in Table 4.2 and their pressure dependencies in Figure 4.5. The goodness of fit is characterised by a factor G, defined as:

$$G(\%) = 100\% \times \left(\frac{\sum \omega \Delta^2}{m-n} \right)^{1/2}$$

where ω is the weight for d_{hkl} , m the number of observed reflections at a given pressure P , and n the number of fitting parameters (*i.e.* three). The weighting scheme used was $\omega \propto d_{hkl}^2$.

The linear axial compressions (Figure 4.5) are anisotropic with gradients corresponding to:

$$a: -5.6 \times 10^{-2} \text{ \AA.GPa}^{-1} \quad b: -3.6 \times 10^{-2} \text{ \AA.GPa}^{-1} \quad c: -2.8 \times 10^{-2} \text{ \AA.GPa}^{-1}$$

The axial compression ratios are therefore, $a:b:c = 1.00:0.64:0.50$. The variation of the unit cell volume with pressure, $\partial V/\partial P$, gives a linear compressibility of $-1.69 \times 10^{-2} \text{ GPa}^{-1}$, as shown in Figure 4.5. This is in good agreement with the macroscopic compressibility measured by Bridgman [5] of $-1.76 \times 10^{-2} \text{ GPa}^{-1}$ (Walrafen *et al* 1982) [12].

4.4 Discussion

4.4.1 X-ray results

Potassium nitrate is an excellent example of a material which displays complex structural polymorphism but which cannot be studied by high-pressure single-crystal diffraction unless, as in Weir's work, the high-pressure phase can be prepared directly. The II/IV phase transition at 0.29 GPa is strongly first-order, with a volume decrease of 11.5%, which always causes single crystals to shatter. A similar decrease (15.54%) occurs at the thermally induced III/IV transition [13].

Little change occurs in b at the II/IV transition but major movements take place in the (ac) planes which result in considerable relative changes in a and c , see Figures 4.6(i) and 4.6(ii). Viewed down a , in phase II the NO_3^- ions are almost overlaid, although with staggered N-O bonds. They are displaced substantially from each other along c on entering phase IV, and are rotated about axes through nitrogen and parallel to b . These rotations result in columns of NO_3^- 's all tilted up (or down) in the same sense. Concurrently, the K^+ ions move along a with two consequences: (1) the coordination number of K^+ is increased from 9 (2.82 to 2.92 Å) to 11 (2.79 to 3.06 Å); (2) the alternating layers of K^+ and NO_3^- in phase II are replaced by mixed K^+ , NO_3^- layers.

**Table 4.1 Observed and calculated d-spacings for
KNO₃ at 2.0 GPa.**

| d(obs) Å | I(obs) % | d(calc) Å | h k l |
|-------------|-------------|--------------|-------|
| 3.6698 | 25.80 | 3.6655 | 2 0 0 |
| 3.3292 | 12.90 | 3.3280 | 0 0 2 |
| 3.2127 | 9.70 | 3.2108 | 2 0 1 |
| 3.0372 | 100.00 | 3.0437 | 2 1 0 |
| 2.7362 | 51.60 | 2.7310 | 0 2 0 |
| 2.6532 | 46.80 | 2.6498 | 1 1 2 |
| 2.4577 | 83.90 | 2.4640 | 2 0 2 |
| 2.2883 | 16.1 | 2.2939 | 3 0 1 |
| 2.1887 | 35.50 | 2.1900 | 2 2 0 |
| 2.1293 | 48.40 | 2.1235 | 1 0 3 |
| 1.8230 | 3.90 | 1.8294 | 2 2 2 |
| 1.7763 | 29.00 | 1.7561 | 0 3 1 |
| 1.6825 | 3.20 | 1.6812 | 4 1 1 |

**Table 4.2 Variation with pressure of the lattice parameters of KNO₃ IV
and unit cell volume***

| P(GPa) | a(Å) | b(Å) | c(Å) | V(Å ³) | G(%) |
|--------|-----------|-----------|-----------|--------------------|------|
| 0.35 | 7.487(3) | 5.565(2) | 6.763(3) | 281.75(30) | 0.12 |
| 1.60 | 7.395(18) | 5.507(15) | 6.696(18) | 272.70(1.2) | 0.21 |
| 2.00 | 7.331(18) | 5.462(14) | 6.656(17) | 266.50(1.2) | 0.21 |
| 2.58 | 7.295(15) | 5.449(12) | 6.662(24) | 264.80(1.3) | 0.17 |
| 3.00 | 7.282(16) | 5.441(13) | 6.650(16) | 263.50(1.0) | 0.18 |
| 4.58 | 7.219(38) | 5.400(27) | 6.639(54) | 258.85(2.8) | 0.38 |
| 5.10 | 7.175(26) | 5.346(18) | 6.613(38) | 253.69(1.9) | 0.26 |
| 7.36 | 7.097(49) | 5.288(35) | 6.571(71) | 246.60(3.5) | 0.51 |
| 9.30 | 6.944(18) | 5.236(11) | 6.461(13) | 234.94 (90) | 0.16 |

(The goodness of fit G for each data-set is also shown)
*estimated standard deviations are shown in parentheses

Figure 4.5

Variation with pressure of
unit cell parameters and volume ratio
(V_0 is the initial value for phase IV)
for KNO_3 IV.

Note:

Solid lines are extrapolated back to zero pressure:
this is *not* meant to represent the
compressibility in phase II.

KNO₃ (IV)

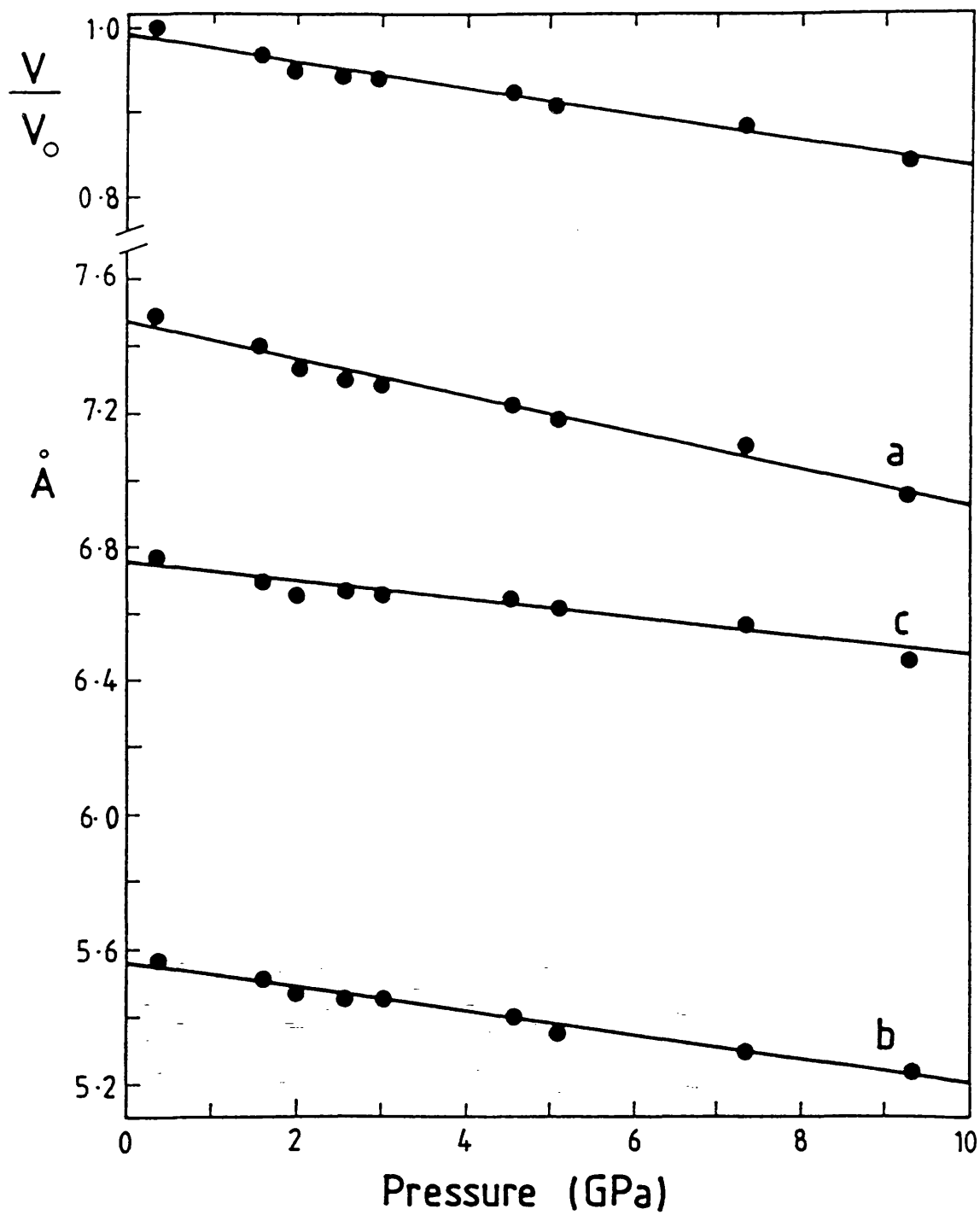
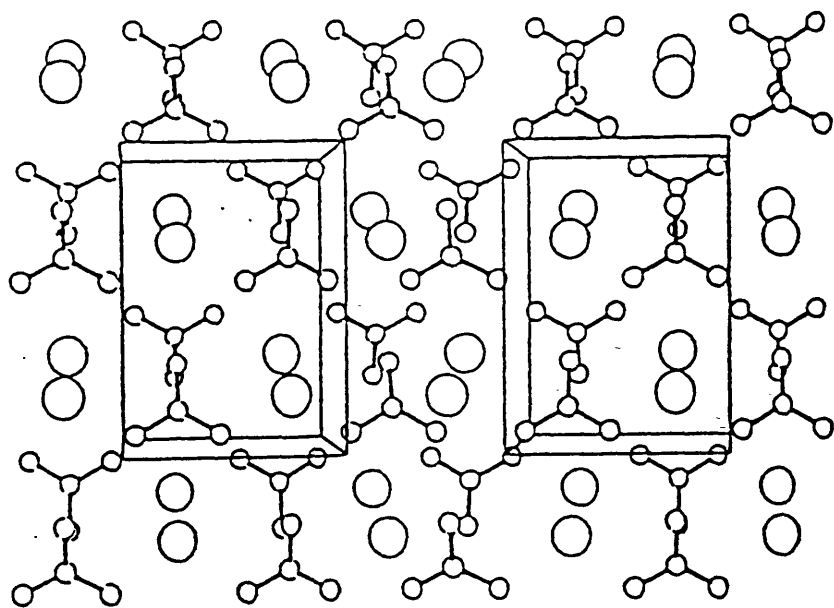
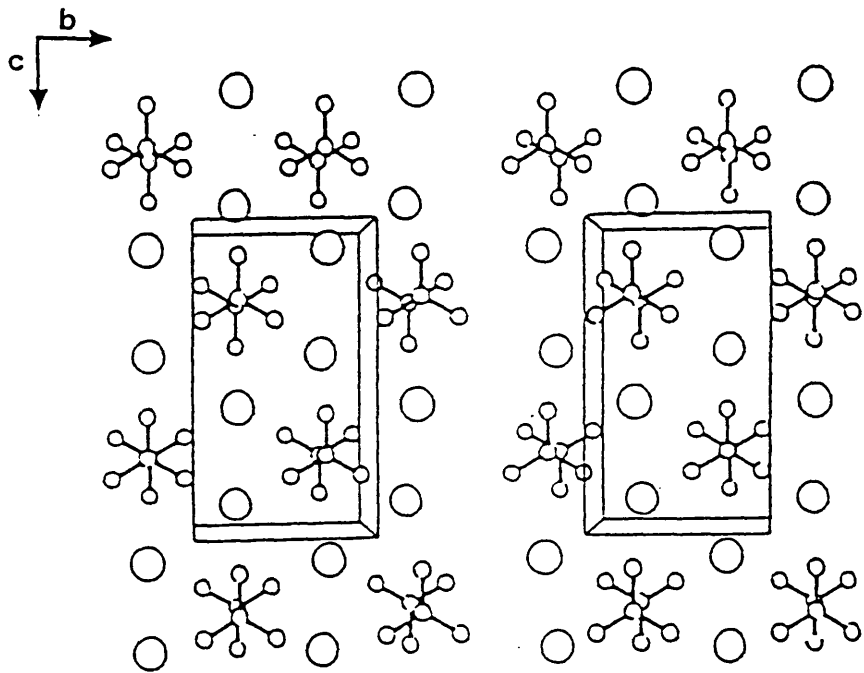


Figure 4.6

(i) Stereoscopic projection
down a for KNO_3 II.

(ii) Stereoscopic projection
down a for KNO_3 IV



Comparison of the unit cell parameters suggests that the equivalences are:

| | II(ambient) | IV(0.29 GPa) | Change/Å |
|----------|-------------|--------------|----------|
| <i>a</i> | 6.4213 | 6.763 | +0.34 |
| <i>b</i> | 5.4119 | 5.565 | +0.15 |
| <i>c</i> | 9.1567 | 7.487 | -1.67 |

where *b* has been kept in common (as it is perpendicular to the (*ac*) mirror plane) and *a* and *c* have been interchanged on moving from phase II to phase IV in order to give the least change in each case.

4.4.2 Raman spectra

In the absence of definitive diffraction-based information a variety of other techniques has been used to search for, and characterise, high-pressure polymorphs. Of these, Raman spectroscopy has been one of the most important. The Raman spectrum of KNO₃ at high pressures has been studied by a number of groups (Fong and Nicol 1971 [14], Buckelmann *et al* 1976 [15], Iqbal *et al* 1977 [4], Medina 1981 [16] and Adams and Sharma 1981 [17]), showing that those of KNO₃ II and IV are so different from each other as to suggest an origin in different space groups. Indeed, Medina concluded that '...it is obvious that phase IV cannot have the same space group as phase II: the spectra are different in both the external mode region and the internal mode region'. The resolution of this dilemma lies in recognising that the packing within the two phases is quite different, despite the common site and factor groups.

Factor group analysis (f.g.a.) for the tetramolecular *Pnma* ($\cong D_{2h}^{16}$) cells of phases II and IV yields the results of Table 4.3. This requires eighteen Raman-active lattice modes. The spectra of KNO₃ II show five bands in this region, and KNO₃ IV has six, although band shape analysis suggests two further (unresolved) contributions.

The spectrum of KNO₃ II has been accounted for by Ismail *et al* [18] who noted that the crystal structure is only very slightly distorted from that of *P3m*₁ (D_{3d}). Selection rules for this structure are also given in Table 4.3. These selection rules allow five Raman-active lattice modes, exactly as is observed. In contrast, the lattice mode spectrum of phase IV is in better agreement with the D_{2h} selection rules. Moreover, in the ν_3 (E' of the D_{3h} ion) $\nu(\text{NO}_3)_a$ region appearance of four bands (1441, 1396, 1387 and 1370 cm^{-1} at 2.6 GPa, [17]) is in precise agreement with the f.g.a. requirements. Phase II also shows four bands (1446, 1385, 1361 and 1345 cm^{-1}) but the two higher ones are very weak. Thus, the intensities are most readily understood on the basis of the D_{3d} -like model.

Table 4.3 Factor group analysis and correlations of KNO_3

A: F.g.a.

| D_{2h}^{16} | N_T^* | T_A | T | R | $\Gamma(\text{vib})$ | Activity |
|---------------|---------|-------|---|---|----------------------|----------|
| A_g | 9 | | 4 | 1 | 4 | Raman |
| B_{1g} | 6 | | 2 | 2 | 2 | Raman |
| B_{2g} | 9 | | 4 | 1 | 4 | Raman |
| B_{3g} | 6 | | 2 | 2 | 2 | Raman |
| A_u | 6 | | 2 | 2 | 2 | Inactive |
| B_{1u} | 9 | 1 | 3 | 1 | 4 | I.r. |
| B_{2u} | 6 | 1 | 1 | 2 | 2 | I.r. |
| B_{3u} | 9 | 1 | 3 | 1 | 4 | I.r. |

| D_{3d}^3 | N_T | T_A | T | R | $\Gamma(\text{vib})$ | Activity |
|------------|-------|-------|---|---|----------------------|----------|
| A_{1g} | 4 | | 2 | 0 | 2 | Raman |
| A_{2g} | 1 | | 0 | 1 | 0 | Inactive |
| E_g | 5 | | 2 | 1 | 2 | Raman |
| A_{1u} | 1 | | 0 | 1 | 0 | Inactive |
| A_{2u} | 4 | 1 | 1 | 0 | 2 | I.r. |
| E_u | 5 | 1 | 1 | 1 | 2 | I.r. |

B: Correlations

| Crystal ^α D_{2h}^{16} | $\xleftarrow{x_4}$ | Site $C_s(xz)$ | Ion D_{3h} | Site $\xrightarrow{x_2}$ | Crystal D_{3d}^3 |
|--|--------------------|-------------------|-----------------|--------------------------|-----------------------|
| $A_g + B_{2g} + B_{1u} + B_{3u}$ | | A' | ν_1, A_1' | A_1 | $A_{1g} + A_{2u}$ |
| $A_g + B_{2g} + B_{1u} + B_{3u}$ | | A' | ν_2, A_1'' | A_1 | $A_{1g} + A_{2u}$ |
| $2(A_g + B_{1u} + B_{2g} + B_{3g} + A_u + B_{1u} + B_{2u} + B_{3u})$ | | $A' + A''$ | ν_3, E' | E | $E_g + E_u$ |
| | | $A' + A''$ | ν_3, E' | E | $E_g + E_u$ |

* N_T = total no. of modes; T_A = acoustic, T = optic branch translations; R = NO_3^- librations; $\Gamma(\text{vib})$ = NO_3^- internal vibrations.

α This column is identical with $\Gamma(\text{vib})$.

The ν_4 (E' in D_{3h}) $\delta(\text{NO}_3)_3$ region shows similar behaviour. In KNO_3 II the D_{2h} factor group require four components whereas only one is seen (715 cm^{-1}), in exact agreement with the D_{3d} rules. By 2.6 GPa in KNO_3 IV, there are two clearly resolved bands together with a hint of an unresolved component on the low frequency side, more nearly in accord with the D_{2h} rules.

Hence, although both KNO_3 II and IV have the same atoms on the same set of Wyckoff sites in the same space group, their vibrational spectra are very different because the packing in phase II is very close to the symmetry of D_{3d} . The spectra faithfully reflect the change of structure accompanying the transition. It follows, however, that a change of structure need not require a change of space group. This highlights the dangers of applying spectroscopic techniques alone to investigate structure, although in recent years they have been used to accumulate a considerable body of information on phase behaviour.

References

1. Wyckoff R.W.G., 1964, "Crystal Structure", Vol. 2, Interscience, New York
2. Leong J.T. and Emerick R.M., 1971, *J. Phys. Chem. Solids*, **32**, 2593
3. Nimmo J.K. and Lucas B.K., 1973, *J. Phys. C: Solid State Phys.*, **6**, 201
4. Iqbal Z., Christoe C.W. and Owens F.J., 1977, *Ferroelectrics*, **16**, 229
5. Bridgman P.W., 1916, *Proc. Am. Acad. Arts. Sci.*, **51**, 582
6. Jamieson J.C., 1956, *Z. Krist.*, **107**, 65
7. Davis B.L. and Adams L.H., 1962, *Z. Krist.*, **177**, 399
8. Weir C.E., Piermarini G.J. and Block S., 1969, *J. Chem. Phys.*, **50**, 2089
9. Rapoport E. and Kennedy G.C., 1965, *J. Phys. Chem. Solids*, **26**, 1995
10. Worlton T.G., Decker D.L., Jorgensen J.D. and Kleb R., 1986, *Physica*, **136b**, 503
11. David W.I.F., Johnson M.W., Knowles K.J., Crosbie G.D., Graham, S.P., Campbell E.P. and Lyall J.S., 1986, *Rutherford Appleton Laboratory Report RAL-86-015*.
12. Walrafen G.E., Abebe M., Mauer F.A., Block S., Piermarini G.J. and Munro R., 1982, *J. Chem. Phys.*, **77**, 2166
13. Chew A. and Chernow F., 1967, *Phys. Rev.*, **154**, 493
14. Fong M.Y. and Nicol M., 1971, *J. Chem. Phys.*, **54**, 579
15. Buckelmann A.K., Sherman W.F. and Wilkinson G.R., 1976, *Proc. 12th Eur. Congr. Molr. Spect.*, 303
16. Medina J.A., 1981, *Ph.D. Thesis*. University of London
17. Adams D.M. and Sharma S.K., 1981, *J. Chem. Soc. (Farad. Trans. II)*, **77**, 1263
18. Ismail M.A., Jogasooriga U.A. and Kettle S.F.A., 1983, *J. Chem. Phys.*, **79**, 4459

CHAPTER 5

A HIGH PRESSURE STUDY OF A VALENCE TRANSITION IN EuPd_2Si_2

CHAPTER 5

A High-Pressure Study of a Valence Transition in EuPd_2Si_2

5.1 Mixed Valence and Valence Transitions

There are many mixed-valence compounds, such as Fe_3O_4 and CsAuCl_3 , in which an element exists simultaneously in two different stable valence states. Thus, Fe_3O_4 is more accurately represented as $(\text{Fe}^{\text{II}})(\text{Fe}^{\text{III}})_2\text{O}_4$ and CsAuCl_3 as $\text{Cs}_2[\text{Au}^{\text{I}}\text{Cl}_2][\text{Au}^{\text{III}}\text{Cl}_4]$.

In the solid state physics literature the term "mixed valence" is used in an entirely different sense, and the field is further confused by application of the synonyms: "mixed configuration", "fluctuating valence", and "fluctuating configuration". These terms describe in a very loose and rather misleading way, complex solid state electronic band structures in materials in which an element may adopt more than one electronic configuration [1].

Under a given set of experimental conditions, the band structure of such a solid may in general be represented as a linear combination of the two notional "parent" configurations,

$$\Psi(\text{total}) = a_k\phi_1 + b_k\phi_2$$

Then, if these two electronic configurations are thought of as different "valence states", the material is aptly described as of "mixed valence", although it is clear that all the atoms of the element in question in the solid have the *same* electron configuration. Thus, the term "homogeneously mixed-valent" is often used to describe these systems, in contrast with the "inhomogeneously mixed-valent" materials familiar to chemists, *e.g.* Fe_3O_4 . The situation is closely analogous to that of an element adopting different hybridisation schemes in its molecular compounds, although no chemist would describe these as representing different valence states.

With variation of temperature or pressure the electronic levels of all materials are altered in absolute and relative terms. It follows that $\Psi(\text{total})$ will then have different values of a_k and b_k and that, in current solid state parlance, a change of valence is deemed to have occurred. The "average valency" R is defined in these circumstances by:

$$R = \frac{\sum |a_k|^2}{\sum |b_k|^2}$$

where the summation is over the occupied part of the conduction band. As temperature or pressure is varied over a range of values, the accompanying changes in a_k and b_k and therefore also in R , are sometimes regarded as constituting a "continuous valence transition". The effect of "pressure tuning" in particular is to affect the relative and absolute values of the electronic energy levels, commonly resulting in creation of a new ground state of the system with radically different properties, *e.g.* insulator-metal and spin-flip systems. The following example is given to help clarify these concepts.

5.2 Example: The case of SmS

This solid has the rock salt structure and at s.t.p. is described nominally as $\text{Sm}^{2+}\text{S}^{2-}$ with the atoms having the outer electron configuration $4f^65d^06s^2$ and $3s^23p^4$ respectively. The $4f$ level is not far below the $5d$. In solids the electron levels broaden into bands. In the case of SmS the d -levels broaden and hybridise with the $6s$ band in the process, but the f -levels, being buried well within the atoms, are little affected and remain atomic to first order [2-4]. The resulting band structure may be represented by Figure 5.1.

Under pressure the bottom of the crystal-field-split d -band is lowered relative to the f -level and eventually (at about 0.6 GPa) crosses it. This crossing is accompanied by large volume and resistivity changes, and the colour turns from gold to black; in other words, there is a classic insulator-metal transition. At and beyond this crossing point the f -levels hybridise with d -levels on neighbouring atoms (symmetry forbids hybridisation with d -levels on the same atom) but they remain close to their atomic levels in energy, constituting a sharp peak in the density-of-states distribution, Figure 5.2.

Near this peak the wave functions are linear combinations of d -like and f -like wave functions, the proportions varying rapidly near the peak. The wave function represents a linear combination of atomic orbitals (l.c.a.o.) which is partly f^5d and partly f^6 . The d -electron is relatively free in the lattice: thus, we may describe $\Psi(\text{total})$ as representing a linear combination of $3+$ and $2+$ valence states on the rare earth ion. This is the *only* sense in which such materials are of "mixed valence". Sm^{2+} and Sm^{3+} do *not* exist in SmS as separate entities, either as ordered or random mixtures.

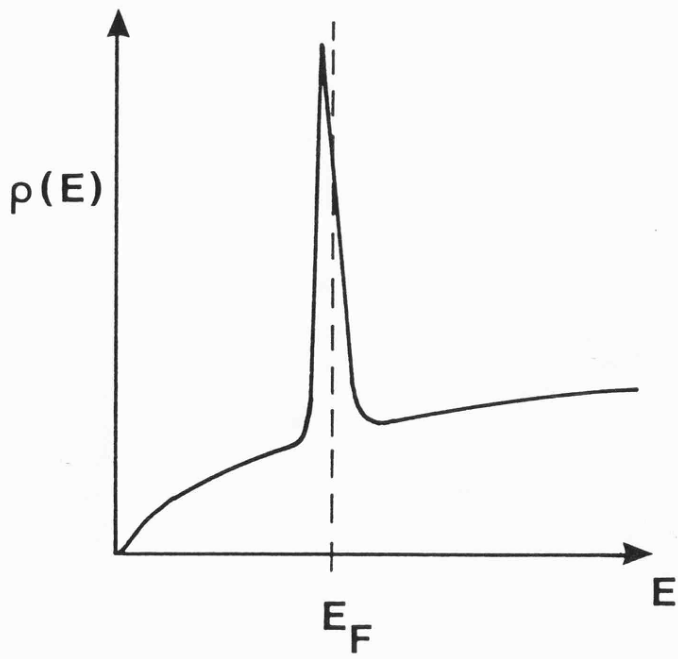
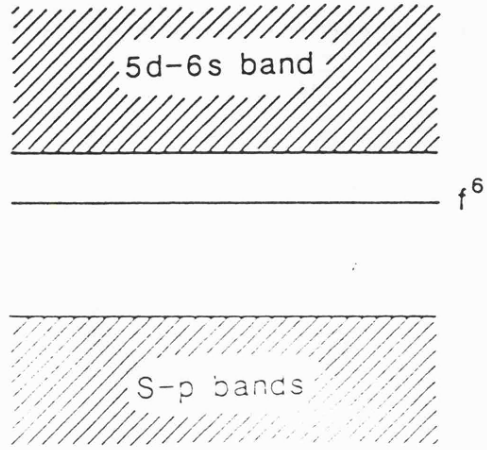
The "average valence" R defined above is not the "instantaneous valence" because there are always fluctuations: thus, the local f -character will fluctuate around the value represented by R . In this sense these compounds have "fluctuating valence".

Figure 5.1

Band structure in SmS
showing hybridisation of
6s, 5d and to a lesser extent, 4f

Figure 5.2

Density-of-states distribution
in SmS, showing sharp peak
around the 4f level
(E_F is the Fermi level)



5.3 Other mixed-valence materials

The concept of "homogeneously mixed valence" in the sense used in solid state physics is thus seen to be a piece of jargon associated with certain electronic band structure effects, observed mainly in materials containing a rare earth (or lanthanide) component. Because there are many possible materials of these types, a huge showcase of physical phenomena exists. Nevertheless, the basic concepts used here are no different from those traditionally associated with semiconductor physics and "band structure engineering", which have delivered many important devices from diode lasers to high- T_c superconductors.

Particularly interesting systems, from the solid state physics angle, are those in which f- and d-levels are in close proximity, such as in Ce and Yb and their compounds; as these show many unusual effects as specific energy levels are tuned relative to each other.

5.4 EuPd_2Si_2 and related materials

A series of materials MRh_2Si_2 and MPd_2Si_2 (where M = lanthanide) exists. They have the tetragonal ($I4/mmm \equiv D_{4h}^{17}$, $Z = 2$) ThCr_2Si_2 structure, represented in Figure 5.3 [5]. This structure type is of note in that the magnitude of the lattice constant a is primarily set by the size of the lanthanide ion, whereas c is mainly determined (in the case of EuPd_2Si_2) by the Pd/Si skeleton [6].

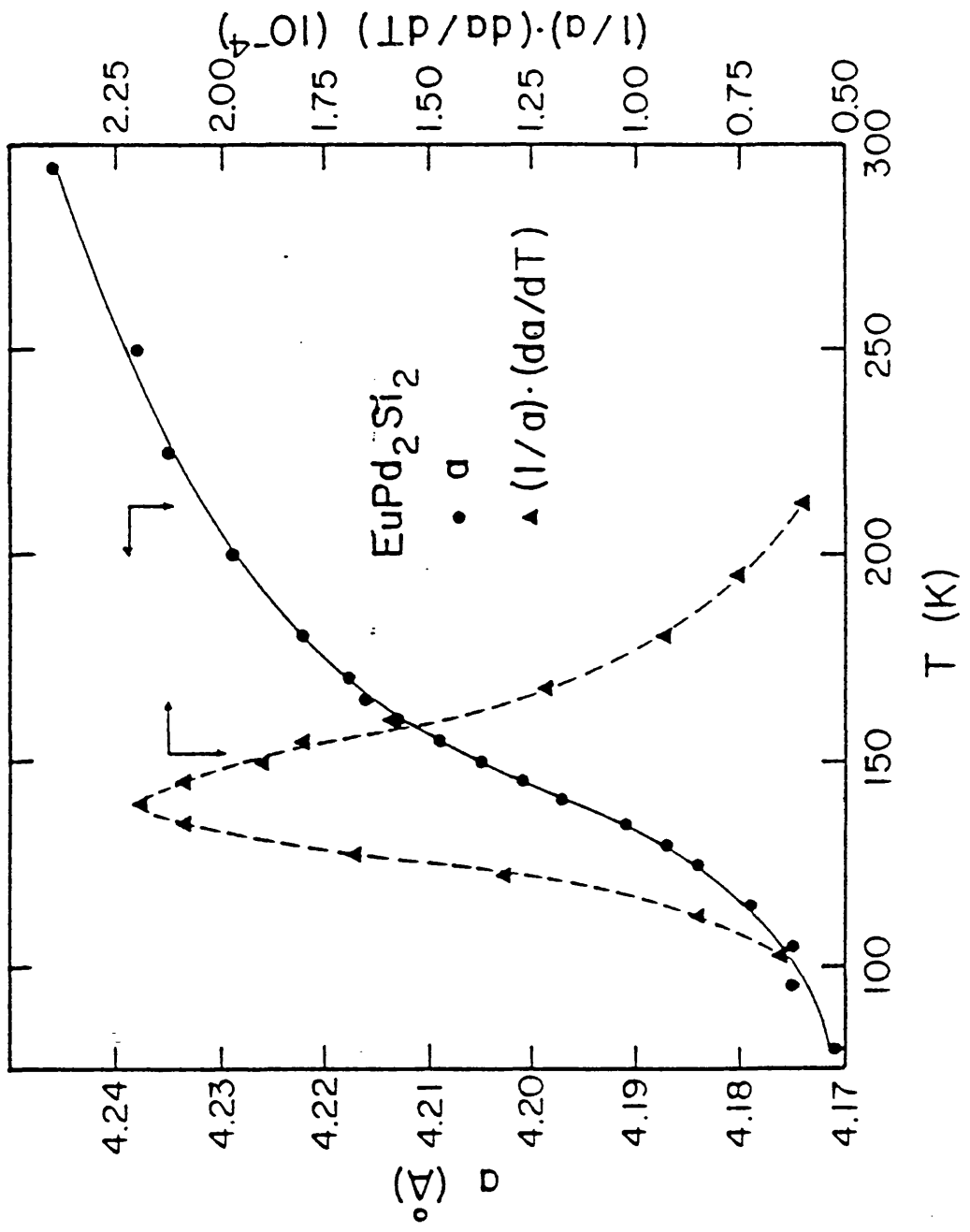
The compound EuPd_2Si_2 is of special interest in that it shows a lattice volume anomaly with respect to the other lanthanide isomorphs. It also shows a strong temperature anomaly near 150 K in several physical properties. Mössbauer data show a large isomer shift (due to the Eu) between 77 and 300 K with reference to the shifts observed in systems of di- and tri-valent europium [7]. The values of the average valence obtained were $\sim +2.2$ at room temperature and $\sim +2.9$ in the limit $T \rightarrow 0$ K. Low temperature x-ray diffraction work (on powders) using monochromatic radiation has shown that the lattice parameter a shortens as T approaches zero [7-9]. Figure 5.4 shows these data, the function $1/a \cdot (\partial a / \partial P)$ giving a maximum representing the transition midpoint. The S-shaped curve is characteristic of the slow change found in these compounds, which follows from the europium ion shrinkage as the average valence increases. We have studied the effect of pressure upon the lattice parameters of this compound at ambient temperature, using energy dispersive x-ray diffraction.

Figure 5.3

ThCr₂Si₂ structure type
(*I4/mmm*, *Z* = 2)

Figure 5.4

Variation of lattice parameter a
with temperature in EuPd_2Si_2 .
Data collected using angle-dispersive
powder diffraction.



5.5 Experimental

The pure sample of EuPd_2Si_2 was prepared in a tri-arc furnace with excess Eu and annealed at 1100 K for one week. The powder diffraction experiments were performed at the Daresbury SRS with the diffractometer operating in energy-dispersive mode without a monochromator and the detector operating at a fixed angle 2θ . A Diacell Products d.a.c. containing inconel gaskets (0.2-0.3mm hole) was used for the high-pressure scans, the pressure being determined by the ruby R-line method (see Chapter 2). A 4:1 mixture of methanol/ethanol was used as a pressure transmitting fluid. The Bragg peak positions were accurately determined using the GENIE data analysis package. Lattice parameters were calculated at varying pressures using the computer program VARVEC (see Chapter 3).

5.6 Results

Two diffraction spectra collected under pressure using the sample of EuPd_2Si_2 are shown in Figures 5.5 and 5.6. The sharp, well-resolved Bragg peaks were indexed successfully based on the tetragonal unit cell with $a = b = 4.237 \text{ \AA}$ and $c = 9.851 \text{ \AA}$. Although dominated by fluorescence peaks, the data collected showed very little elastic (Compton) scattering which would manifest itself as background. The relatively small number of reflections observed was due to the high symmetry crystal lattice.

The observed values for d_{hkl} were fitted to calculated d_{hkl} using a and c as fitting parameters. Table 5.1 contains values of a and c calculated at various pressures with their corresponding errors in parentheses. Figure 5.7 represents the variation of both lattice parameters, a and c to the highest recorded pressure, 3.1 GPa. These data show a wide scatter, such that no attempt of any type of least squares fit should be attempted. However, this behaviour is not totally unexpected (*vide infra*). Values of a calculated from shifts in the d_{200} reflection fit the familiar S-shaped curve noted previously, Figure 5.8. The point of inflexion observed in the steepest portion of the curve implies a volume decrease occurs around 0.8 GPa.

5.7 Discussion

Figure 5.7 shows a wide scatter of data-points; the data do *not* fit using either a linear regression analysis or, indeed, the S-shaped curve represented in Figure 5.8. These results can easily be accounted for by the effects of uni-axial stress present in the sample system. The anisotropic stress components affect differently the d_{hkl} spacings. Another

Figure 5.5

Energy dispersive powder
pattern of EuPd_2Si_2 at
0.2 GPa

e = escape peak of detector
In = inconel gasket material
F = fluorescence

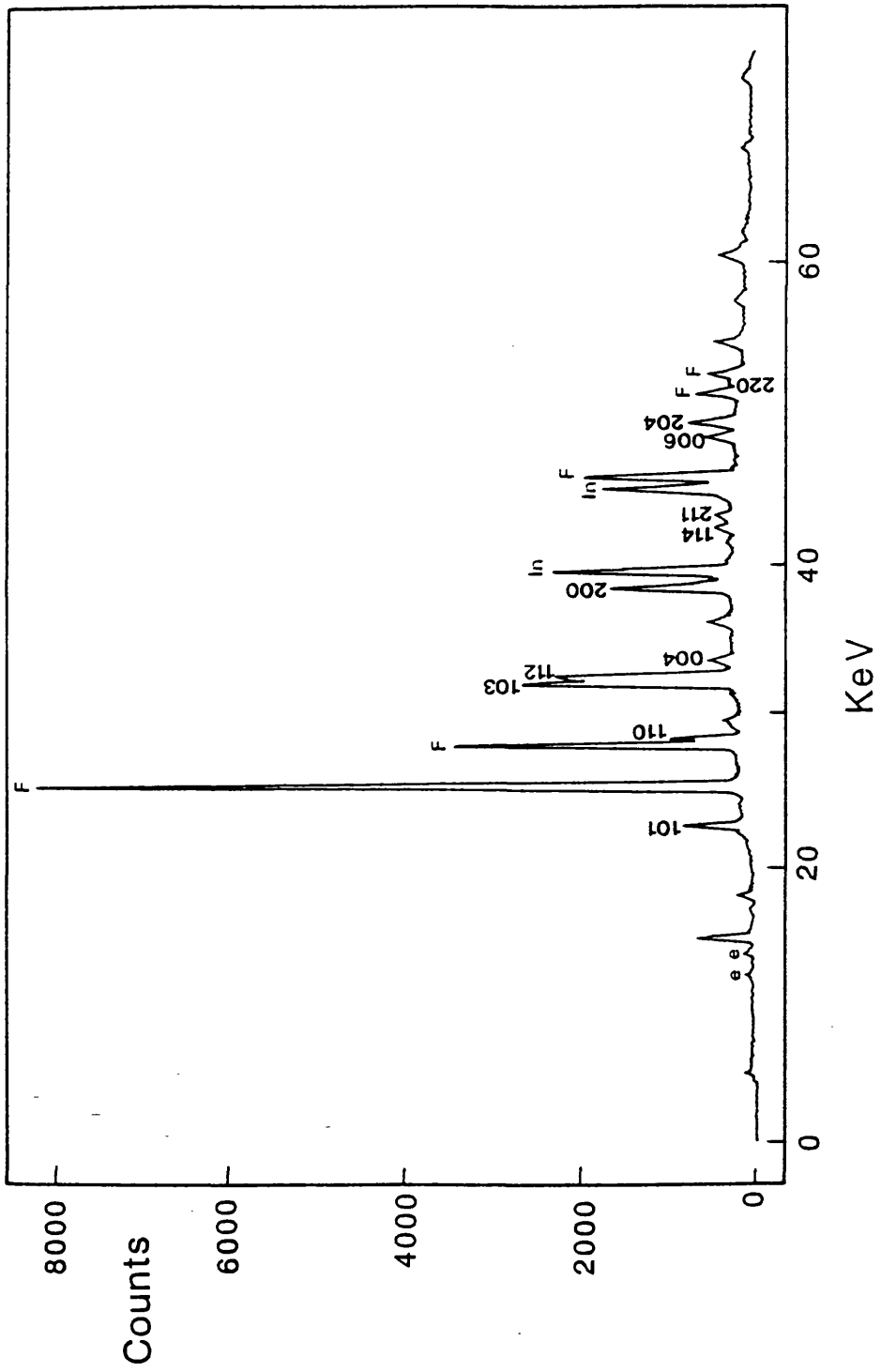


Figure 5.6

Energy dispersive powder
pattern of EuPd_2Si_2 at
2.0 GPa

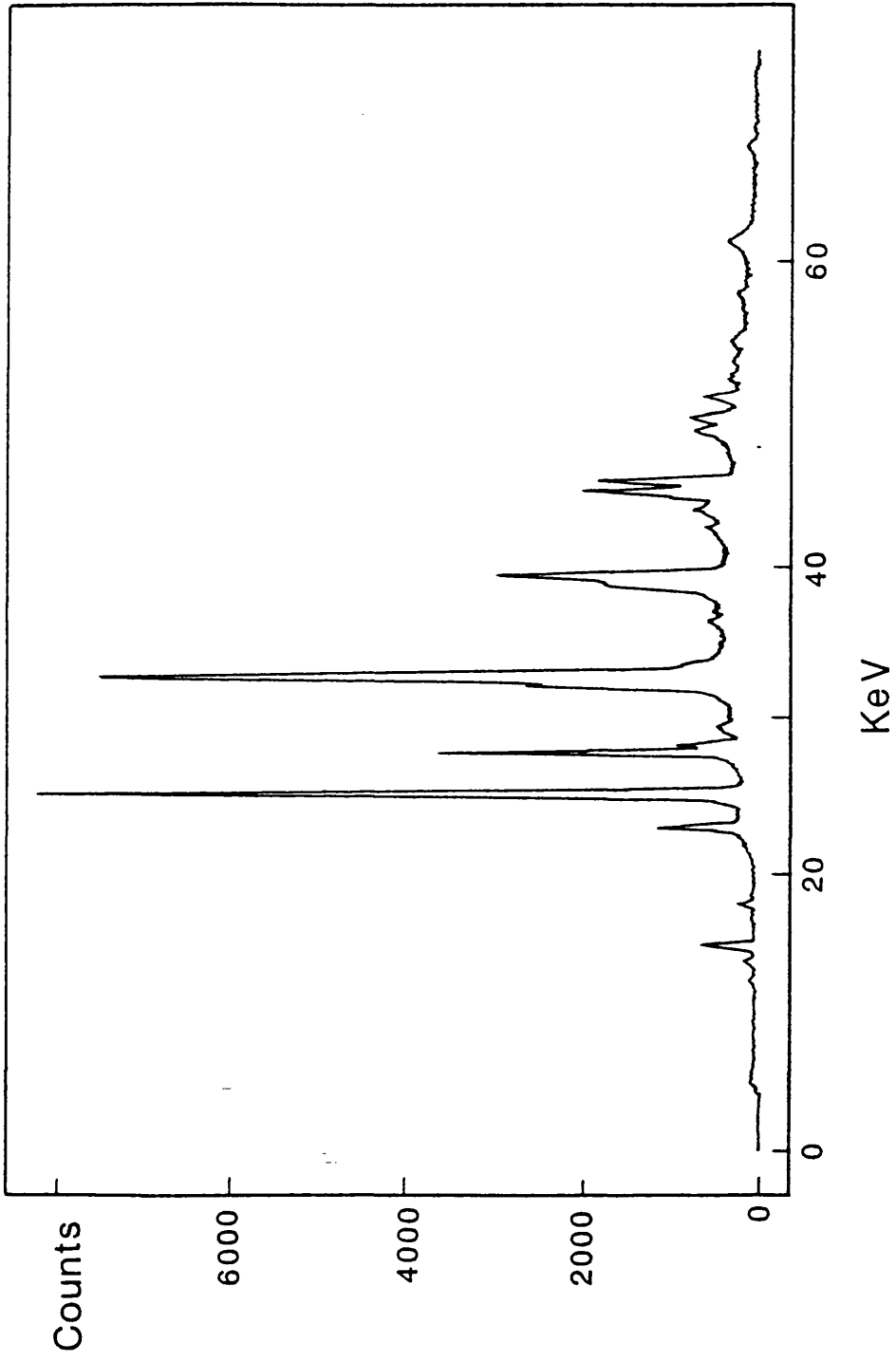


Table 5.1 Variation of lattice parameters with pressure in EuPd₂Si₂*

| P(GPa) | <i>a</i> (Å) | <i>c</i> (Å) | V(Å ³) |
|--------|--------------|--------------|--------------------|
| 0.43 | 4.123(30) | 9.723(132) | 165.2(3.3) |
| 0.63 | 4.118(26) | 9.790(287) | 166.0(5.3) |
| 0.79 | 4.115(28) | 9.761(315) | 165.3(5.8) |
| 0.92 | 4.105(28) | 9.520(147) | 160.4(3.3) |
| 1.31 | 4.138(25) | 9.676(164) | 165.7(3.4) |
| 1.81 | 4.140(25) | 9.673(160) | 165.8(3.4) |
| 3.11 | 4.116(38) | 9.381(370) | 159.0(6.9) |

*calculated standard deviations are shown in parentheses

Figure 5.7

Variation of lattice parameters
 a (top) and c between
0 and 3.1 GPa

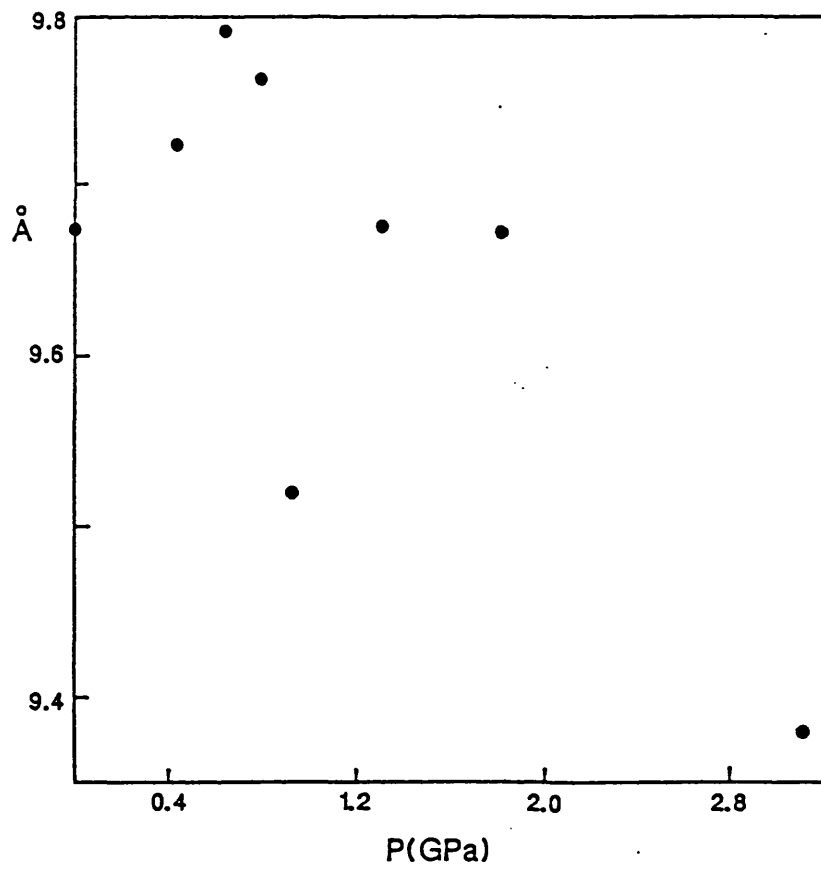
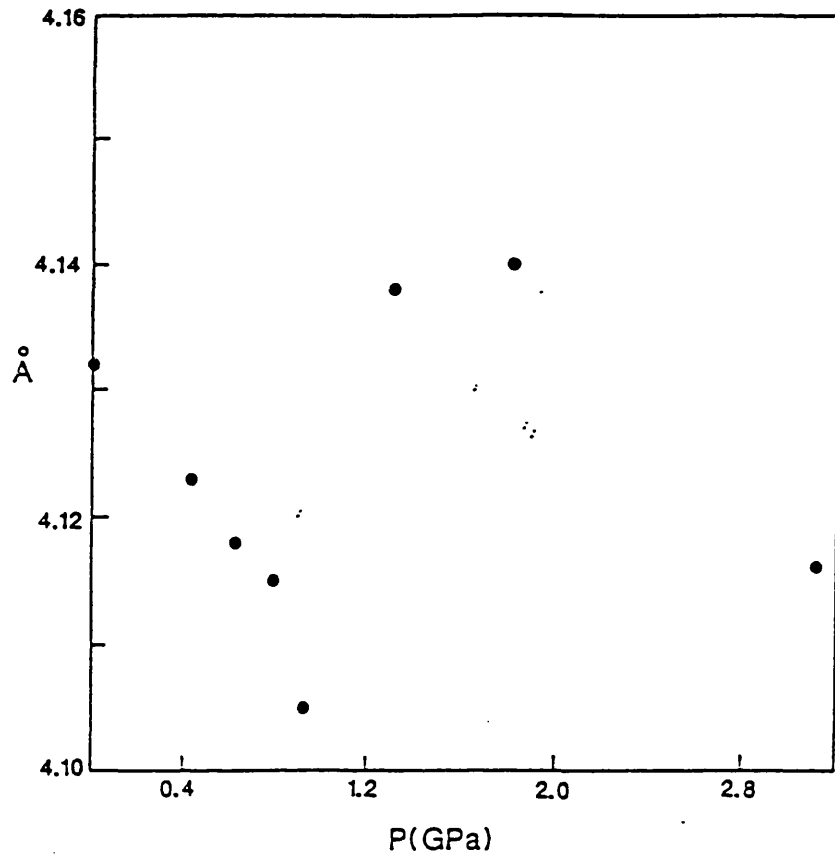
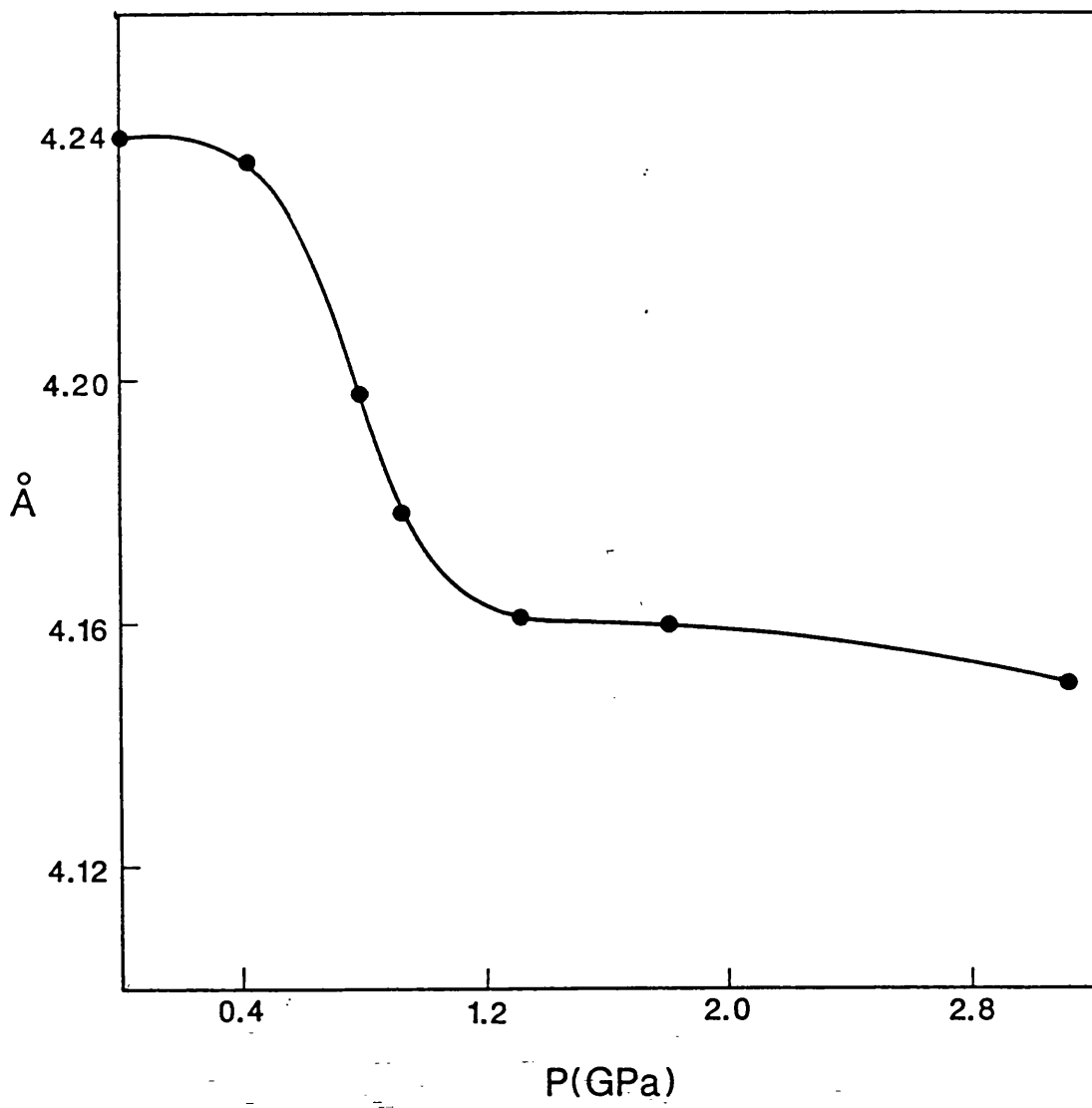


Figure 5.8

Variation of a with pressure
(where a is calculated
using d_{200} data)



very clear example of this phenomena is found in CeS [10] where the stress components effect on the cubic lattice can be represented by the function:

$$\Gamma(hkl) = (h^2k^2 + k^2l^2 + l^2h^2)/(h^2 + k^2 + l^2)^2 \quad (5.1)$$

which is minimum for h,0,0 reflections and maximum for h,h,h lines [11]. Clearly then, the value of a should be calculated from h,0,0 lines as opposed to an average value derived from all possible h,h,h lines. This conclusion has also been verified in the case of CeAl₂ [12]. All experiments presented here were carried out in the hydrostatic methanol/ethanol medium, and the ruby R-lines showed no sign of the formation of a non-hydrostatic sample chamber. It is suspected that the very hard crystallites could have been orientated in the sample chamber to be in contact with the diamond faces, and therefore would experience greater pressure on some axes than the homogeneous pressure produced by the surrounding fluid. This would explain the similar effects to those seen in CeS and CeAl₂, these cubic cases being extrapolated to this tetragonal problem. These observations would not have affected the low temperature data shown in Figure 5.4.

The a parameter variation calculated from the d_{200} line gives a true representative diagram. Again, this follows equation 5.1 in so much as h,0,0 lines provide reliable information. The curve follows a smooth path over a 1.0 GPa range suggesting a gentle contraction of a around 0.8 GPa. At ~2.0 GPa EuPd₂Si₂ has lattice constants ($a = 4.16 \text{ \AA}$, $c = 9.87 \text{ \AA}$) which compare exactly with those of SmPd₂Si₂. These two compounds are isomorphous and hence this suggests the europium ion approaches the tri-valent state (and size) at high pressure, the value of a depends primarily upon the europium ion radius. The sample has undergone a "valence transition" between ~0.6 and 0.16 GPa resulting from a hybridisation of 4f and 6ds bands and a volume collapse of 3.4%. This volume reduction is equivalent to a decrease of the europium ion radius by 0.0385 \AA , and assuming a linear relationship between valence and atomic radii ($r^{2+} = 1.17 \text{ \AA}$, $r^{3+} = 0.947 \text{ \AA}$) this gives an increase to the europium "valence" of about 0.2 at 2.0 GPa.

We are seeing the same band structure tuning effect with pressure as that observed with temperature variation. The calculated increase in "valence" on the europium ion of ~0.2 is of the same order of magnitude as that seen in CeS, where the increase is ~0.25 but over a much greater pressure range (0 to 25 GPa) [10].

References

1. Varma C.M., 1976, *Rev. Mod. Phys.*, **48**, 219
2. Wachter P., 1969, *Solid State Commum.*, **7**, 693
3. Kaldis E. and Wachter P., 1972, *Solid State Commum.*, **11**, 907
4. Narayanamurti V., Jayaraman A. and Bucher E., 1974, *Phys. Rev.*, **9**, 2521
5. Rossi D., Marazza R. and Ferro R., 1979, *J. Less-Common Met.*, **66**, 17
6. Ballestracci M.R., 1976, *C.R. Acad. Sc. (Paris)*, **B282**, 291
7. Sampathkumaran E.V., Gupta L.C., Vijayaraghavan R., Gopatakrishnan K.V., Pilley R.G. and Devare H.G., 1981, *J. Phys. C: Solid State Phys.*, **14**, L237
8. Jahns H., *Private Communication*
9. Sampathkumaran E.V., Vijayaraghavan R., Gopatakrishnan K.V., Pilley R.G. and Devare H.G., Gupta L.C., Post B. and Parks R.D., 1981, "Valence Fluctuations in Solids", edited by Falicov L.M., Hanke W. and Maple M.P., Amsterdam, N. Holland, p.193
10. Vedel I., Redon A.M., Legert J.M., Mignod-Rossat J. and Vogt O., 1986, *J. Phys. C: Solid State Phys.*, **19**, 6297
11. Smith A.K. and Kennedy G.C., 1974, *J. Appl. Phys.*, **45** 4686
12. Vedel I., Redon A.M., Leger J.M., Mignot J.M. and Flouquet J., 1986, *J. Magn. Magn. Mater.*, **54-57**, 361

CHAPTER 6

STRUCTURAL INVESTIGATIONS OF THE METHYL MERCURIC HALIDES CH_3HgX ($\text{X} = \text{Cl}, \text{Br}, \text{I}$)

CHAPTER 6

Structural Investigations of the Methyl Mercuric Halides (CH_3HgX , $\text{X} = \text{Cl, Br, I}$)

Introduction

The series of compounds CH_3HgX ($\text{X} = \text{Cl, Br, I}$) have been studied in detail under high-pressure using Raman spectroscopy. This group of molecular solids is of interest to the spectroscopist because its members exhibit phase transitions in which a molecular internal torsion is implicated. These materials are ideal candidates for study because of the simplicity of their structures and the existence of a single torsional mode. Previous study [1] has shown that each compound exhibits at least one phase transition, either with temperature or pressure, and a vibrational 'soft mode' has also been observed in each. Detailed structural information is essential for unambiguous assignment of spectra, and thus the understanding of phase transitions and their mechanisms.

In this chapter two of the series of compounds have been studied using x-ray diffraction. The ambient crystal structure of the iodide has been solved. Structure solution and low temperature investigation of the solid state phase transition for the chloride has been attempted using Rietveld refinement and Bragg indexing methods.

6.1 Crystal Structure of Methyl Mercuric Iodide

6.1.1 Introduction

As the structure of CH_3HgI was unknown a single crystal x-ray diffraction study was undertaken to complete the structural information available for the methyl mercuric halide phases under ambient conditions. The three crystal structures vary in detail but comparisons are drawn between CH_3HgI and the analogous chloride and bromide.

6.1.2 Experimental

A commercial sample of Analar quality CH_3HgI was recrystallised from ethanol/methanol and further purified by sublimation using a 'cold-finger' apparatus. The crystals were found to be thin platelets which over a certain size exhibited 'twinning'; consequently a small crystal was chosen. Methyl mercuric iodide sublimes in the

atmosphere at s.t.p. and the resulting vapours are also very toxic by inhalation. Therefore, the crystal was sealed in a glass capillary prior to diffraction.

6.1.3 Symmetry and Cell

Oscillation and Weissenberg photographs were taken to establish cell constants, crystal orientation and space group. The observed systematic absences indicated either orthorhombic or monoclinic unit symmetry fitting the space groups $Pbcm$ (D_{2h}^{11}), $Pbc2_1$ or $P2_1/c$ (C_{2h}^5) respectively. The unit cell parameters were later refined from 2θ -scan data measured on the diffractometer.

6.1.4 Crystal Data

CH_3HgI formula weight = 342
Space group $Pbcm$
 $a = 8.704 \text{ \AA}$ $b = 7.404 \text{ \AA}$ $c = 7.226 \text{ \AA}$
 $\alpha = \beta = \gamma = 90^\circ$ $F(000) = 568$
Cell volume = 465.7 \AA^3 $Z = 4$ $D_c = 4.88 \text{ gcm}^{-3}$
Crystal size = $0.26 \times 0.016 \times 0.24 \text{ mm}$ {001}, {010}, {100}
 $\lambda(\text{Mo-K}\alpha) = 0.7107 \text{ \AA}$ $\mu(\text{Mo-K}\alpha) = 379 \text{ cm}^{-1}$

6.1.5 Data Collection

All intensity data were collected on a Digital PDP-8 controlled Stoe 2-circle diffractometer using the ω -scan method. Acquisition of data, experimental control parameters and data transfer were managed by a Sirius microcomputer interfaced to the PDP-8. A total of 2208 reflections hkl was collected from all four quadrants (*i.e.* $\pm h$, $\pm k$ and $l = 0$ to 8) and these data transferred to a mainframe Digital VAX 8600. Data work-up was carried out by a locally written program STOWK [2]. The computer program SHELX76 [3] was used for all subsequent calculations. The data were checked against the symmetry specified by the orthorhombic space group and 123 reflections were rejected as systematically absent. The conditions limiting possible reflections in the space group are:

$$\begin{aligned}0 k l \quad k &= 2n \\h 0 l \quad l &= 2n\end{aligned}$$

However, some 'absent' reflections which had been rejected were found to diffract significantly (particularly those associated with the b glide perpendicular to a , *e.g.*

0 1 2). These reflections are allowed in the monoclinic space group ($P2_1/c$). However, from the results of various refinement models (*vide infra*), the highest symmetry model ($Pbcm$) was eventually chosen. The presence in the data of these 'absences' could arise from double reflection (Renninger effect), in which radiation reflected from two strongly diffracting planes appears to arise by single reflection from a third [4]. Glide planes give rise to many absences and apparent contradictions can usually be ascribed to double reflection, although the Renninger effect generally exhibits itself by contributing additional intensity to an allowed reflection. Imperfections in the crystal lattice (*e.g.* a minor degree of 'twinning') may cause some unit cells to be misaligned with respect to the mounting axis giving anomalous results. The resulting 2085 reflections in the data were merged in order to average symmetry related peaks and 557 unique reflections were obtained. This operation gave an R-factor of 3.5% indicating a favourable 'merge'. Check reflection measurements made every 50 reflections in each layer indicated no noticeable decay of the crystal during diffraction.

6.1.6 Structure Solution and Refinement

Structure solution and refinement were achieved again using SHELX76. The heavy atom approach using the Patterson technique was employed to determine the positions of the mercury and iodine atoms. A difference Fourier synthesis elucidated the carbon position; unsurprisingly, the hydrogen atoms were not located.

A full-matrix least squares refinement of atomic positional parameters was undertaken allowing anisotropic thermal parameters for all determined atoms. The application of a standard weighting scheme resulted in the following crystallographic R-factors:

$$R = 5.89\% \quad R_w = 5.10\%$$

where $R = \sum ||F_o| - |F_c||^2 / \sum |F_o|^2$

and $R_w = \sum w \{ (|F_o| - |F_c|)^2 / \sum w |F_c|^2 \}^{1/2}$ with $w = 8.837 / \{ \sigma^2(|F_o|) + 0.00017 |F_o|^2 \}$

Initial observations of Weissenberg photographs suggested the space group symmetry for CH_3HgI to be either $Pbcm$, $Pbc2_1$ (orthorhombic) or $P2_1/c$ (monoclinic). The lattice parameters of the unit cell suggested the orthorhombic lattice ($\alpha = \beta = \gamma = 90^\circ$) but some reflections expected to be systematically absent were found to be have significant intensity. The possible explanations for this phenomenon are given above in section 6.1.5. The original data were merged in both the orthorhombic and monoclinic symmetries (monoclinic merge gave 1006 unique reflections, $R = 3.1\%$) and separate least squares refinement carried out for each model. $Pbc2_1$ is a polar space group and

therefore the position of Hg was fixed to define the origin. The enantiomeric model for this space group was also refined as a possible solution. Table 6.1 compares the least squares parameters for each model and details any constraints imposed in refinement.

The lowest R-factors were found for the $Pbc2_1$ models but the thermal parameter component U_{33} was of the same order throughout. U_{33} is the thermal parameter perpendicular to the mirror plane in the $Pbcm$ model. Here all atoms are forced to lie in this mirror plane and therefore a significantly higher value of U_{33} would be expected if this constraint were incorrect. The difference in the R-factors was very small between the orthorhombic options; those of the monoclinic model having relatively high values. The e.s.d.s of the diagonal thermal parameter components were lower in the higher symmetry orthorhombic model than those of their counterparts where the screw axis replaced the mirror plane. Consequently, the highest symmetry group (*i.e.* $Pbcm$) was chosen, with all the atoms on sites $4d$ *i.e.* Hg, I, and C on special positions $(x, y, 1/4)$.

6.1.7 Discussion

CH_3HgI has near-linear molecules packed along a , with adjacent chains oriented in opposite directions. The final positional and thermal parameters for all refined atoms are given in Tables 6.2 and 6.3. Table 6.4 contains the relevant bond distances and angle calculated in the final structural model. The crystal structure of CH_3HgI is shown in Figure 6.1.

6.1.8 Comparison of CH_3HgX ($X = Cl, Br, I$) structures

Table 6.5 lists the crystal data for the methyl mercuric series CH_3HgX ($X = Cl, Br, I$). The structure of CH_3HgCl was reported by Grdenic and Kitaigorodskii in 1949 [5] to be tetragonal with $Z = 2$ in space group $P4/nmm$ (D_{4h}^{74}). However, comparison of the Hg-Cl bond distance (2.5 Å) with that in $HgCl_2$ (2.25 Å) [6] and $HgCl$ vapour (2.34 Å) [6] casts suspicion on the validity of this determination. An attempt was made to repeat the structure determination but no quality single crystals could be grown, possibly due to the high degree of disorder suspected in the chloride (*vide infra*). Oscillation and Weissenberg photographs (although of very poor quality) agreed with the published lattice parameters and tetragonal symmetry. However, the analysis derived from this publication should be viewed with suspicion. The reported crystal structure is shown in Figure 6.2. The bromide also adopts a tetragonal unit cell, $P\bar{4}2_1m$ with $Z = 4$ [7], the structure is shown in Figure 6.3.

Table 6.1 Comparison of refinement parameters for CH₃HgI*

| Symmetry | NP [♦] | R(%) | R _w (%) | RG(%) | U ₃₃ (Hg) | U ₃₃ (I) | U ₃₃ (C) |
|---------------------------------------|-----------------|------|--------------------|-------|----------------------|---------------------|---------------------|
| 1 <i>P2₁/c</i> | 28 | 6.43 | 6.13 | 7.43 | 0.0732(8) | 0.0717(12) | 0.0504(148) |
| 2 <i>Pbc2₁</i> | 27 | 5.47 | 4.78 | 5.34 | 0.0758(10) | 0.0733(15) | 0.0558(412) |
| 2 <i>Pbc2₁^e</i> | 27 | 5.60 | 4.94 | 5.46 | 0.0751(10) | 0.0750(14) | 0.0603(325) |
| 3 <i>Pbcm</i> | 19 | 5.89 | 5.10 | 5.59 | 0.0732(8) | 0.0725(12) | 0.0641(155) |

Constraints placed on 1 to 3:

- 1 None
- 2 Hg z co-ord. fixed
- 2e " " " " with enantiomeric atomic positions
- 3 All atoms fixed on (x,y,1/4), U₁₃ and U₂₃ fixed

♦NP = number of refinement parameters.

*estimated standard deviations are shown in parentheses.

Crystallographic results for CH₃HgI

Table 6.2 Atomic parameters*

| | <i>x/a</i> | <i>y/b</i> | <i>z/c</i> |
|----|------------|------------|------------|
| Hg | 0.1504(2) | 0.0536(1) | 0.2500 |
| I | -0.1527(3) | 0.0534(2) | 0.2500 |
| C | 0.4028(28) | 0.0667(31) | 0.2500 |

All atoms on special positions (*x,y,1/4*)

Table 6.3 Thermal parameters*

| | <i>U</i> ₁₁ | <i>U</i> ₂₂ | <i>U</i> ₃₃ | <i>U</i> ₁₂ |
|----|------------------------|------------------------|------------------------|------------------------|
| Hg | 0.0477(9) | 0.0625(7) | 0.0732(8) | -0.0006(8) |
| I | 0.0507(14) | 0.0620(10) | 0.0725(12) | 0.0007(14) |
| C | 0.0056(104) | 0.0508(131) | 0.0641(155) | 0.0001(11) |

*U*₁₃, *U*₂₃ lie in mirror plane and are constrained in refinement

Table 6.4 Bond distances and angle*

| | |
|-----------------------|-------------|
| Hg-I | 2.638(3) Å |
| Hg-CH ₃ | 2.199(24) Å |
| H ₃ C-Hg-I | 177.5(6)° |

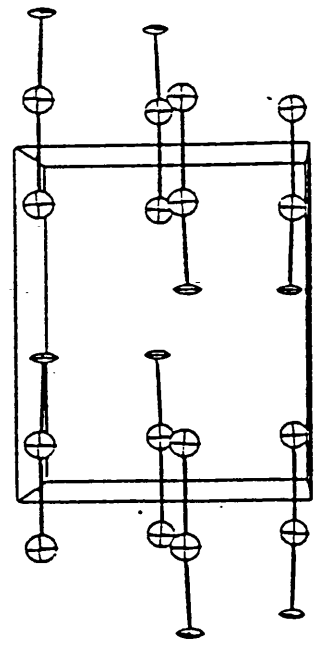
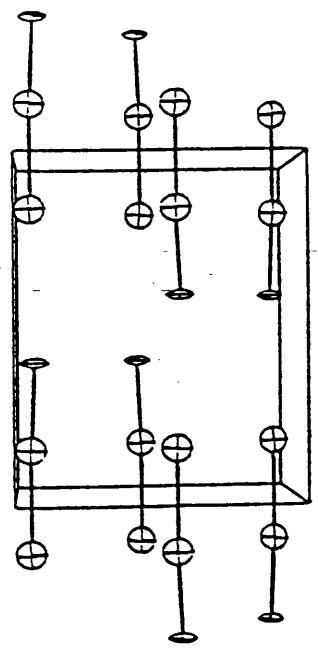
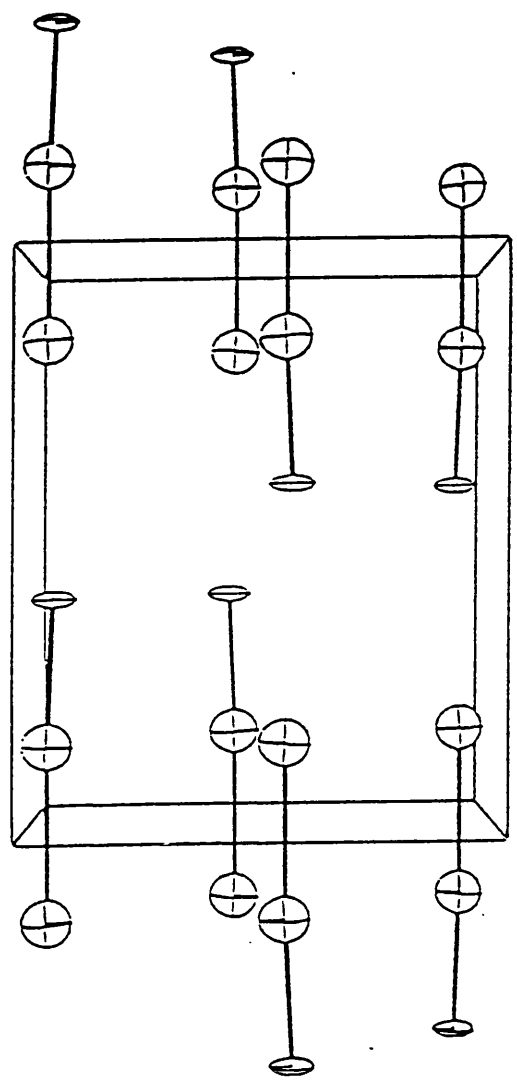
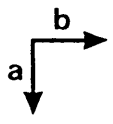
*estimated standard deviations are shown in parentheses.

Figure 6.1

a) The crystal structure of methyl
mercuric iodide, CH_3HgI

(- CH_3 groups are shown by the narrowest ellipsoids)

b) Stereoscopic projection of CH_3HgI



Comparison of structure in the CH₃HgX series

Table 6.5 Crystal data for the CH₃HgX (X = Cl, Br, I) series*

| X | a(Å) | b(Å) | c(Å) | Hg-X | Hg-C | C-Hg-X | Z |
|----|------|------|------|----------|---------|---------|-----|
| Cl | 4.62 | 4.62 | 9.39 | 2.51 | 2.06 | 180° | 2 |
| Br | 6.91 | 6.91 | 8.83 | 2.499(7) | 2.40(9) | 177(2)° | 4 |
| I | 8.70 | 7.40 | 7.23 | 2.638(3) | 2.20(2) | 178(1)° | 4 |
| (I | 7.23 | 7.40 | 8.70 | " | " | " | ")♦ |

♦a' = c in *Pbcm*

Table 6.6 Contact distances for Hg...X and CH₃...CH₃ in CH₃HgX*

| X | Hg...X(Å) | N♦ | CH ₃ ...CH ₃ (Å) | N♦ |
|----|-----------|----|--|----|
| Cl | 3.27 | 4 | 4.2 | 4 |
| Br | 3.289(4) | 2 | 3.76(9) | 4 |
| | 3.640(4) | 2 | | |
| I | 3.699(0) | 2 | 4.07(3) | 2 |
| | 3.704(2) | 2 | | |

♦N = number of closest contacts

*estimated standard deviations (where possible) are shown in parentheses.

The three structures are basically the same, with layers of methyls and HgX alternating along z throughout the lattice. Table 6.6 lists the contact distances between Hg-halogen and methyl-methyl groups calculated using the locally written computer program GEOM [8]. Halving the $\text{CH}_3\cdots\text{CH}_3$ distance gives an estimate of the overlap (if any) of the methyl groups in neighbouring molecules taking the radius of a freely rotating methyl group to be 2.1 Å. Hence, the chloride with $\text{CH}_3\cdots\text{CH}_3 = 4.2$ Å is expected to have overlap to a small extent, it is postulated that hydrogen atoms of one group intermesh with those of its nearest neighbour, like cogs in a gearwheel. The methyl groups must be rotating in the chloride since they inhabit sites $2c$, the symmetry of the latter in $P4/nmm$ being $4mm$ (C_{4v}), a static methyl would require threefold site symmetry (*i.e.* C_{3v}). The resulting disorder could account for the inability of the chloride to produce good quality single crystals, which in turn makes further single crystal x-ray work very difficult. The $\text{CH}_3\cdots\text{CH}_3$ contact distances in the bromide and iodide suggest higher degrees of overlap, especially in the bromide. The site symmetry found in both the above (on $4e$ in $P\bar{4}2_1m$ and $4d$ in $Pbcm$) is m (σ_v); this mirror plane is compatible with a static methyl group and hence ordered hydrogen positions.

By exchanging a and c in the CH_3HgI unit cell the orthorhombic lattice can be thought of as pseudo-tetragonal with $a = 7.23$ $b = 7.40$ Å and $c = 8.70$ Å. The packing arrangements in all three structures are similar, the C-Hg-X skeleton shows a small deviation from linearity when $X = \text{Br}$ and I but is supposedly linear in the chloride. The fractional co-ordinates of each set of atoms along the packing direction z also show a marked similarity (if $c' = a$ in $Pbcm$). In all three structures the contacting methyls are central to the unit cell. It is interesting to note that the c lattice parameter shortens as the halogen size increases, the most densely packed of the three is the bromide, the increased size of the halogen in the iodide driving the lattice to be pseudo-tetragonal (*i.e.* orthorhombic) on crystallisation.

Figure 6.2

a) The crystal structure of methyl
mercuric chloride, CH_3HgCl

b) Stereoscopic projection of CH_3HgCl

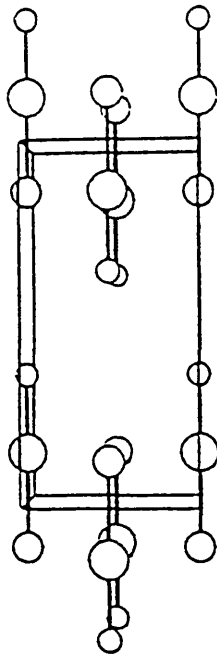
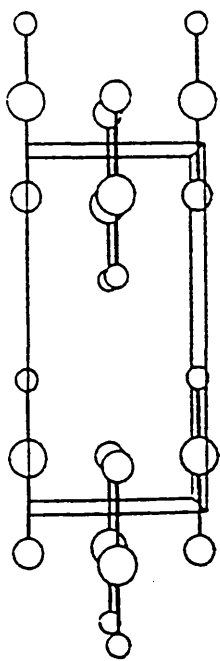
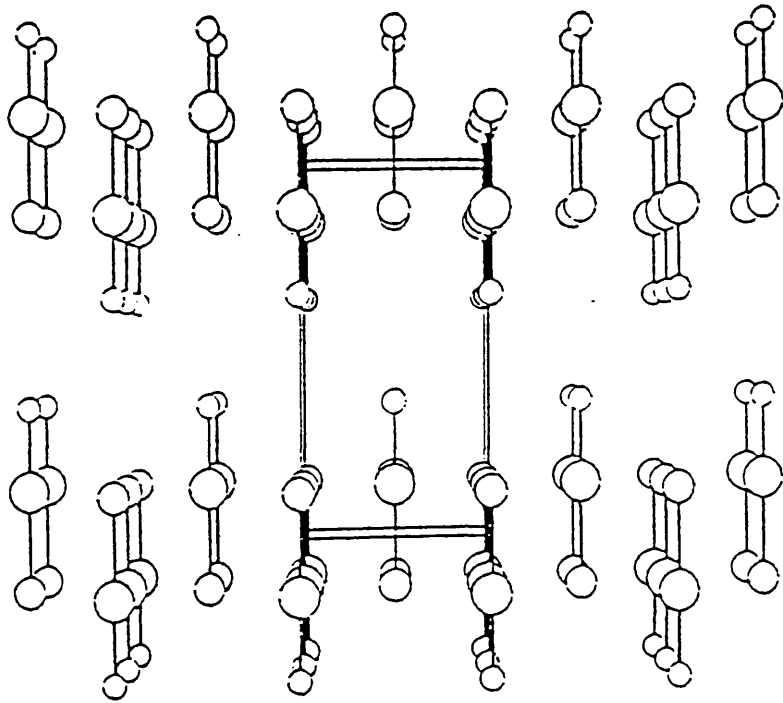
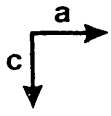
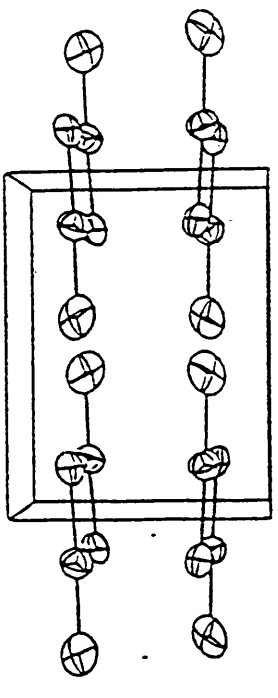
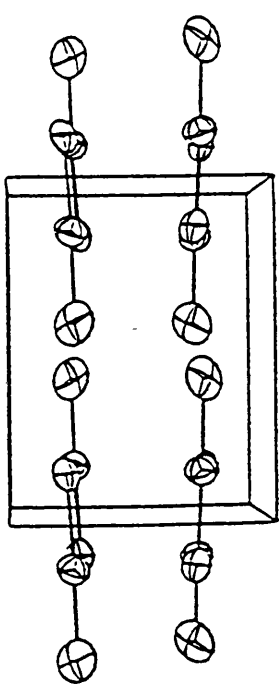
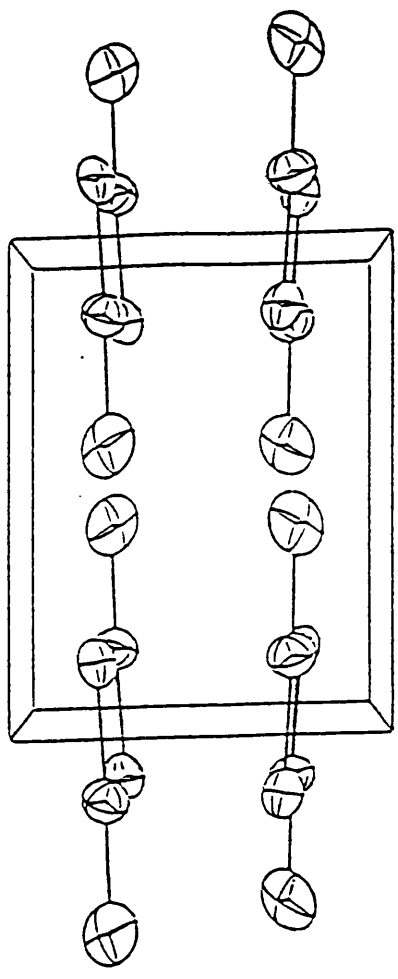
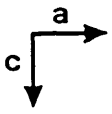


Figure 6.3

a) The crystal structure of methyl
mercuric bromide, CH_3HgBr

b) Stereoscopic projection of CH_3HgBr



6.2 Powder Investigations of CH₃HgCl at different Temperatures

6.2.1 Introduction

Orthodox single crystal methods of structure determination in the case of CH₃HgCl proved impossible because of the poor quality of the single crystals obtained. In the light of this, angle dispersive powder diffraction was used in an attempt to confirm the structural model proposed by Grdenic *et al* [5] for the ambient phase of this compound.

The phase diagram of CH₃HgCl deduced from Raman spectroscopy [1] is shown in Figure 6.4. The vibrational spectra suggest that the low temperature phase II of CH₃HgCl is iso-structural with the tetragonal ambient phase II of CH₃HgBr (*P42₁m*, see Table 6.5 for lattice parameters). The CH₃HgCl (II) spectra were analysed to show a cell doubling in the reported transition from phase I at 162.5 K. Diffraction data were collected for CH₃HgCl at 75 K in order to test the hypothesis of structural similarity between the two phases of the chloride and bromide.

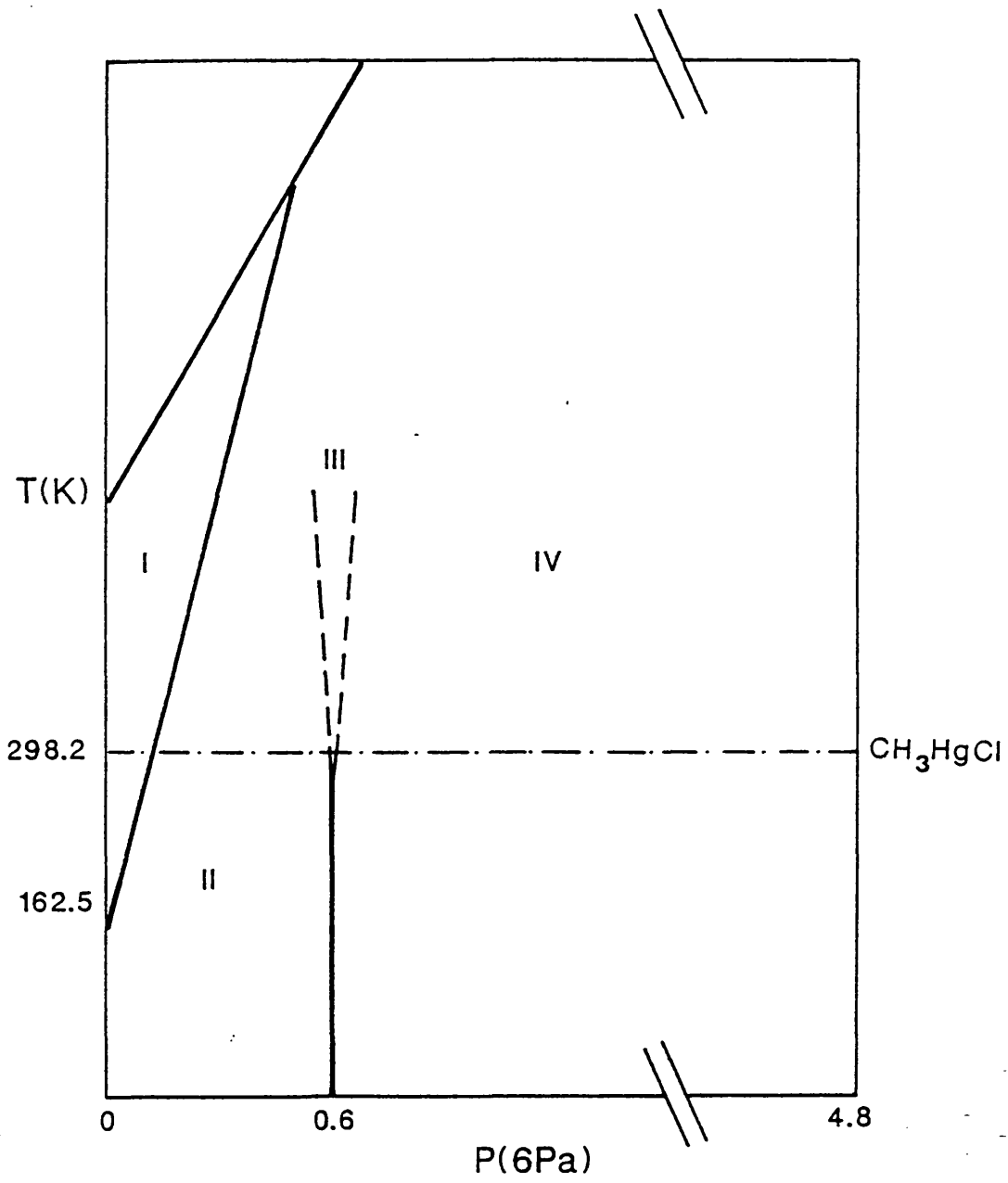
Rietveld analysis was attempted using the data collected at higher temperature but this was not possible following the phase change as no complete structural model has yet been proposed. The low temperature diffraction pattern was used to attempt Bragg peak indexing of CH₃HgCl (II).

6.2.2 Experimental

A commercial sample of CH₃HgCl was recrystallised from methanol/ethanol and further purified by sublimation in a 'cold-finger' apparatus. The sample was ground to a fine powder and sealed in a 0.5 mm glass capillary. The powder diffraction experiments made use of the wiggler enhanced synchrotron radiation source at Daresbury on station 9.1. An incident wavelength of 1.0098 Å was selected using a Si triple crystal monochromator. Both experiments were carried out in an Oxford Instruments cryostat. A copper block acts as a heat exchanger between helium gas, which cools the rotating capillary sample and liquid helium in contact with the block. The cryostat was calibrated using the lattice parameter of silicon to be accurate within 0.2 K at temperatures above 30 K. Further calibration experiments using the inter-planar spacings of silicon showed the zero-point-theta error to be -0.019°. The ambient phase was observed at 180 K to minimise thermal disorder and the low temperature phase at 75 K. The use of the cryostat restricted the maximum 2θ which could be used for data collection to approx. 80° but

Figure 6.4

Phase diagram of CH_3HgCl
(Adams *et al*, 1988)



preliminary experiments suggested measurable Bragg intensities could only be observed in a collection range of 5-60°.

6.2.3 Analysis of Ambient phase data

The diffraction pattern of CH₃HgCl collected at 180 K is shown in Figure 6.5. Where possible the Bragg reflections *hkl* have been indexed on the basis of the tetragonal unit cell (*P4/nmm*, *Z* = 2, *a* = *b* = 4.62 Å, *c* = 9.39 Å) put forward by Grdenic *et al.* The resolution of the Bragg peaks was ~0.05° and the signal/noise ratio high enough to allow measurement of even very low intensities.

The data were analysed using the computer program BENDALL MULTIPATTERN [9,10] which consists of two separate parts resident in the PDPL program library available on the mainframe Dec VAX 11/780 at Daresbury. The initial preparation of the data for Rietveld analysis was carried out by the program MPREP. This allowed a user-defined baseline to be subtracted from the pattern and calculated peaks to be indexed. The output was a data file suitable as input to the refinement program MPROF. Refinement of the data began with determining the scale factor relating the observed and calculated intensity between the diffraction and model patterns. The next step in the process was to refine the Bragg peak parameters (*i.e.* the half-width components and line-shape parameters). Several starting values for these parameters were used but all yielded least squares convergence with a set of very high values for the calculated R-factors. The calculated and observed intensities of a large proportion of the Bragg reflections were found to differ by substantial amounts as shown by the difference plot of the pattern in Figure 6.6. In order to remedy the large differences the temperature factors associated with Hg, Cl and C were refined separately but this yielded no improvement in the R-factors obtained.

6.2.4 Discussion of ambient phase results

The inability of the refinement to achieve R-factors below 40% (a plausible starting value for further refinement [11]) suggests that the model on which the calculations in the Rietveld program were based was incorrect. The pattern can be indexed efficiently using measured peak positions which suggests that the tetragonal cell and unit vectors proposed in the original structural analysis are correct. Unfortunately, the nature of Rietveld analysis does not allow a model that is 'nearly' correct to be the basis of a successful procedure towards the required goal. Hence, any information regarding the actual molecular structure could not be used.

Figure 6.5

Powder diffraction pattern of CH_3HgCl (I)
($T = 180 \text{ K}$, $\lambda = 1.0098 \text{ \AA}$)
I = impurity

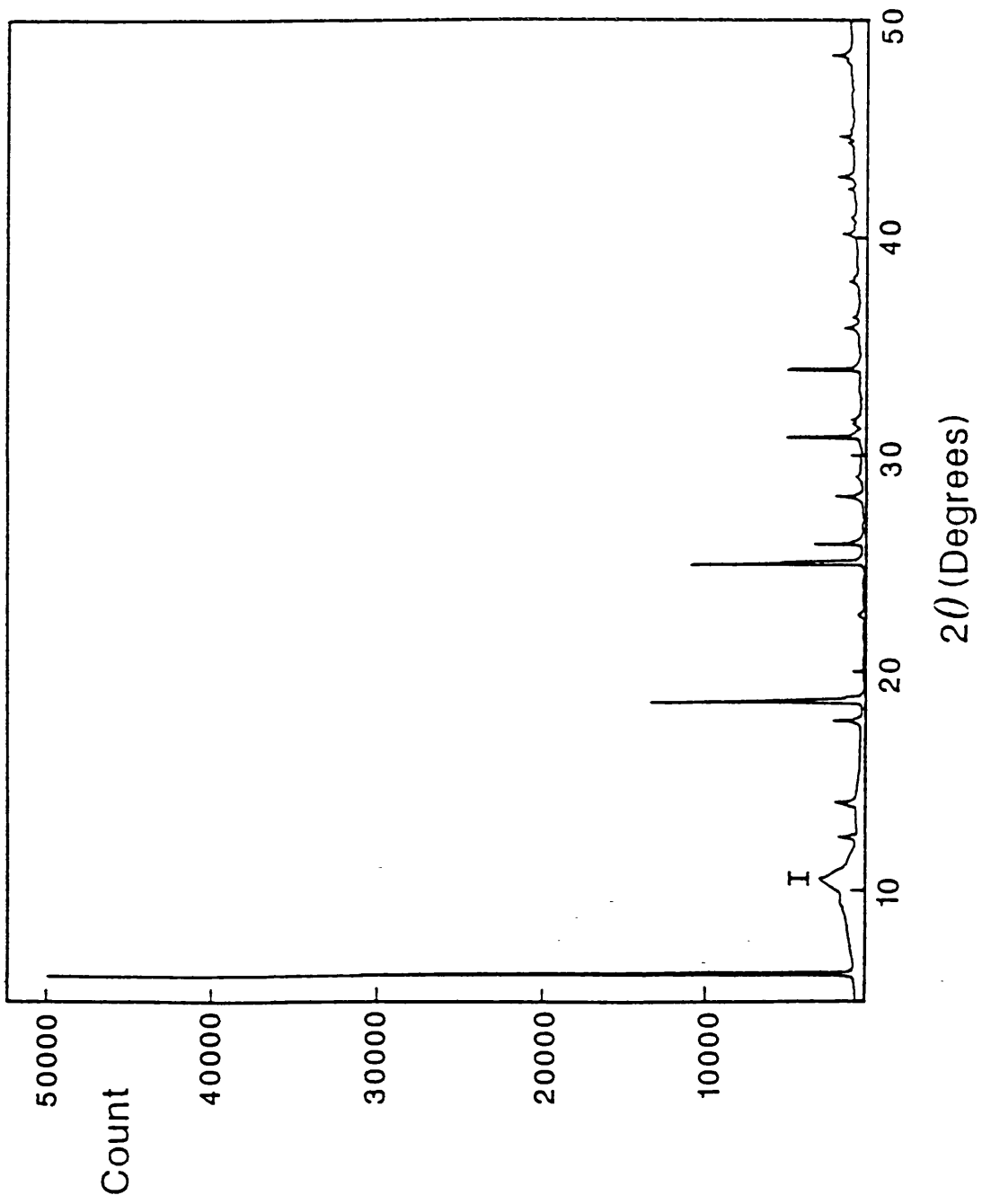


Figure 6.6

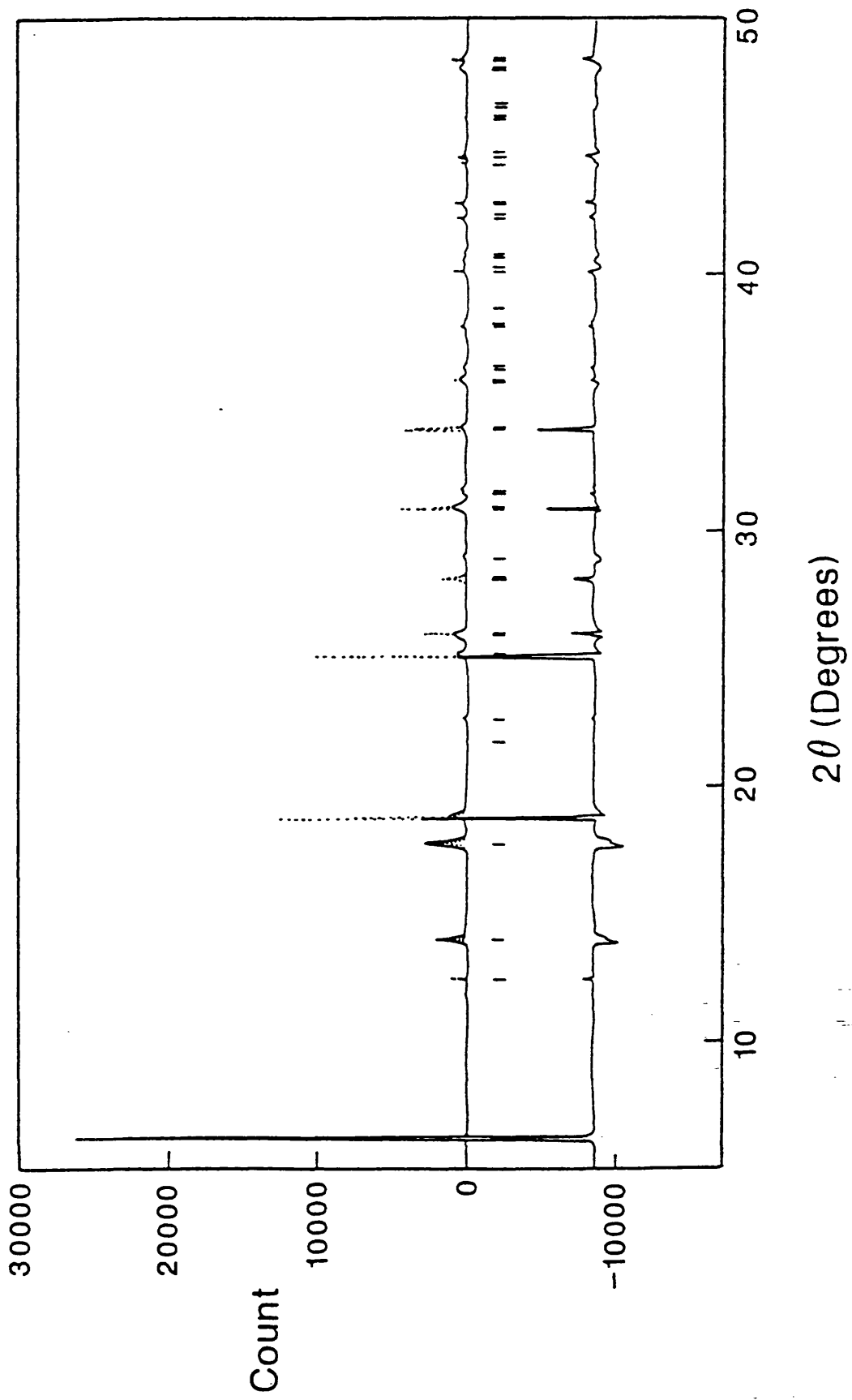
Difference plot of observed and calculated
diffraction patterns for CH_3HgCl (I)

Broken line - observed pattern

Solid line - calculated pattern

D - difference plot

'|' - peak positions



The original model postulated that Hg, Cl and C all were sited on special positions $2c$ in the primitive space group. The scattering cross-section of Cl and C from x-rays is sufficiently similar to allow the interchange of these two atoms between their special positions which could produce confusion in the refinement of the structure. The original space group is possibly incorrect giving extra intensity to some peaks whilst still fulfilling the geometric constraints of the tetragonal symmetry. The neutron scattering lengths of Cl and C are approx. 6 and 9 respectively. A neutron diffraction study may well yield much more fruitful results since the site occupancy of these two atoms could not be inter-changed without significant intensity alterations in the observed pattern. Another possible solution could be found in collecting many more data with x-rays and attempting structure solution *ab initio* using the conventional methods of single crystal diffraction data.

In conclusion, without good single crystals of CH_3HgCl in the ambient phase, and access to further neutron or x-ray powder data, this structure cannot be solved to an acceptable level. However, the work presented here challenges the original analysis and should be further investigated using the complementary techniques outlined above.

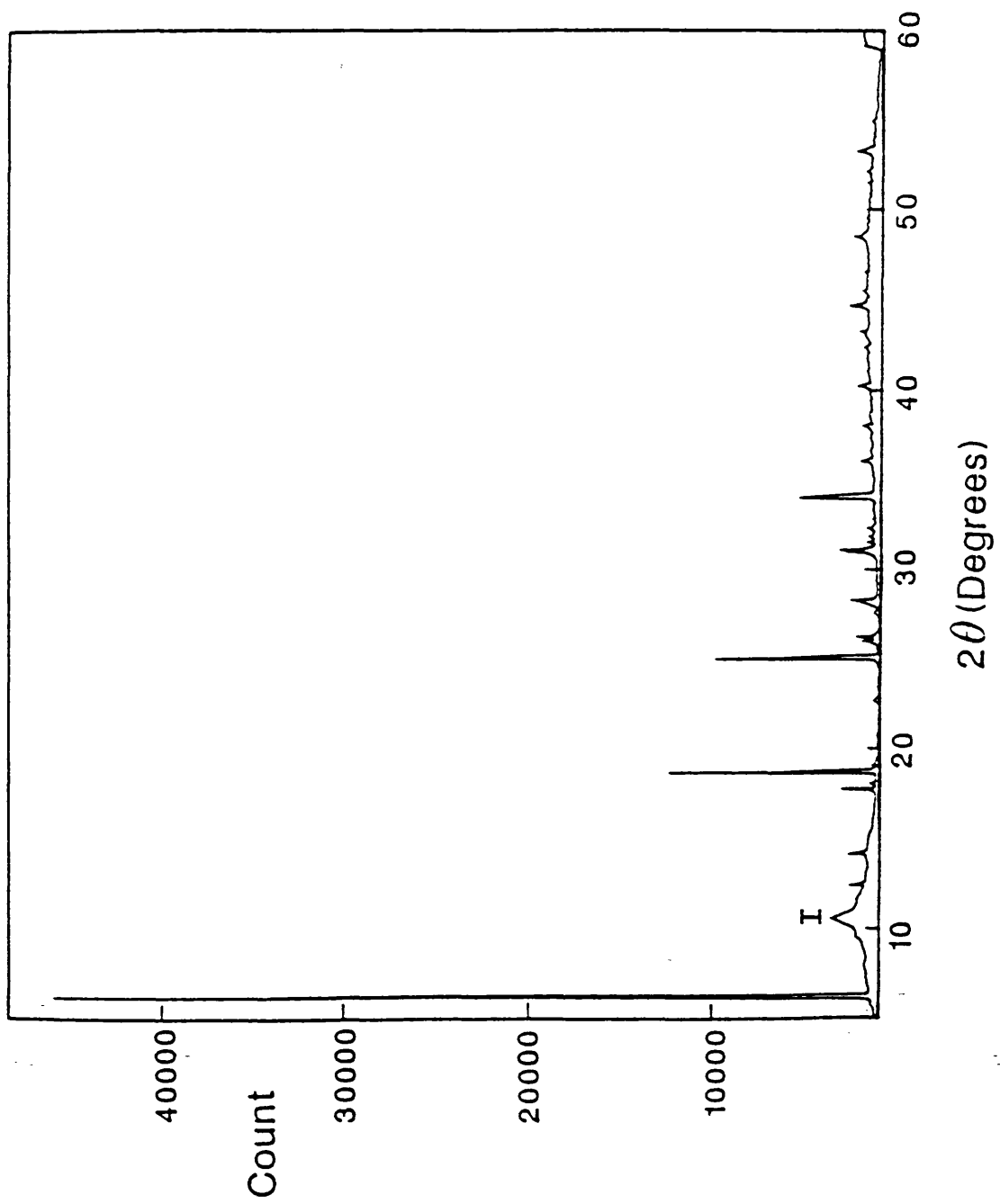
6.2.5 Analysis of Low temperature phase data

The diffraction pattern obtained from the sample of CH_3HgCl at 75 K is shown in Figure 6.7. The pattern bears a strong resemblance to that collected at higher temperature. However, some peak splitting and intensity variation suggests entry into a new phase. The structure of this phase is unknown but the peak positions (hence the inter-planar spacings) can be measured. Bragg peaks were fitted in turn to a pseudo-Voigt function and their positions calculated. 37 reflections were measured successfully. The pattern was initially indexed using a computer program written by Visser [12] based on a method proposed by de Wolff [13]. The most promising solution was a monoclinic unit ($a = 4.857$, $b = 9.311$, $c = 3.460$ Å, $\beta = 109.64^\circ$). The program attempts to index only the first 20 lines from the input data; of these 18 were successfully assigned Miller indices indicating a high degree of success. This cell was further examined using the computer program NEWLAT [14] which yielded another monoclinic cell ($a = 3.46$, $b = 9.311$, $c = 9.151$ Å, $\beta = 91.22^\circ$) having a volume twice that of the parent.

The similarity of the lattice parameters of this transformed cell to those of a tetragonal unit cell prompted further analysis. The lattice constants a and c were interchanged and an average value taken between a' and b giving a 'tetragonal' cell with $a = b = 9.23$, $c = 3.46$ Å and β set to 90° . A prediction of Bragg positions based on this cell was calculated using the locally written computer program POWDER [15]. This

Figure 6.7

Powder diffraction pattern of CH_3HgCl (II)
($T = 75 \text{ K}$, $\lambda = 1.0098 \text{ \AA}$)
I = impurity



prediction allowed the observed data to be re-indexed. These indexed d-spacings were used as input to VARVEC (Chapter 3.2) with a tetragonal Bravais lattice specified. The refined solution was a cell with $a = b = 9.26$, $c = 3.41$ Å. Table 6.7 lists the observed and calculated d-spacings of the 2θ reflections used in the refinement.

6.2.6 Discussion of low temperature phase results

Adams and Pogson [1] suggest the I/II phase transition is first order in type and related to a cell doubling of the $Z = 2$ asymmetric unit to that of the analogous ambient bromide phase. The tetragonal cell refined for the low temperature phase of the chloride (above) agrees with this conclusion. The density of CH_3HgCl I is 4.16 gcm^{-3} at s.t.p.; this quantity is calculated using the refined cell with $Z = 4$ at 75 K to be $\sim 5.7 \text{ gcm}^{-3}$. The material is expected to be more dense after the transition and the latter value is reasonable. However, it seems improbable that the unit cells of the chloride (phase II) and ambient bromide belong to the same space group. The first (and most intense) reflection in the chloride pattern is the 100 at 6.27° (2θ). If the chloride had the space group $P\bar{4}2_1m$ the first reflection would be the 110 at 8.84° since 100 is absent.

The powder data collected cannot be used to decide the space group of phase II unambiguously between the proposed tetragonal or re-set monoclinic cell. Indeed, in the tetragonal case the Laue symmetry of the space group could be either $P4/m$ or $P4/mmm$; the one dimensional nature of powder data cannot distinguish between the two. Although 37 reflections were measured in the low temperature pattern this is only a fraction of the expected Bragg peaks for either Bravais type. There are too few data indexed unambiguously to show the specific groups of reflections which allow the conditions limiting possible reflections to be observed; hence selection from the possible space groups cannot be made.

In conclusion, CH_3HgCl II appears to show tetragonal or pseudo-tetragonal (monoclinic) symmetry with a tetra-molecular unit cell. These results support the previous Raman work but the definitive space group of the low temperature phase of this material remains unknown.

Table 6.7 Observed and calculated values of d_{hkl} for $\text{CH}_3\text{HgCl II}$ (tetragonal model)

| hkl | $d_{(\text{obs})}$ | $d_{(\text{calc})}$ |
|-------|--------------------|---------------------|
| 1 0 0 | 9.3380 | 9.2604 |
| 2 0 0 | 4.6610 | 4.6302 |
| 1 2 0 | 4.1100 | 4.1414 |
| 2 2 0 | 3.2620 | 3.2740 |
| 1 0 1 | 3.2130 | 3.1997 |
| 3 0 0 | 3.1050 | 3.0868 |
| 1 1 1 | 3.0370 | 3.0243 |
| 1 3 0 | 2.9250 | 2.9284 |
| 3 2 0 | 2.5680 | 2.5684 |
| 4 0 0 | 2.3280 | 2.3151 |
| 3 0 1 | 2.2870 | 2.2884 |
| 4 1 0 | 2.2470 | 2.2460 |
| 3 1 1 | 2.2320 | 2.2216 |
| 4 2 0 | 2.0750 | 2.0707 |
| 4 0 1 | 1.8940 | 1.9153 |
| 4 1 1 | 1.8850 | 1.8756 |
| 3 4 0 | 1.8620 | 1.8521 |
| 3 3 1 | 1.8410 | 1.8383 |
| 5 1 0 | 1.8170 | 1.8161 |
| 4 4 0 | 1.6310 | 1.6370 |

References

1. Adams D.M. and Pogson M., 1988, *J. Phys. C:Solid State Phys.*, **21**, 1065-1079
2. Russell D.R., 1983, *STOWK: Program for analysis of STADI2 data*, University of Leicester
3. Sheldrick G.M., 1976, *SHELX76: Program for crystal structure determination*, University of Cambridge
4. Renniger M., 1937, *Z. Physik.*, **106**, 141
5. Grdenic D.R. and Kitaigorodskii A.I., 1949, *Zhur. Fiz Khim.*, **23**, 1161-1166
6. Wells A.F., 1975, "Structural Inorganic Chemistry". Clarendon Press, Oxford, 921
7. Russell D.R., 1987, *Private Communication*
8. Russell D.R., 1985, *GEOM: Program for molecular geometry calculations*, University of Leicester
9. Thomas M.W. and Bendall P.J., 1978, *Acta Cryst.*, **A34**, S351
10. Bendall P.J., Fitch A.N. and Fender B.E., 1983, *J. Appl. Cryst.*, **16**, 164
11. Cernik R.J. and Murray A., 1988, *Private Communication*
12. Visser J.W., 1969, *J. Appl. Cryst.*, **2**, 89
13. Wolff de, 1957, *Acta Cryst.*, **10**, 590
14. Mugnoli A., 1985, *J. Appl. Crystallgr.*, **18**, 183
15. Russell D.R., 1978, *POWDER: Program for powder pattern calculations*, University of Leicester

APPENDIX 1

Source code listing of program VARVEC

The function of this computer program is to refine the unit cell parameters of a given crystal system, at different pressures, by fitting calculated inter-layer (d) spacings to indexed observed data. These input data are calculated from the measured Bragg peak centroids observed in either an angle or energy dispersive x-ray powder pattern. The least squares procedure used in the refinement is non-linear and is described in Chapter 3. Hence, the program requires starting values for the unit cell (lattice) parameters.

VARVEC was written in FORTRAN 77 on a DEC Vax 8600 mainframe computer. The program is menu-driven with a help facility. Only one input data file is required and two output files are produced. The content and format of these files are explained in Chapter 3. The starting values given by the user are checked to ensure they agree with the lattice system specified. One subroutine, SECURE, is very specific to the VMS operating system but may be omitted. Two NAG (Numerical Algorithms Group) library subroutines are used to solve linear equations and invert matrices. Chapter 3 includes a summary of the important subroutine functions. The source code contains comments throughout.

Program Varvec

```
c -----
c
c *****
c *
c * Author: Andy Heath *
c * University of Leicester *
c * Date: 20/1/87 *
c * Last *
c * Update: 2/3/88 *
c *
c *****
c
c
c
c MODULES used are all subroutines (in FORTRAN77).
c Modules are in alphabetic order and are:
c CALCON
c CHARCK
c CHECK
c DCALC
c ECHO
c ERROR
c FO1ABF (from NAG fortran library)
c FO4AAF (from NAG fortran library)
c HELP
c HEXA
c INTSUM
c LOTOUP
c MENOUT
c MENU
c MONO
c ORTHO
c OUTPUT
c RHOMB
c SETMAT
c SECURE
c SOLVE
c TETRA
c TRIC
c
c All variables are specified at the beginning of each module.
c All format statements are in the order in which they are used
c (as much as possible).
```

```

c All format statements are at the beginning of any module which
c contains any I/O to disk or terminal.
c FORMAT labels start at 100 and increase monotonically.
c GOTO labels are few and have values between 1 and 10
c ERROR labels have the value 999
c
c
c          ***** MAIN PROGRAM BEGINS *****
c
c
common /index/index(100),dspace(100),line(79),dc(100)
common /param/latpar(6),sd(6),vol,sv
common /matrix/mat(7,7),inv(7,7),vec(7,1),corec(7,1)
common /infil/infile,title
real*8 mat,inv,vec,corec,oldpar(6),latpar,param(7)
real*8 pres,dspc(100),sd,R,Gmin
integer nob, temp(100),ncycle,iflag2,ESC
integer index,npres,ncol,ixtal,nindex,nout
character infile*20,line*1,go*1,title*80
data nout /6/
c
100 format(1h$,a1,'[3;1H',a1,'[?J')
101 format(1h$,a1,'[10;4H',a1,'#6',
*      a1,'[1mProcessing ...',a1,'[0m',$)
102 format(1h$,a1,'[12;4H',a1,'#6Requested input file: ',a1,
& '[1m',a20,a1,'[0m',a1,'[13;4H',a1,'#6',
& 'cannot be opened - check access and spelling.'//)

103 format(1h$,a1,'[23;1H',a1,'#6',a1,
& '[1mPress return to continue...',a1,'[0m')
104 format(1h$,a1,'[62;1"p',a1,'[?71',a1,'[?3h')
c
ESC = 27
c
c Set the terminal up to the correct type and settings
c
write(nout,104) ESC,ESC,ESC
c
c Create LINE marker
c
do i = 1,79
  line(i) = '-'
enddo
c

```

```

c Set HELP flag to zero to precipitate interactive additions to the
c menu. I.e. flag is reset if a default menu is loaded from disk.
c
ihelp = 0
c
c Execute front end of program - i.e. menu system
c
  2 Call menu(ncol,ixtal,oldpar,infile,ihelp)
c
c Check the information given is consistent
c
Call Check(ixtal,oldpar,ncol,infile,iflag3)
c
c Check the value of FLAG3: a value of 1 indicates that CHECK found
c an error with the input parameters and will have given the user
c a relevant error message. Thus, return and reload the menu to allow
c modifications to take place.
c
c Set HELP flag to 1 to indicate to MENU to reload previous menu
c from scratch file on disk.
c
if (iflag3.eq.1) then
  ihelp = 1
  goto 2
endif
c
c All input parameters are now OK and hence program can now
c be executed.
c
write(nout,100) ESC,ESC
write(nout,101) ESC,ESC,ESC,ESC
c
c Open unit 1 (INPUT) as the d-space file, unit 2 (OUTPUT) as the main
c output file, unit 3 (OUTPUT) as the datagraf formatted file for plotting
c results.
c
open(unit=1,file=infile,status='old',err=999)
open(unit=2,file=infile//'.out',status='new')
open(unit=3,file=infile//'.grf',status='new')
c
c Write out OUTPUT file header
c
iflag2 = 2
call output(nobs,Gmin,pres,ncycle,iflag2,r,

```

```

*           npres,nparam,ixtal)
c
c Set error flag FLAG2 to zero - this indicates an error:
c
c 1) in a Bravias routine if the number of degrees of freedom
c    for the least squares is insufficient.
c 2) if the output file header is to be written.
c 3) if the output file END-OF-FILE marker is to be written.
c
iflag2 = 0
c
c Read title
c
read(1,'(a80)') title
c
c Read in the hkl's for each dspacing from INPUT file
c
nindex = ncol*3
read(1,*) (temp(i),i=1,nindex)
c
c Set Number of pressure records to zero
c
npres = 0
c
c Read in record of pressure and d(hkl)
c Begin main loop to work down the INPUT file.
c

  1 read(1,*,end=10) pres,(dspc(i),i=1,ncol)
c
c Count number of pressures
c
npres = npres+1
c
c Find any missing data in the dspacings at the given pressure and
c arrange dspace and index arrays accordingly.
c Therefore, count the number of observed d-spacings.
c
nobs = 0
c
do ii = 1,ncol
  if (dspc(ii).ne.0.0) then
    nobs = nobs+1
  do i = 1,3

```

```

        npti = (nobs*3-3)+i
        nptt = (ii*3-3)+i
        index(npti) = temp(nptt)
    enddo
        dspace(nobs) = dspc(ii)
    endif
enddo
c
c Call the appropriate Bravias routine for the structure given.
c This is dependant on the value of IXTAL.
c
If (ixtal.eq.1) then
    call tric(nobs,Gmin,ncycle,R,iflag2)
    nparam = 6
else if (ixtal.eq.2) then
    call mono(nobs,Gmin,ncycle,R,iflag2)
    nparam = 4
else if (ixtal.eq.3) then
    call hexa(nobs,Gmin,ncycle,R,iflag2)
    nparam = 2
else if (ixtal.eq.4) then
    call rhomb(nobs,Gmin,ncycle,R,iflag2)
    nparam = 2
else if (ixtal.eq.5) then
    call ortho(nobs,Gmin,ncycle,R,iflag2)
    nparam = 3
else
    call tetra(nobs,Gmin,ncycle,R,iflag2)
    nparam = 2
endif
c
c Output the processed information into OUTFILE for each pressure
c
call output(nobs,Gmin,pres,ncycle,iflag2,r,
           *           npres,nparam,ixtal)
c
c Reset error flag (if necessary)
c (e.g. if a Bravias routine encountered a sparse data record)
c
iflag2 = 0
c
c Repeat with the next pressure
c
goto 1

```

```

c
c Control comes here when pointer reaches the end of INPUT data file.
c Hence, end of main program.
c
c Set IFLAG2 to indicate to OUTPUT to write END-OF-FILE marker
c
  10   continue
c
c Check SECURITY before closing OUTPUT file.
c
Call Secure(2)

iflag2 = 3
call output(nobs,Gmin,pres,ncycle,iflag2,r,
           *          npres,nparam,ixtal)
iflag2 = 0
c
c Close all input and output channels.
c
close (1)
close (2)
close (3)
c
c Return control to the menu for further I/O or to allow
c the user to save the set menu.
c
ihelp = 1
goto 2
c
c Error message sent out if input file (d-spacing data file)
c is inaccessible for any reason.
c
  999   write(nout,102) ESC,ESC,ESC,infile,ESC,ESC,ESC
write(nout,103) ESC,ESC,ESC,ESC
read(5,'(a)') go
ihelp = 1
goto 2
c
End
c
c          ***** END OF MAIN PROGRAM *****
c
c-----
c

```

```

Subroutine Calcon(d,delta,G,Rtop,Rbot,w)
c -----
c
c Calculate Condition factors for each iteration
c
real*8 d,delta,G,Rtop,Rbot,w
c
c Decide on a criterion for the weighting factor
c
w = d**2
c
G = G + w*(delta**2)
Rtop = Rtop + w*(delta**2)
Rbot = Rbot + w*(1/d)**4
c
Return
End
c
c-----
c
Subroutine Charck(string,ierr)
c -----
c
integer ierr
character string*20
c
c Set error flag to zero value before checking the input
c
ierr = 0
c
c Check to see if user has entered option code and nothing else.
c
if (string(1:8).eq.'          ') then
  ierr = 1
  return
endif
c
c Check string which should be a number for any characters
c which may cause an internal conversion error.
c
do i = 1,20
  if (string(i:i).lt.'0'.or.string(i:i).gt.'9') then
    if (string(i:i).ne.' ') then
      if (string(i:i).ne.' ') then

```

```

ierr = 1
return
    endif
endif
endif
enddo
c
return
end
c
c-----
c
Subroutine Check(ixtal,oldpar,hklmax,infile,iflag3)
c-----
c
common /param/latpar(6),sd(6),vol,sdv
real oldpar(6)
real*8 latpar,sd
integer ixtal,iflag3,ierror,hklmax,ihelp,ierr1,ierr2,ierr3
character infile*20
c
c Routine to check the input parameter data against the type of
c Bravis lattice requested. If parameters are missing they are filled
c in with default values.
c
c Set all internal error flags to zero
c
ierr1 = 0
ierr2 = 0
ierr3 = 0
c
c For orthorhombic lattice case
c All vectors should be non-zero
c
If (ixtal.eq.5) then
do i = 1,3
if (oldpar(i).eq.0.0) then
ierr1 = 5
ierr2 = 1
goto 10
else
latpar(i) = oldpar(i)
endif
endif
enddo

```

```

c
c All angles should be 90.0 degrees
c
do i = 4,6
  if (oldpar(i).ne.90.0) then
    if (oldpar(i).ne.0.0) then
      ierr1 = 5
    ierr2 = 2
      goto 10
    endif
  endif
  latpar(i) = 0.0
enddo

c
c For rhombohedral lattice case
c All vectors should be equal and non-zero
c
else if (ixtal.eq.4) then
  if(oldpar(1).eq.0.0) then
    ierr1 = 4
    ierr2 = 1
    goto 10
  endif
  do i = 1,3
    if(oldpar(1).ne.oldpar(i)) then
      if (oldpar(i).ne.0.0) then
        ierr1 = 4
      ierr2 = 1
        goto 10
      endif
    else
      latpar(1) = oldpar(1)
    endif
  enddo

c
c All angles should be equal and non-zero
c
if (oldpar(4).eq.0.0) then
  ierr1 = 4
  ierr2 = 2
  goto 10
endif
do i = 4,6
  if(oldpar(4).ne.oldpar(i)) then

```

```

        if (oldpar(i).ne.0.0) then
            ierr1 = 4
ierr2 = 2
            goto 10
        endif
        else
            latpar(2) = oldpar(4)
        endif
    enddo
c
c For hexagonal case
c a = b <> 0 and c should be non-zero
c
else if (ixtal.eq.3) then
    if (oldpar(1).eq.0.0.or.oldpar(3).eq.0.0) then
        ierr1 = 3
        ierr2 = 1
        goto 10
    else if (oldpar(1).ne.oldpar(2)) then
        ierr1 = 3
        ierr2 = 1
        goto 10
    else
        latpar(1) = oldpar(1)
        latpar(2) = oldpar(3)
    endif
c
c alpha = beta = 90.0 degrees and gamma = 120.0 degrees
c
do i = 4,5
    if (oldpar(i).ne.90.or.oldpar(i).ne.0.0) then
        ierr1 = 3
        ierr2 = 2
        goto 10
    endif
enddo
if (oldpar(6).ne.120.0) then
    ierr1 = 3
    ierr2 = 2
    goto 10
endif
c
c For Monoclinic lattice case
c All vectors should be non-zero

```

```

c
else if (ixtal.eq.2) then
  do i = 1,3
    if (oldpar(i).eq.0.0) then
      ierr1 = 2
      ierr2 = 1
      goto 10
    else
      latpar(i) = oldpar(i)
    endif
  enddo
c
c alpha = gamma = 90.0 (second monoclinic setting) and beta non-zero
c
  if (oldpar(5).eq.0.0) then
    ierr1 = 2
    ierr2 = 2
    goto 10
  endif
  do i = 4,6
    if (oldpar(i).ne.90.0) then
      if (oldpar(i).ne.0.0) then
        if (i.ne.5) then
          ierr1 = 2
          ierr2 = 2
          goto 10
        else
          latpar(4) = oldpar(5)
        endif
      endif
    endif
  enddo
c
c For tetragonal case
c
else if (ixtal.eq.6) then
  do i = 1,3
    if (oldpar(i).eq.0.0) then
      ierr1 = 6
      ierr2 = 1
      goto 10
    endif
  enddo
  latpar(1) = oldpar(1)

```

```

    latpar(2) = oldpar(3)
c
c All angles should be 90.0 degrees
c
  do i = 4,6
    if (oldpar(i).ne.90.0) then
      if (oldpar(i).ne.0.0) then
        ierr1 = 6
      ierr2 = 2
      goto 10
    endif
  endif
  latpar(i) = 0.0
enddo
c
c For anything else which has yet to be commissioned
c
else
  ierr3 = 1
  ierr1 = ixtal
  goto 10
endif
c
c Set error flag to zero - this prohibits recalling of MENU
c
iflag3 = 0
c
  return
c
c Come here on error with input parameters
c Error routine delivers error message and flags are set up
c to save the previous menu, recall the drawing of a menu and
c cause the new menu to be taken from the scratch file created
c by routine MENOUP.
c
  10  call error(ierr1,ierr2,ierr3)
ihelp = 1
call menout(hklmax,ixtal,oldpar,infile,ihelp,proc)
iflag3 = 1
c
return
end
c
c-----

```

```

c
Subroutine Dcalc(nobs,rca,rcb,rcc,ral,rbe,rga)
c -----
c
c Calculate dspacing for each observed hkl reflection from refined
c lattice parameters and compare with observed with respect to
c standard deviation of delta(hkl) function.
c
common /index/index(100),dspace(100),line(79),dc(100)
real dspace,dc,dcal,ra(3),rv(3),rca,rcb,rcc
real ral,rbe,rga
integer index,h(3),i,j,k,ii
character line*1
c
rv(1) = rca
rv(2) = rcb
rv(3) = rcc
ra(1) = ral
ra(2) = rbe
ra(3) = rga
c
do 20 ii = 1,nobs
  dcal = 0.0
  npoint = (3*ii-3)
  do 10 i = 1,3
    h(i) = index(npoint+i)
    dcal = dcal + (h(i)**2)*(rv(i)**2)
  10 continue
  do 15 i = 1,3
    j = MOD(i,3) + 1
    k = MOD(j,3) + 1
    dcal = dcal + 2*h(j)*h(k)*rv(j)*rv(k)*cosd(ra(i))
  15 continue
  dc(ii) = 1/sqrt(dcal)
  20 continue
c
return
end
c
c-----
c
Subroutine Echo(on)
c
c Description:

```

```

c Routine causes terminal to switch in and out of NOECHO mode for
c password entries. Very device dependant and will only work
c with a VAX. The other possible method is to use RTL calls to
c the LIB$ library routines but although this is successful it
c is time consuming and uses large CPU.

```

```

c
include '($todef)'
integer istat,sys$qiow,sys$assign,bw2,on,sys$dassgn
integer*2 iosb(4),bw1(2)
external io$_setmode,io$_sensemode
character*3 devnam
character*1 buffer(8)
equivalence (bw1(1),buffer(1)), (bw2,buffer(5))
data devnam /'TT:'/

```

```

c
c Assign the terminal
c
istat=sys$assign(devnam,%ref(ichan),)
if(.not.istat) call lib$signal(%val(istat))
c
c Sense the current characteristics
c
istat=sys$qiow(%val(ichan),io$_sensemode,iosb,,
& %ref(buffer),%val(8),,,)
if(.not.istat) call lib$signal(%val(istat))
c
c Modify and reset characteristics
c
bw1(2)=132
if (on.eq.1) then
  bw2=ibset(bw2,TT$V_NOECHO) ! IBSET TO INVOKE
  istat=sys$qiow(%val(ichan),io$_setmode,iosb,,
& %ref(buffer),%val(8),,,)
else
  bw2=ibclr(bw2,TT$V_NOECHO) ! IBCLR TO CANCEL
  istat=sys$qiow(%val(ichan),io$_setmode,iosb,,
& %ref(buffer),%val(8),,,)
endif
c
if(.not.istat) call lib$signal(%val(istat))
istat=sys$dassgn(%val(ichan))
if(.not.istat) call lib$signal(%val(istat))
c

```

```

Return

```

```

      End
c
c-----

c
Subroutine Error(ierr1,ierr2,ierr3)
c -----
c
integer   ierr1,ierr2,ierr3,ESC,BELL
character system(6)*12,errpar(2)*6,go*1,info(2,6)*31
data      system(1) /'triclinic'/,system(2)
*          /'monoclinic'/,
*          system(3) /'hexagonal'/,system(4)
*          /'rhombohedral'/,
*          system(5) /'orthorhombic'/,system(6)
*          /'tetragonal'/
data      errpar(2) /'angle'/, errpar(1) /'vector'/
data      info(2,4) /'alpha = beta = gamma; alpha<>0 '/,
*          info(1,4) /'a = b = c; a non-zero      '/,
*          info(2,5) /'alpha = beta = gamma = 90  '/,
*          info(1,5) /'a, b, c, <> 0.0          '/,
*          info(2,2) /'alpha = gamma = 90 <> beta <> 0'/,
*          info(1,2) /'a, b, c, <> 0.0          '/,
*          info(1,3) /'a = b <> c all non-zero    '/,
*          info(2,3) /'alpha = beta = 90, gamma = 120 '/,
*          info(1,6) /'a = b <> c all non-zero    '/,
*          info(2,6) /'alpha = beta = gamma = 90  '/
data      nout      /6/, ESC /27/, BELL /7/
c
c Print error message to screen dependant on the value of IERR1,2,3
c
100  format(1h$,a1,'[H',a1,'[2J')
101  format(1h$,a1,'[3;25H',a1,'#6',a1,a1,'[7m INPUT ERROR DETECTED
,
*          ,a1,'[0m')
102  format(///1h$,a1,'#6',
* 'Error detected .. Parameter input is not consistent with the
,/'
* 1h$,a1,'#6',
* 'crystal system specified.'//
* 1h$,a1,'#6',
* 'System specified was ',a1,'[1m',a12,a1,'[0m',
* ' and ',a1,'[1m',a6,a1,'[0m', ' data is inconsistent'/
* 1h$,a1,'#6',

```

```

* 'with the symmetry demanded by this lattice type. '//)
103 format(1h$,a1,'#6','The ',a6,
* ' data should have ',a31)
104 format(1h$,a1,'[23;1H',a1,'#6',a1,
* '[1mPress return to continue...',a1,'[0m')
105 format(///1h$,a1,'#6','Program not yet commissioned for the
',
* a1,'[1m',a12,a1,'[0m crystal system. '//
* 1h$,a1,'#6','Consult author about implementing this
* new routine. ')
106 format(//1h$,a1,'#6','This error will be corrected for you. ')
c
c IERR1 holds the code for the lattice type
c IERR2 holds the code for the type of cock-up (1=vector, 2=angle)
c IERR3 has a value of 1 if a Bravias routine dosen't yet exist
c
write(nout,100) ESC,ESC
write(nout,101) ESC,ESC,BELL,ESC,ESC
if (ierr3.eq.1) then
write(nout,105) ESC,ESC,system(ierr1),ESC,ESC
goto 10
endif
write(nout,102) ESC,ESC,ESC,ESC,system(ierr1),ESC,
* ESC,errpar(ierr2),ESC,ESC
write(nout,103) ESC,errpar(ierr2),info(ierr2,ierr1)
write(nout,106) ESC
10 write(nout,104) ESC,ESC,ESC,ESC
read(5,'(a)') go
write(nout,100) ESC,ESC
c
return
end
c
c-----
c
Subroutine Help
c -----
c
integer ESC,BELL
character go*1
data ESC /27/, BELL /7/
c
100 format(1h$,a1,'[2J')
101 format(1h$,a1,'[1;25H',a1,'#6',a1,'[7m ON-LINE HELP ',a1,'[0m')

```

```

102  format(//1h$,a1,'#6',
      &'Data file should contain powder peaks measured in units'/
      & 1h$,a1,'#6',
      & 'of angstroms. The file should have INDEXS of each row of'/
      & 1h$,a1,'#6',
      & 'data as the first record and the following records are'/
      & 1h$,a1,'#6',
      & 'formatted such that (eg. Pressure) is followed by columns'/
      & 1h$,a1,'#6',
      & 'of D-SPACINGS. XS refers to the Bravias lattice type'/
      & 1h$,a1,'#6',
      & '(i.e. Orthorhombic, triclinic, etc.) and are coded thus: '//
      & 1h$,a1,'#6',
      & '  TRICLINIC      1  MONOCLINIC    2   HEXAGONAL      3'//
      & 1h$,a1,'#6',
      & '  RHOMBOHEDRAL  4  ORTHORHOMBIC  5   TETRAGONAL     6'//
      & 1h$,a1,'#6',
      & 'The max no. hkls refers to the greatest number of indexed'/
      $ 1h$,a1,'#6',
      & 'd-spacings in any one pressure record.'//))
103 format(1h$,a1,'[23;1H',a1,'#6',a1,a1,
      &          '[1mPress return to continue...',a1,'[0m')

```

```

c
c Draw help page
c
write(6,100) ESC
write(6,101) ESC,ESC,ESC,ESC
write(6,102) ESC,ESC,ESC,ESC,ESC,ESC,ESC,ESC,ESC,ESC
write(6,103) ESC,ESC,BELL,ESC,ESC
read(5,'(a)') go
write(6,100) ESC
c
return
end
c
c-----
c
Subroutine Hexa(nobs,G,ncycle,R,iflag2)
c -----
c
c Calculate delta,partial derivatives, and sets of linear equations
c for the hexagonal bravias system.
c

```

```

c
common /index/index(100),dspace(100),line(79),dc(100)
common /param/latpar(6),sd(6),vol,svd
common /matrix/mat(7,7),inv(7,7),vec(7,1),corec(7,1)
real*8 inv,R,Rtop,Rbot,latpar,sd,w,G,delta,d,mat
real*8 part1(3),param(3),dummy1(10,10),dummy2(10,10)
integer npoint,ncycle,nobs,iflag1,iflag2,nparam
c
c Set up number of parameters in iteration
c
nparam = 2
c
c Check for singularity of sparsity in matrix to be produced
c (i.e. the no. of degrees of freedom of the least squares is sufficient)
c
if (nobs.le.nparam) then
  iflag2 = 1
  return
endif
c
c Create fitting parameters from guessed lattice parameters
c
param(1) = 2.0/(latpar(1)*sqrt(3.0))
param(2) = 1.0/latpar(2)
c
ncycle = 0
c
c Initialise Variables to be summed to zero
c
1    Call Intsum(G,R,Rtop,Rbot,Delta)
c
c Count number of iterations
c
ncycle = ncycle + 1
c
c Start main loop over all the data at pressure P
c
Do 10 ii = 1,nobs
c
d = dspace(ii)
c
c Calculate partial derivatives of the equation
c
npoint = (3*ii-3)

```

```

X = (index(npoint+1)**2 + index(npoint+2)**2
      & + index(npoint+1)*index(npoint+2) )
part1(1) = -2.0 * X * param(1)
part1(2) = -2.0 * (index(npoint+3)**2) * param(2)
c
c Calculate the minimum function
c
delta = X * (param(1)**2) +
      & (index(npoint+3)**2) * (param(2)**2)
c
c Calculate condition factors
c
Call Calcon(d,delta,G,Rtop,Rbot,w)
c
c Set up linear equations of the form Ax=B
c
Call Setmat(part1,delta,w,nparam)
c
10 continue
c
c Solve set of linear equations
c
idum = nparam+1
c
Call Solve(param,nparam,nobs,G,ncycle,idum,iflag1,
      * dummy1,dummy2)
c
c Test iflag1 to see if reiteration is necessary (1=re-iterate)
c
If (iflag1.eq.1) goto 1
c
c Calculate standerd deviation on final parameter values
c and reform into origanal parameter type
c
latpar(1) = 2.0/(param(1)*sqrt(3.0))
latpar(2) = sqrt(1/param(2))
sd(1) = sqrt((4.0/(3.0*(param(1)**4)))*(G**2)*Inv(1,1))
sd(2) = sqrt((1.0/(4.0*(param(2)**3)))*Inv(2,2)*(G**2))
c
c Calculate the cell volume and the standard deviation on this result
c
vol = (latpar(1)**2) * latpar(2) * sqrt(1.5)
sdv = (latpar(2)*latpar(3)*sqrt(1.5))**2*sd(1)**2
      * + (latpar(1)*latpar(3)*sqrt(1.5))**2*sd(2)**2

```

```
      *      + (latpar(1)*latpar(2)*sqrt(1.5))**2*sd(3)**2
```

```
sdv = sqrt(sdv)
```

```
c
```

```
c Calculate the R factor
```

```
c
```

```
R = sqrt((Rtop/Rbot))*100
```

```
c
```

```
Return
```

```
End
```

```
c
```

```
c-----
```

```
c
```

```
Subroutine Intsum(G,R,Rtop,Rbot,Delta)
```

```
c -----
```

```
c
```

```
c Initialise variables to be summed over each iteration
```

```
c Set all original matrix elements to zero
```

```
c
```

```
common /matrix/mat(7,7),inv(7,7),vec(7,1),corec(7,1)
```

```
real*8 mat,inv,vec,corec,G,R,Rtop,Rbot,Delta
```

```
c
```

```
    G = 0.0
```

```
R = 0.0
```

```
Rtop = 0.0
```

```
Rbot = 0.0
```

```
Do 10 i = 1,7
```

```
    vec(i,1) = 0.0
```

```
    corec(i,1) = 0.0
```

```
    Do 10 j = 1,7
```

```
        mat(i,j) = 0.0
```

```
        inv(i,j) = 0.0
```

```
    10 continue
```

```
c
```

```
Return
```

```
End
```

```
c
```

```
c-----
```

```
c
```

```
Subroutine lotoup(opt)
```

```
c -----
```

```
c
```

```
c Takes a character, finds it's ascii value, into the uppercase
```

```
c value if necessary, and returns the uppercase character.
```

```
c
```

```

character*20 opt
c
  idiff = ichar('a') - ichar('A')
c
do 10 i=1,20
  if(opt(i:i) .ge. 'a' .and. opt(i:i) .le. 'z') then
    opt(i:i) = char(ichar(opt(i:i)) - idiff)
  endif
  10 continue
c
return
end
c
c-----
c
Subroutine menout(hklmax,ixtal,oldpar,infile,ihelp,proc)
c -----
c
common /files/menoutfil
real      oldpar(6)
integer   hklmax,ixtal,ihelp,proc
character infile*20,optcod(9)*2,menoutfil*20
Data optcod(1) /'DN'/,optcod(2) /'LA'/,optcod(3) /'LB'/,
  &      optcod(4) /'LC'/,optcod(5) /'AA'/,optcod(6) /'AB'/,
  &      optcod(7) /'AG'/,optcod(8) /'XS'/,optcod(9) /'NI'/
c
  100  format(a2,1x,a20)
  101  format(a2,1x,f7.3)
  102  format(a2,1x,i2)
c
c Simply write out the present menu to a scratch file in the same
c format that would be expected from the user_input and then
c it's quite straight forward to redirect the input channel to the
c scratch file.
c
c Create default parameters dependant on the value of IXTAL and
c what the user has already given.
c
if (proc.eq.1) goto 2
if (ihelp.eq.1.and.ixtal.ne.0) then
  if (ixtal.eq.6) then
    oldpar(2) = oldpar(1)
    do i = 4,6
      oldpar(i) = 90.0

```

```

        enddo
    else if (ixtal.eq.5) then
        do i = 4,6
            oldpar(i) = 90.0
        enddo
    else if (ixtal.eq.4) then
        do i = 1,3
            oldpar(i) = oldpar(1)
        enddo
        do i = 4,6
            oldpar(i) = oldpar(4)
        enddo
    else if (ixtal.eq.3) then
        do i = 1,2
            oldpar(i) = oldpar(1)
        enddo
        do i = 4,5
            oldpar(i) = 90.0
        enddo
        oldpar(6) = 120.0
    else if (ixtal.eq.2) then
        oldpar(4) = 90.0
        oldpar(6) = 90.0
    endif
endif
c
  2 if (ihelp.eq.1) then
    open(unit=10,status='scratch')
    nout = 10
  else
    open(unit=20,file=menoutfil//'.men',status='new')
    nout = 20
  endif
c
c Write out the menu to either a scratch file or a pre-defined
c file to be written to disk and stored for another day
c
  1 write(nout,100) optcod(1),infile
do i=1,6
    write(nout,101) optcod(i+1),oldpar(i)
enddo
write(nout,102) optcod(8),ixtal
write(nout,102) optcod(9),hklmax
if (nout.eq.20) then

```

```

close (20)
open(unit=10,status='scratch')
nout = 10
goto 1
endif
rewind 10
c
return
end
c
c-----
c
Subroutine Menu(hklmax,ixtal,oldpar,infile,ihelp)
c -----
c
common /files/menfil
real fval,oldpar(6)
Integer ESC,BELL,nline,ival,ixtal,hklmax,
& ihelp,ierror,ierr,proc
Character optrec(9)*40,optcod(9)*2,opt*2,val*20,infile*20
Character ans*2,menfil*20
c
c Store all options and codes in character data statements
c
Data optrec(1) /'Data file containing d-spacings' //,
& optrec(2) /'Lattice vector a' //,
& optrec(3) /'Lattice vector b' //,
& optrec(4) /'Lattice vector c' //,
& optrec(5) /'Lattice angle alpha' //,
& optrec(6) /'Lattice angle beta' //,
& optrec(7) /'Lattice angle gamma' //,
& optrec(8) /'Crystal System' //,
& optrec(9) /'Max. no. indexed reflections' //
Data optcod(1) /'DN'/,optcod(2) /'LA'/,optcod(3) /'LB'/,
& optcod(4) /'LC'/,optcod(5) /'AA'/,optcod(6) /'AB'/,
& optcod(7) /'AG'/,optcod(8) /'XS'/,optcod(9) /'NI'/'
Data nout /6/, ESC /27/, BELL /7/
c
100 format(1h$,a1,'[2J')
101 format(1h$,a1,['i1',';8H',a1,'#6',a32)
105 format(1h$,a1,['i2',';8H',a1,'#6',a32)
102 format(1h$,a1,['1A',a1,'[47C',a1,'#6',a2)
106 format(1h$,a1,'[21;11H',a1,'#6', ' Enter Option Code and
& new value:')/

```

```

& 1h$,a1,'#6',a1,'[11CEnter ',a1,'[1mGO',a1,'[0m to execute,'
& ,a1,'[1m HE',a1,'[0mlp,',a1,'[1m SA',a1,'[0mve menu,'
& ,a1,'[1m EX',a1,'[0mit')
107 format(1h$,a1,'[21;46H',,$)
108 format(a2,1x,a20)
109 format(1h$,a1,['',i1,',',51H',f8.4)
110 format(1h$,a1,['',i2,',',51H',f8.4)
111 format(1h$,a1,['',i1,',',51H',a20)
112 format(1h$,a1,['',i2,',',51H',i2)
113 format(1h$,a1,'[21;46H',a1,'[?K')
114 format(1h$,a1,'[1;11H',a1,'#6',a1,'[7m
    &CALCULATION OF CRYSTAL LATTICE PARAMETERS',a1,'[0m')
115 format(1h$,a1,'[3;6H',a1,'#6',,'Do you wish to load
    &a default menu file [N] ? ',,$)
116 format(1h$,a1,'[5;6H',a1,'#6',,'File containing
    * default menu ? ',,$)
117 format(///1h$,a1,'#6',a1,'Requested default menu file: ',
    & a1,'[1m',a20,a1,'[0m',/1h$,a1,'#6',
    & 'does not exist - rerun or enter menu manually'//)
118 format(1h$,a1,'[23;11H',a1,'#6',a1,a1,'[1m INCORRECT RESPONSE
    & - TRY AGAIN',a1,'[0m',,$)
119 format(1h$,a1,'[23;11H',a1,'[0m',a1,'[?J')
120 format(1h$,a1,'[2;1H',a1,'[?J')
121 format(1h$,a1,'[10;6H',a1,a1,'#6
    *Menu file_name for writing to disk ? ',,$)
122 format(1h$,a1,'[23;1H',a1,'#6',a1,
    * '[1mPress return to continue...',a1,'[0m')
123 format(1h$,a1,'[23;11H',a1,'#6',a1,a1,'[1m INPUT/VARIABLE
    & MISMATCH - TRY AGAIN',a1,'[0m',,$)
124 format(1h$,a1,'[!p',a1,'[?31')
c
if (ihelp.eq.1) goto 1
c
6 ierror = 0
c
c Clear the screen and write the program title at the top of the screen.
c
write(nout,100) ESC
write(nout,114) ESC,ESC,ESC,ESC
write(nout,115) ESC,ESC
c
c Inquire if the user wishes to load a default menu file.
c
read(5,'(a)') ans

```

```

call lotoup(ans)
c
c If the answer is affirmative then inquire the menu_file name
c and open the file.
c
if (ans(1:1).eq.'Y') then
  write(nout,116) ESC,ESC
  read(5,'(a)') menfil
  call lotoup(menfil)
  ihelp = 2
  open(unit=11,file=menfil//' .men',status='old',err=999)
endif
c
c Clear the screen of all output except the program title
c
  write(nout,120) ESC,ESC
c
c Execute SECURITY for start of program
c
Call Secure(1)
c
c Start of main routine to draw the menu to the screen
c
  1 if (ihelp.eq.1) write(nout,114) ESC,ESC,ESC,ESC
c
c Loop over 9 times to get all data statements to the screen.
c nline points to correct row on the screen for the output.
c Format specifies either i1 or i2 for the row position in the output
c therefore, must test to see if greater than row 9 has been reached.
c
Do i = 1,9
  nline = 2*i+1
  if (nline.lt.11) then
    write(nout,101) ESC,nline,ESC,optrec(i)
  else
    write(nout,105) ESC,nline,ESC,optrec(i)
  endif
  write(nout,102) ESC,ESC,ESC,optcod(i)
enddo
c
c Write out question banner.
c
write(nout,106) ESC,ESC,ESC,ESC,ESC,ESC,ESC,ESC,ESC,
*          ESC,ESC,ESC,ESC

```

```

c
c Control is returned to this label whenever input is required
c Position cursor after question banner.
c
  2 write(nout,107) ESC
c
c If the 'HELP' option was specified by the user the program reads
in
c the most previous menu from a scratch file opened in MENOUP as unit
10
c
if (ihelp.eq.1) then
  read(10,108,end=3) opt,val
  goto 4
else if (ihelp.eq.2) then
  read(11,108,end=3) opt,val
  goto 4
endif
c
c Read input from terminal for option code and new value for this option.
c
  3 read(5,108) opt,val
c
c If the menu has just been redrawn due to help being asked for then
c destroy the scratch file and reset the help flag (IHELP) back to
zero.
c
if (ihelp.eq.1) then
  close (10)
  ihelp = 0
endif
c
c Here the input is converted to uppercase and the input area in front
c of the original cursor position is cleared.
c Control jumps here if a menu is being loaded from a disk or scratch
file
c i.e. control does not wait for user interference.
c
  4 call lotoup(opt)
write(nout,113) ESC,ESC
c
c If an error has been encountered in the input from either a menu_file
c or the interactive user a message to that effect is displayed.
c The error flag (IERROR) is reset to it's original value of zero.

```

```

c
if (ierror.eq.1) then
  write(nout,119) ESC,ESC,ESC
  ierror = 0
endif
c
c This loop checks the input (from either disk or scratch file or from
the
c interactive user) for errors and then reads in the option values
into
c variables with the correct format corresponding to their station
in life.
c This loop also writes out the updated information in the correct
place
c on the screen in the correct format.
c
Do i = 1,9
c
c Check the inputed option against all options stored in data array
OPTCOD
c
  If (opt.eq.optcod(i)) then
    nline = i*2+1
    if (nline.eq.3) then
c
c Deals with d-space filename
c
      call lotoup(val)
      write(nout,111) ESC,nline,val
      infile = val
      else if (nline.eq.17) then
c
c Deals with the Bravias lattice type code
c
        call charck(val,ierr)
        if (ierr.eq.1) goto 10
        read(val,*) ival
        write(nout,112) ESC,nline,ival
        if (ival.ne.ixtal) then
          ixtal = ival
          ihelp = 1
          call menout(hklmax,ixtal,oldpar,infile,ihelp,proc)
          goto 2
        else

```

```

        ixtal = ival
    endif
    else if (nline.eq.19) then
c
c Deals with maximum nummber of observed d-spacings for any one pressure
c
        call charck(val,ierr)
        if (ierr.eq.1) goto 10
        read(val,*) ival
        write(nout,112) ESC,nline,ival
        hklmax = ival
    else
c
c The only thing that is left here is either a vector or an angle
c
        call charck(val,ierr)
        if (ierr.eq.1) goto 10
        read(val,*) fval
        oldpar(i-1) = fval
        if (nline.lt.11) then
            write(nout,109) ESC,nline,fval
        else
            write(nout,110) ESC,nline,fval
        endif
    endif
c
c Return control to the input-side of things since the option code
c entered was a valid one.
c
        goto 2
    endif
enddo
c
if (opt.eq.'GO') then
c
c 'GO' executes calculations
c
        goto 5
c
else if (opt.eq.'HE') then
c
c Write help to the screen
c
        ihelp = 1

```

```

    call menout(hklmax,ixtal,oldpar,infile,ihelp,proc)
    call help
    goto 1
c
else if (opt.eq.'SA') then
    ihelp = 0
    write(nout,120) ESC,ESC
    write(nout,121) ESC,BELL,ESC
    read(5,'(a)') menfil
    call menout(hklmax,ixtal,oldpar,infile,ihelp,proc)
    write(nout,120) ESC,ESC
    ihelp = 1
    close (20)
    goto 1
c
else if (opt.eq.'EX') then
    write(nout,100) ESC
    write(nout,124) ESC,ESC
    stop 'COITUS INTERUPTUS'
c
else
c
c If control ever gets here then the user has made a mistake and typed
c in the wrong option code (ie not included in the set OPTCOD).
c
10    if (ierr.eq.1) then
        write(nout,123) ESC,ESC,BELL,ESC,ESC
    else
        write(nout,118) ESC,ESC,BELL,ESC,ESC
    endif
    ierr = 0
    ierror = 1
endif
c
c Control is returned to the input-side from here with an illegal error
flag.
c
goto 2
c
c No menu file found
c
999  write(nout,117) ESC,BELL,ESC,menfil,ESC,ESC,ESC
write(nout,122) ESC,ESC,ESC,ESC,ESC
read(5,'(a)') ans

```

```

call lotoup(ans)
if (ans.eq.'EX') stop
write(nout,100) ESC
ihelp = 0
goto 6
c
c Control comes here when it gets tired or the user so bored he/she
decides
c to actually run the program - God forbid !
c
c The menu is saved in a scratch file to be retrived when the program
c has processed the d-spacing data file
c
  5      ihelp = 1
proc = 1
call menout(hklmax,ixtal,oldpar,infile,ihelp,proc)
proc = 0
ihelp = 0
c
return
end
c
c-----
c
Subroutine Mono(nobs,G,ncycle,R,iflag2)
c      -----
c
c Calculate sets of parameters, partial derivatives, delta, R and
c G values for an monoclinic unit cell
c
common /index/index(100),dspace(100),line(79),dc(100)
common /param/latpar(6),sd(6),vol,sdv
common /matrix/mat(7,7),inv(7,7),vec(7,1),corec(7,1)
real*8 inv,R,Rtop,Rbot,latpar,sd,w,G,delta,d,mat
real*8 part1(4),param(4),dummy1(10,10),dummy2(10,10)
integer npoint,ncycle,nobs,iflag1,iflag2,nparam
c
c Set up number of parameters in iteration
c
nparam = 4
c
c Check for singularity of sparsity in matrix to be produced
c (i.e. no. of degrees of freedom of the least squares is sufficient)
c

```

```

if (nobs.le.nparam) then
  iflag2 = 1
  return
endif
c
c Create fitting parameters from guessed lattice parameters
c
param(1) = 1.0/(latpar(1)*sind(latpar(4)))
param(2) = 1.0/(latpar(2))
param(3) = 1.0/(latpar(3)*sind(latpar(4)))
param(4) = 180.0 - latpar(4)
c
ncycle = 0
c
c Initialise Variables to be summed to zero
c
  1      Call Intsum(G,R,Rtop,Rbot,Delta)
c
c Count number of cycles
c
ncycle = ncycle + 1
c
c Start main loop over all the data at pressure P
c
Do 10 ii = 1,nobs
c
d = dspace(ii)
c
c Calculate partial derivatives of the equation
c
npoint = (3*ii-3)
X = index(npoint+1)*index(npoint+3)*cosd(param(4))
part1(1) = -2.0*((index(npoint+1))**2*param(1)
&
          + X*param(3))
part1(2) = -2.0*(index(npoint+2)**2)*param(2)
part1(3) = -2.0*((index(npoint+3))**2*param(3)
&
          + X*param(1))
part1(4) = 2.0*(index(npoint+1)*index(npoint+3)
&
          *param(1)*param(3)*sind(param(4)))
c
c Calculate the minimum function
c
delta = (1.0/d)**2
Do i = 1,(nparam-1)

```

```

        delta = delta - (index(npoin+1)**2)*(param(1)**2)
    enddo
    delta = delta - 2.0*X*param(1)*param(3)
c
c Calculate condition factors
c
    Call Calcon(d,delta,G,Rtop,Rbot,w)
c
c Set up linear equations of the form Ax=B
c
    Call Setmat(part1,delta,w,nparam)
c
    10 continue
c
c Solve set of linear equations
c
    idum = nparam+1
c
    Call Solve(param,nparam,nobs,G,ncycle,idum,iflag1,
        *          dummy1,dummy2)
c
c Test iflag1 to see if re-iteration is necessary
c
    If (iflag1.eq.1) goto 1
c
c Calculate standerd deviation on final parameter values
c and reform into orignal parameter type
c
    latpar(4) = 180.0 - param(4)
    latpar(1) = 1.0/(param(1)*sind(latpar(4)))
    latpar(2) = 1.0/(param(2))
    latpar(3) = 1.0/(param(3)*sind(latpar(4)))
    sd(1) = sqrt((1.0/((latpar(1)**2)*sind(latpar(4))**2)
        & + (cosd(latpar(4))**2/(latpar(1)*(sind(latpar(4))**2)**2)
        & *(G**2)*Inv(1,1)))
    sd(2) = sqrt((1.0/(param(2)**4))*Inv(2,2)*(G**2))
    sd(3) = sqrt((1.0/((latpar(3)**2)*sind(latpar(4))**2)
        & + (cosd(latpar(4))**2/(latpar(3)*(sind(latpar(4))**2)**2)
        & *(G**2)*Inv(3,3)))
    sd(4) = sqrt(Inv(4,4)*(G**2))
c
c Calculate the cell volume and the standard deviation on this result
c
    vol = 1.0

```

```

do i = 1,(nparam-1)
  vol = vol*latpar(i)
enddo
vol = vol*sind(latpar(4))
c
sdv = ((latpar(2)*latpar(3)*sind(latpar(4)))**2)*(sd(1)**2)
&      + ((latpar(1)*latpar(3)*sind(latpar(4)))**2)*(sd(2)**2)
&      + ((latpar(1)*latpar(2)*sind(latpar(4)))**2)*(sd(3)**2)
&      + ((latpar(1)*latpar(2)*latpar(3)
&          *cosd(latpar(4)))**2)*(sd(4)**2)
sdv = sqrt(sdv)
c
c Calculate the R factor
c
R = sqrt((Rtop/Rbot))*100
c
Return
End
c
c-----
c
Subroutine Ortho(nobs,G,ncycle,R,iflag2)
c -----
c
c Calculate sets of parameters, partial derivatives, delta, R and
c G values for an orthorhombic unit cell
c
common /index/index(100),dspace(100),line(79),dc(100)
common /param/latpar(6),sd(6),vol,svd
common /matrix/mat(7,7),inv(7,7),vec(7,1),corec(7,1)
real*8 inv,R,Rtop,Rbot,latpar,sd,w,G,delta,d,mat
real*8 part1(3),param(3),dummy1(10,10),dummy2(10,10)
real rparam(3)
integer npoint,ncycle,nobs,iflag1,iflag2,nparam
c
c Set up number of parameters in iteration
c
nparam = 3
c
c Check for singularity of sparsity in matrix to be produced
c
if (nobs.le.nparam) then
  iflag2 = 1
  return

```

```

endif
c
c Create fitting parameters from guessed lattice lengths
c
do i = 1,nparam
  param(i) = 1.0/(latpar(i)**2)
enddo
c
ncycle = 0
c
c Initialise Variables to be summed to zero
c
  1    Call Intsum(G,R,Rtop,Rbot,Delta)
c
c Count number of iterations
c
ncycle = ncycle + 1
c
c Start main loop over all the data
c
Do 10 ii = 1,nobs
c
d = dspace(ii)
c
c Calculate partial derivatives of the equation
c
  Do i = 1,nparam
    npoint = (3*ii-3)+i
    partl(i) = -1.0*(index(npoin)**2)
  enddo
c
c Calculate the minimum function
c
  delta = (1.0/d)**2
  Do i = 1,3
    delta = delta + partl(i)*param(i)
  enddo
c
c Calculate condition factors
c
  Call Calcon(d,delta,G,Rtop,Rbot,w)
c
c Set up linear equations of the form Ax=B
c

```

```

    Call Setmat(part1,delta,w,nparam)
c
    10 continue
c
c Solve set of linear equations
c
idum = nparam+1
c
Call Solve(param,nparam,nobs,G,ncycle,idum,iflag1,
*          dummy1,dummy2)
c
c Test iflag1 to see if reiteration is necessary
c
If (iflag1.eq.1) goto 1
c
c Calculate set of dspacing from refined parameters
c
rparam(1) = sqrt(param(1))
rparam(2) = sqrt(param(2))
rparam(3) = sqrt(param(3))
Call Dcalc(nobs,rparam(1),rparam(2),rparam(3),90,90,90)
c
c Calculate standerd deviation on final parameter values
c and reform into orignal parameter type
c
do i = 1,nparam
    sd(i) = sqrt((1.0/(4*(param(i)**3)))*Inv(i,i)*(G**2))
    latpar(i) = sqrt(1/param(i))
enddo
c
c Calculate the cell volume and the standard deviation on this result
c
vol = 1.0
do i = 1,nparam
    vol = vol*latpar(i)
enddo
sdv = (latpar(2)*latpar(3))**2*sd(1)**2
*      + (latpar(1)*latpar(3))**2*sd(2)**2
*      + (latpar(1)*latpar(2))**2*sd(3)**2
sdv = sqrt(sdv)
c
c Calculate the R factor
c
R = sqrt((Rtop/Rbot))*100

```

```

c
Return
End
c
c-----
c
Subroutine Output(nobs,Gmin,pres,ncycle,iflag2,r,
&                npres,nparam,ixtal)
c-----
c
common /index/index(100),dspace(100),line(79),dc(100)
common /param/latpar(6),sd(6),vol,sdv
common /matrix/mat(7,7),inv(7,7),vec(7,1),corec(7,1)
common /infil/infile,title
real*8 mat,inv,vec,corec
real*8 pres,dspc(100),sd,R,Gmin,latpar
real*4 spres,slat(3),svol0,svol
integer nobs,ncycle,index,iflag2,ixtal,iparam,nparam
character pnam(6)*5,line*1,system(6)*12,infile*20,title
c
data pnam(1) /' a  '/,pnam(2) /' b  '/,
*      pnam(3) /' c  '/,pnam(4) /'alpha'/,
*      pnam(5) /'beta '/,pnam(6) /'gamma'/
data      system(1) /'TRICLINIC'/,system(2)
*          /'MONOCLINIC'/,
*          system(3) /'HEXAGONAL'/,system(4)
*          /'RHOMBOHEDRAL'/,
*          system(5) /'ORTHORHOMBIC'/,system(6)
*          /'TETRAGONAL'/
c
100  format(1h1,79a1)
101  format(/' Pressure = ',f6.2,' GPa',3x,'Number of obs. = ',i3,
* 3x,'R = ',f6.2,'% ',3x,'G = ',f8.4/)
102  format(1h0,'Obs. hkl: ',8(3(i2),2x))
103  format(1h0,'Param.',6x,'Value ',10x,'Standard Dev.',11x,
* 'Cell vol. = ',f8.3,/,1x,'-----',7x,'-----',10x,
* '-----',11x,'s.d. vol. = ',1Pe10.4/)
104  format(/2x,a5,5x,f7.3,11x,1Pe10.4/)
105  format(/' Minimised matrix equation:'//)
106  format(4x,'(',',3f9.4,2x,')',2x,'(',',1Pe11.3,2x,')',
* 10x,'(',',1Pe11.3,2x,')')
107  format(4x,'(',',29x,')',2x,'(',',13x,')',10x,'(',',13x,')')
108  format(/' Number of iterations performed in refinement = '
* ,i4,/)

```

```

109  format(' Inverted matrix derived from final Iteration: '//)
110  format(4x,'(,3(1Pe10.3,1x),)',15x,'Element(',i1,',',i1,')
= ,
    * ,1Pe10.3)
111  format(4x,'(,33x,')')
112  format(1h , 'Obs. d: ',8(f6.4,2x))
113  format(///' ERROR IN DATA at Pressure ',f6.2,' GPa'
    * /' -----'//)
    * ' Data too sparse for calculation of least squares analysis.'//
    * ' Only data available is ',3(3(i2),2x),' reflections'//
    * ' Advise guessed value at low weighting point ',
    * '(ie. low d-spacing)')
114  format(4x,'(,2f9.4,2x,)',2x,'(,1Pe11.3,2x,)',
    * 10x,'(,1Pe11.3,2x,')')
115  format(4x,'(,20x,)',2x,'(,13x,)',10x,'(,13x,')')
116  format(4x,'(,4f9.4,2x,)',2x,'(,1Pe11.3,2x,)',
    * 10x,'(,1Pe11.3,2x,')')
117  format(4x,'(,38x,)',2x,'(,13x,)',10x,'(,13x,')')
118  format(4x,'(,2(1Pe10.3,1x),)',15x,'Element(',i1,',',i1,')
= ,
    * ,1Pe10.3)
119  format(4x,'(,22x,')')
120  format(4x,'(,4(1Pe10.3,1x),)',15x,'Element(',i1,',',i1,')
= ,
    * ,1Pe10.3)
121  format(4x,'(,44x,')')
if (iparam.eq.2.and.i.eq.2) j = 4
122  format(///' *** END OF OUTPUT DATA FILE')
123  format(1h1,///' *** CRYSTAL LATTICE PARAMETER CALCULATIONS'/
    * , -----'//)
124  format(//' Calculation of the variation of unit cell parameters
    * with respect to'// an extrinsic variable (e.g. Temperature or
    * Pressure). '// The Bravias system which the calculations are
    * based on is ',a12// The least squares analysis requires starting
    * values for'// the lattice parameters which are to be
    * calculated. '// These were given as: '//)
125  format(1h0,2x,a5,10x,f8.4)
126  format(//' The program also requires a file containing indexed
    * d-spacings'// as they change with the extrinsic variable.'//
    * ' d-spacing file from which data drawn was : ',a20//
    * ' Chronically bad data will be dealt with as is befitting to
its
    * very nature.'// REMEMBER: "Garbage In - Garbage Out")
127  format(1h ,4x,f6.2,4x,3(f6.3,4x),4x,f7.2)

```

```

128  format(1h0,'Data correlation'//
      * 5x,' h k l',5x,'Observed',5x,'Calculated',5x,'Difference'//)
129  format(5x,3(i2),6x,f6.4,7x,f6.4,7x,f6.4)
c
nindex = nob*3
c
c Check the error flag
c
if (iflag2.eq.1) then
  write(2,100) (line(i),i=1,79)
  write(2,113) pres/10.0,(index(i),i=1,nindex)
  return
else if (iflag2.eq.2) then
  write(2,123)
  write(2,124) system(ixtal)
  if (ixtal.eq.2) then
    iparam = 4
  else if (ixtal.eq.4) then
    iparam = 2
  else if (ixtal.eq.5) then
    iparam = 3
  endif
  do i = 1,iparam
    j = i
    if (ixtal.eq.6.and.i.eq.2) j = 3
    if (ixtal.eq.4.and.i.eq.2) j = 4
    if (iparam.eq.4.and.i.eq.4) j = 5
    write(2,125) pnam(j),latpar(i)
  enddo
  write(2,126) infile
  return
else if (iflag2.eq.3) then
  write(2,122)
  return
endif
c
write(2,'(a80)') title
write(2,100) (line(i),i=1,79)
write(2,101) pres/10.0,nob,r*10.0,gmin*100.0
if (nindex.gt.24) then
  write(2,102) (index(i),i=1,24)
  write(2,112) (dspace(i),i=1,8)
  write(2,102) (index(i),i=25,nindex)
  write(2,112) (dspace(i),i=9,nob)

```

```

else
  write(2,102) (index(i),i=1,nindex)
  write(2,112) (dspace(i),i=1,nobs)
endif
write(2,103) vol,sdv
do i = 1,nparam
  j = i
  if (ixtal.eq.6.and.i.eq.2) j = 3
  if (ixtal.eq.4.and.i.eq.2) j = 4
  if (nparam.eq.4.and.i.eq.4) j = 5
  write(2,104) pnam(j),latpar(i),sd(i)
enddo
write(2,105)
if (nparam.eq.2) then
  do i = 1,nparam
    write(2,114) (mat(i,j),j=1,nparam),corec(i,1),vec(i,1)
    if(i.le.1) write(2,115)
  enddo
else if (nparam.eq.3) then
  do i = 1,nparam
    write(2,106) (mat(i,j),j=1,nparam),corec(i,1),vec(i,1)
    if(i.le.2) write(2,107)
  enddo
else if (nparam.eq.4) then
  do i = 1,nparam
    write(2,116) (mat(i,j),j=1,nparam),corec(i,1),vec(i,1)
    if(i.le.3) write(2,117)
  enddo
endif
c
write(2,108) ncycle
c
write(2,109)
if (nparam.eq.2) then
  do i = 1,nparam
    write(2,118) (inv(i,j),j=1,nparam),i,i,inv(i,i)
    if(i.le.1) write(2,119)
  enddo
else if (nparam.eq.3) then
  do i = 1,nparam
    write(2,110) (inv(i,j),j=1,nparam),i,i,inv(i,i)
    if(i.le.2) write(2,111)
  enddo
else if (nparam.eq.4) then

```

```

do i = 1,nparam
  write(2,120) (inv(i,j),j=1,nparam),i,i,inv(i,i)
  if(i.le.3) write(2,121)
enddo
endif
c
write(2,128)
Do ii = 1,nobs
  npoint = (3*ii-3)
  write(2,129) (index(npoint+i),i=1,3),dspace(ii),dc(ii)
enddo
c
c Write out to datagraf type file.
c

spres = pres/10.0
do i = 1,nparam
  slat(i) = latpar(i)
enddo
svol = vol
if (npres.eq.1) svol0 = vol
c svol = vol/svol0
write(3,127) spres,(slat(i),i=1,3),svol
c
  Return
End
c
c-----
c
Subroutine Rhomb(nobs,G,ncycle,R,iflag2)
c -----
c
c Calculate sets of parameters, partial derivatives,delta, R and G
c values for a rhombohedral unit cell.
c
common /index/index(100),dspace(100),line(79),dc(100)
common /param/latpar(6),sd(6),vol,svd
common /matrix/mat(7,7),inv(7,7),vec(7,1),corec(7,1)
real*8 inv,R,Rtop,Rbot,latpar,sd,w,G,delta,d,mat
real*8 part1(2),param(2),X,Y,dummy1(10,10),dummy2(10,10)
real rparam(3)
integer iflag1,iflag2,npoint,ncycle,nobs,nparam,idum
c
c Set up number of parameters in iteration

```

```

c In R type space grp. have one vector and one angle
c
nparam = 2
c
c Check for singularity or sparsity in matrix to be produced
c (i.e. no. degrees of freedom in least squares is sufficient)
c
If (nobs.le.nparam) then
  iflag2 = 1
  Return
endif
c
c Create fitting parameters from guessed lattice parameters
c
param(1) = (sind(latpar(2))/
  &          (latpar(1)*sqrt
  &          (1.0 - 3.0*(cosd(latpar(2))**2)
  &          + 2.0*(cosd(latpar(2))**3))))**2
param(2) = acosd(-1.0*(cosd(latpar(2))/
  &          (1.0+cosd(latpar(2)))))
c
c Initialise variables which are to be summed over each iteration
c and set all matrix elements in MAT and VEC to zero.
c
ncycle = 0
c
  1 Call intsum(G,R,Rtop,Rbot,Delta)
c
c Count number of iterations
c
ncycle = ncycle + 1
c
c Start loop over all data
c
Do 10 ii = 1,nobs
c
  d = dspace(ii)
c
c Calculate partial derivatives
c
  npoint = (3*ii-3)
  X = index(npoint+1)**2+index(npoint+2)**2+index(npoint+3)**2
  Y = ((index(npoint+1)*index(npoint+2)) +
  &      (index(npoint+2)*index(npoint+3)) +

```

```

      &      (index(npoin+1)*index(npoin+3))*2.0
partl(1) = -1.0*X - Y*cosd(param(2))
partl(2) = Y*param(1)*sind(param(2))
c
c Calculate the minimum function
c
delta = 1.0/(d**2)-(X*param(1))-(Y*param(1)*cosd(param(2)))
c
c Calculate condition factors
c
  Call Calcon(d,delta,G,Rtop,Rbot,w)
c
c Set up linear equations of the form Ax=B
c
  Call Setmat(partl,delta,w,nparam)
c
10  continue
c
c Solve set of linear equations
c
idum = nparam+1
c
Call Solve(param,nparam,nobs,G,ncycle,idum,iflag1,
*          dummy1,dummy2)
c
c Test iflag1 to see if reiteration is necessary
c
if (iflag1.eq.1) goto 1
c
c Calculate standerd deviation on final parameter values
c
c NOT EASY !!
c
rparam(1) = param(1)
rparam(2) = param(2)
Call Dcalc(nobs,rparam(1),rparam(1),rparam(1),rparam(2),
&         rparam(2),rparam(2))
c
c Reform into original parameter type
c
latpar(2) = acosd(1.0/(-1.0*(1+(1.0/cosd(param(2))))))
latpar(1) = sind(latpar(2))/
&         (sqrt(param(1))*sqrt
&         (1.0 - 3.0*(cosd(latpar(2))**2))

```

```

&          + 2.0*(cosd(latpar(2))**3))

c
c Calculate cell volume and standard deviation on this result
c
vol = (latpar(1)**3)*sqrt(1.0-(3.0*(cosd(latpar(2))**2)
&      + (2.0*(cosd(latpar(2))**3)))
sdv = 0.0 ! Give up.

c
c Calculate R factor
c
R = sqrt((Rtop/Rbot))*100
c
Return
End
c
c-----
c
Subroutine Setmat(partl,delta,w,nparam)
c      -----
c
c Set up linear equations of the form Ax=B
c
common  /matrix/mat(7,7),inv(7,7),vec(7,1),corec(7,1)
real*8  mat,inv,vec,corec,delta,w,partl(nparam)
integer nparam
c
Do 10 i = 1,nparam
  vec(i,1) = vec(i,1) + w*delta*partl(i)
  Do 10 j = 1,nparam
    Mat(i,j) = Mat(i,j) + w*partl(i)*partl(j)
  10 Continue
Return
End
c
c-----
c
Subroutine Solve(param,nparam,nobs,G,ncycle,idum,iflag1,
*          dummy1,dummy2)
c      -----
c
c Use NAG routine to solve the set of linear equations for the system
c

```

```

common /matrix/mat(7,7),inv(7,7),vec(7,1),corec(7,1)
real*8 mat,inv,vec,corec,param(nparam)
real*8 wkspce(100),dummy1(idum,idum),dummy2(idum,idum)
real*8 G,gold,gcomp
integer nobs,nparam,idum,ivec,icorec,m,ifail,ncycle,iflag1
data ivec /7/,icorec /7/,m /1/
c
iflag1 = 0
c
c Vector on right of equation is negative
c
do i = 1,nparam
  vec(i,1) = -1.0*vec(i,1)
enddo
c
c Move matrix into dummy variable since NAG routine converts
c the true symmetric matrix into a condensed version with the
c leading diagonal understood
c
do i = 1,nparam
  do j = 1,nparam
    dummy1(i,j) = mat(i,j)
  enddo
enddo
c
ifail = 0
c
Call f04aaf(Dummy1,idum,vec,ivec,nparam,
&          m,corec,icorec,wkspce,ifail)
c
c
c Update the parameter values with corrections from equations
c
Do i = 1,nparam
  param(i) = param(i) + corec(i,1)
enddo
c
G = sqrt(G/(nobs-nparam))
c
c Force the iteration around six times
c Returns control to Bravias routine from which was called
c
if (ncycle.le.6) then
  Gold = G

```

```

    iflag1 = 1
    Return
endif
c
c Set up comparison of G values found in the calculation
c
Gcomp = abs(1.0-(G/Gold))
c
if (Gcomp.gt.1d-04) then
    Gold = G
    iflag1 = 1
    Return
endif
c
c Call a NAG routine to invert the final matrix of sums
c which gave best fit of parameters
c
c Fill the upper triangle of the matrix to be inverted
c with the final matrix elements
c
do i = 1,nparam
    do j = 1,nparam
        if (j.ge.i) then
            dummy2(i,j) = mat(i,j)
        else
            dummy2(i,j) = 0.0
        endif
    enddo
enddo
c
ifail = 0
c
call f01abf(dummy2,idum,nparam,inv,ivec,wkspce,ifail)
c
c Replace upper triangle of symmetric matrix with the inverse
c elements from the lower triangle
c
do i = 1,nparam
    do j = 1,nparam
        if(j.ge.i) then
            inv(i,j) = inv(j,i)
        endif
    enddo
enddo
enddo

```

```

c
Return
End
c
c-----
c
Subroutine Secure(passnum)
c
c Stop other users from making use of this software system apart
c from privileged users and also demand program passwords for
c continuation of the system.
c
Integer  usernum,attempt,passnum,ESC,nin,nout
Character username*10,symbol*20,password(2)*10,priv*10,
      &          pruser(8)*10,name(8)*10,passat*10
Data     password(1) /'NIVEA'/, password(2) /'FELDENE'/
Data     pruser(1) /'TED      '/, name(1) /'Andy'/
Data     pruser(2) /'NJA     '/, name(2) /'Lab Junior'/
Data     pruser(3) /'HEATH   '/, name(3) /'Andy'/
Data     pruser(4) /'SEN     '/, name(4) /'Simon'/
Data     pruser(5) /'HATTON  '/, name(5) /'Pete'/
Data     pruser(6) /'UNKNOWN '/, name(6) /'Harjiit'/
Data     pruser(7) /'DMA     '/, name(7) /'David'/
Data     pruser(8) /'PWR     '/, name(8) /'Phil'/
Data     ESC /27/, nin /5/, nout /6/
c
100  format(1h$,a1,'[2;1H',a1,'[?J')
101  format(1h$,a1,'[6;11H',a1,'#6',
      &  'User status: ',a1,'[1m',a10,a1,'[0m', ' for user ',
      &  a1,'[1m',a10,a1,'[0m')
102  format(1h$,a1,'[8;11H',a1,'#6',
      &  'Password ? ',a1,$)
103  format(1h$,a1,'[10;11H',a1,'#6',
      &  'Password matches - hello ',a10)
104  format(1h$,a1,'[23;1H',a1,'#6',a1,
      &  '[1mPress Return to continue ...',a1,'[0m,$)
105  format(1h$,a1,'[10;11H',a1,'#6',
      &  'Password mis-match - you have ',a1,'[1m',
      &  i1,a1,'[0m', ' attempts remaining.')
106  format(1h$,a1,'[10;11H',a1,'[?K')
107  format(1h$,a1,'[10;11H',a1,'#6',
      &  'Password matches - goodbye ',a10)
108  format(1h$,a1,'[4;11H',a1,'#6',a1,
      &  '[4mIntroductory Security',a1,'[0m')

```

```

109  format(1h$,a1,'[4;11H',a1,'#6',a1,
      & '[4mOutput Security',a1,'[0m')
110  format(1h$,a1,'[4;11H',a1,'#6
      ')
c
c Clear the screen from the title down the page to the bottom.
c
write(nout,100) ESC,ESC
if (passnum.eq.1) then
  write(nout,108) ESC,ESC,ESC,ESC
else
  write(nout,109) ESC,ESC,ESC,ESC
endif
c
c Get the username from the VMS global symbol table.
c
Call lib$get_symbol('user',symbol)
username = '      '
do i = 1,20
  if (symbol(i:i).eq.',') then
    j = i
    jj = 0
10    j = j+1
    jj = jj+1
    if (symbol(j:j).ne.']) then
      username(jj:jj) = symbol(j:j)
      goto 10
    else
      goto 20
    endif
  endif
enddo
c
c Check the username entered against the look-up table of
c allowed users.
c
20 do i = 1,8
  if (username.eq.pruser(i)) then
    priv = 'privileged'
    namenum = i
    write(nout,101) ESC,ESC,ESC,priv,ESC,ESC,username,ESC
    goto 25
  endif
enddo
c

```

```

c Control comes here if username not matched.
c
priv = 'intruder'
write(nout,fmt='(1h$,a1)') 7 ! Sound terminal bell.
write(nout,101) ESC,ESC,ESC,priv,ESC,ESC,username,ESC
stop

c
c Get password from the now privileged user.
c
25 attempt = 3
30 if (attempt.eq.0) then
if (passnum.eq.2) then
close (2)
call lib$spawn('$ delete for002.dat')
stop
endif
stop
endif
write(nout,102) ESC,ESC
Call echo(1)
read(nin,fmt='(a)') passat
Call echo(0)
Call lotoup(passat)
if (passat.eq.password(passnum)) then
write(nout,106) ESC,ESC
if (passnum.eq.1) then
write(nout,103) ESC,ESC,name(namenum)
else
write(nout,107) ESC,ESC,name(namenum)
endif
write(nout,104) ESC,ESC,ESC,ESC
read(nin,fmt='(a)')
write(nout,110) ESC,ESC
write(nout,100) ESC,ESC
else
attempt = attempt-1
write(nout,105) ESC,ESC,ESC,attempt,ESC
goto 30
endif
c
Return
End
c

```

```

c-----
c
c Subroutine Tetra(nobs,Gmin,ncycle,R,iflag2)
c-----
c
c Calculate delta,partial derivatives, and sets of linear equations
c for the tetragonal bravias system.
c
common /index/index(100),dspace(100),line(79),dc(100)
common /param/latpar(6),sd(6),vol,sv
common /matrix/mat(7,7),inv(7,7),vec(7,1),corec(7,1)
real*8 inv,R,Rtop,Rbot,latpar,sd,w,G,delta,d,mat
real*8 part1(2),param(2),dummy1(10,10),dummy2(10,10)
real rparam(3)
integer npoint,ncycle,nobs,iflag1,iflag2,nparam
c
c Set up number of parameters in iteration
c
nparam = 2
c
c Check for singularity of sparsity in matrix to be produced
c
if (nobs.le.nparam) then
  iflag2 = 1
  return
endif
c
c Create fitting parameters from guessed lattice lengths
c
do i = 1,nparam
  param(i) = 1.0/(latpar(i)**2)
enddo
c
ncycle = 0
c
c Initialise Variables to be summed to zero
c
1 Call Intsum(G,R,Rtop,Rbot,Delta)
c
c Count number of iterations
c
ncycle = ncycle + 1
c
c Start main loop over all the data

```

```

c
Do 10 ii = 1,nobs
c
d = dspace(ii)
c
c Calculate partial derivatives of the equation
c
  npoint = (3*ii-3)
  part1(1) = -1.0*(index(npoin+1)**2+index(npoin+2)**2)
  part1(2) = -1.0*(index(npoin+3)**2)
c
c Calculate the minimum function
c
  delta = (1.0/d)**2
  do i = 1,nparam
    delta = delta + part1(i)*param(i)
  enddo
c
c Calculate condition factors
c
  Call Calcon(d,delta,G,Rtop,Rbot,w)
c
c Set up linear equations of the form Ax=B
c
  Call Setmat(part1,delta,w,nparam)
c
  10 continue
c
c Solve set of linear equations
c
idum = nparam+1
c
Call Solve(param,nparam,nobs,G,ncycle,idum,iflag1,
*          dummy1,dummy2)
c
c Test iflag1 to see if reiteration is necessary
c
If (iflag1.eq.1) goto 1
c
c Calculate dspacings for refined parameters
c
rparam(1) = sqrt(param(1))
rparam(2) = sqrt(param(1))
rparam(3) = sqrt(param(2))

```

```

Call Dcalc(nobs,rparam(1),rparam(2),rparam(3),90.,90.,90.)
c
c Calculate standerd deviation on final parameter values
c and reform into origanal parameter type
c
do i = 1,nparam
  sd(i) = sqrt((1.0/(4*(param(i)**3)))*Inv(i,i)*(G**2))
  latpar(i) = sqrt(1/param(i))
enddo
c
c Calculate the cell volume and the standard deviation on this result
c
vol = 1.0
vol = latpar(1)**2*latpar(2)
sdv = (2*latpar(1)*latpar(2))**2*sd(1)**2
      *      + (latpar(1)**4*sd(2)**2)
sdv = sqrt(sdv)
c
c Calculate the R factor
c
R = sqrt((Rtop/Rbot))*100
c
Return
End
c
c-----
c
Subroutine Tric(nobs,Gmin,ncycle,R,iflag2)
c
c Calculate delta,partial derivatives, and sets of linear equations
c for the trigonal bravias system.
c
c*****
c YET TO BE COMMISSIONED FOR TRICLINIC CASE
c*****
c
c Return
End
c
c-----

```

APPENDIX 2

Source code listings for BBC micro-computer programs

Chapter 2 describes the design of a spectroscopic system used to detect ruby fluorescence from a diamond anvil cell. This system was interfaced to a BBC micro-computer, the computer was used to record the fluorescence spectrum. The first listing is for the 'peaking' program. An analogue signal from the detector is maximised by translation of the sample in a laser beam. The program uses colour graphics to display the signal strength as an animated histogram. The histogram is drawn as a ladder (with one rung) using 6502 Assembler language to make the process as rapid as possible.

The second listing is for the data acquisition and analysis program. The input to the computer is from a pulse produced by a scan controller every 0.1 nm. The program reads the detector signal from an analogue to digital converter built into the BBC. A real-time plot of intensity against wavelength is displayed. The pulse from the controller is treated as an interrupt, and Assembler language is used to redirect the default interrupt polling procedures to a routine which collects the data. When the scan is complete, the stored data are searched for the ruby fluorescence peaks. The pressure exerted on the sample is calculated from the shifted peak positions.

The high-level language used was BBC BASIC. The shortage of comments reflects the limited memory space of this computer. Chapter 2 includes flow diagrams for these programs and detailed explanations of how they operate.

Listing of 'Peaking' program

```
10*FX 16,1
20DIM SPACE% 400
30OSWRCH = &FFEE
40Data% = SPACE%
50Flag%=0
60START_OF_PROG% = SPACE%+12
70Oldadc%=0
80Sen%=8:Sen_level%=4
90REM
100REM=====
110REM Start of machine code program
120REM
130FOR PASS% = 0 TO 3 STEP 3
140P% = START_OF_PROG%
150REM
160[
170 OPT 0
180\
190\SETUP THE COUNTER
200\
210.NO_MODE_CHANGE% LDX #0
220\
230\PUSH THE 'X' POSITION ONTO STACK
240\
250LDA Data%
260PHA
270LDA Data%,+1
280PHA
290\
300\MOVE TO THE START POINTS
310\
320.Main_prog% LDA #25
330JSR OSWRCH
340LDA #4
350JSR OSWRCH
360LDY #0
370.Move_TO_POINT% LDA Data%,Y
380JSR OSWRCH
390INY
```

```
400CPY #4
410BNE Move_TO_POINT%
420\
430\DRAW TO FOLLOWING POINTS
440\
450LDA #25
460JSR OSWRCH
470LDA #5
480JSR OSWRCH
490LDA Data%
500JSR OSWRCH
510LDA Data%+1
520JSR OSWRCH
530LDA Data%+4
540JSR OSWRCH
550LDA Data%+5
560JSR OSWRCH
570INX
580CPX #2
590BEQ LADDER_TOP%
600LDA Data%
610CLC
620ADC Data%+6
630STA Data%
640BCC Main_prog%
650LDY Data%+1
660INY
670STY Data%+1
680JMP Main_prog%
690\
700\TOP OF THE LADDER
710\
720.LADDER_TOP%
730PLA
740STA Data%+1
750PLA
760STA Data%
770\
780\MOVE TO TOP OF LEFT STRUT
```

790\
800LDA #25
810JSR OSWRCH
820LDA #4
830JSR OSWRCH
840LDA Data%
850JSR OSWRCH
860LDA Data%+1
870JSR OSWRCH
880LDA Data%+4
890JSR OSWRCH
900LDA Data%+5
910JSR OSWRCH
920\
930\CALCULATE TOP OF RIGHT STRUT
940\
950LDA Data%
960CLC
970ADC Data%+6
980STA Data%
990BCC Draw_to_right%
1000LDY Data%+1
1010INY
1020STY Data%+1
1030\
1040\DRAW TOP OF BLOCK
1050\
1060.Draw_to_right%
1070LDA #25
1080JSR OSWRCH
1090LDA #5
1100JSR OSWRCH
1110LDA Data%
1120JSR OSWRCH
1130LDA Data%+1
1140JSR OSWRCH
1150LDA Data%+4
1160JSR OSWRCH
1170LDA Data%+5

1180JSR OSWRCH
119ORTS
1200\
1210\DRAW MARKER FOR MAXIMUM
1220\
1230.Do_marker%
1240LDA #25
1250JSR OSWRCH
1260LDA #4
1270JSR OSWRCH
1280LDA Data%+7
1290JSR OSWRCH
1300LDA Data%+8
1310JSR OSWRCH
1320LDA Data%+4
1330JSR OSWRCH
1340LDA Data%+5
1350JSR OSWRCH
1360\
1370\CALCULATE MARKER RIGHT
1380\
1390CLC
1400LDA Data%+7
1410ADC Data%+9
1420STA Data%+7
1430BCC Draw_marker%
1440LDY Data%+8
1450INY
1460STY Data%+8
1470\
1480\NOW DRAW THE MARKER
1490\
1500.Draw_marker%
1510LDA #25
1520JSR OSWRCH
1530LDA #5
1540JSR OSWRCH
1550LDA Data%+7
1560JSR OSWRCH

1570LDA Data%,+8
1580JSR OSWRCH
1590LDA Data%,+4
1600JSR OSWRCH
1610LDA Data%,+5
1620JSR OSWRCH
1630RTS
1640\
1650\DELETE MARKER FROM OLD MAXIMUM
1660\
1670.Del_marker%
1680\
1690\MOVE TO CORRECT POSITION
1700\
1710LDA #25
1720JSR OSWRCH
1730LDA #4
1740JSR OSWRCH
1750LDA Data%,+7
1760JSR OSWRCH
1770LDA Data%,+8
1780JSR OSWRCH
1790LDA Data%,+10
1800JSR OSWRCH
1810LDA Data%,+11
1820JSR OSWRCH
1830\
1840\CALCULATE THE MARKER RIGHT
1850\
1860CLC
1870LDA Data%,+7
1880ADC Data%,+9
1890STA Data%,+7
1900BCC Draw_del_marker%
1910LDY Data%,+8
1920INY
1930STY Data%,+8
1940\
1950\DELETE THE MARKER

```
1960\  
1970.Draw_del_marker%  
1980LDA #25  
1990JSR OSWRCH  
2000LDA #5  
2010JSR OSWRCH  
2020LDA Data%+7  
2030JSR OSWRCH  
2040LDA Data%+8  
2050JSR OSWRCH  
2060LDA Data%+10  
2070JSR OSWRCH  
2080LDA Data%+11  
2090JSR OSWRCH  
2100RTS  
2110]  
2120REM  
2130NEXT PASS%  
2140REM  
2150REM End of machine code  
2160REM=====
```

```
2170INPUT "PRESS RETURN KEY WHEN READY"$  
2180REMOVEDU 23;8202;0;0;0  
2190VDU 28,20,30,39,1  
2200MODE 1  
2210REPEAT  
2220*FX 17,1  
2230Adc% = ADVAL(1)  
2240IF Adc%>0 THEN Adc%=Adc%/Sen% ELSE PROCerror  
2250FOR II=1 TO 0 STEP -1  
2260?Data% = 200 MOD 256  
2270Data%?1 = 200 DIV 256  
2280Data%?2 = 100 MOD 256  
2290Data%?3 = 100 DIV 256  
2300Data%?6 = 200  
2310Data%?4 = Adc% MOD 256  
2320Data%?5 = Adc% DIV 256  
2330GCOL 0,II  
2340CALL START_OF_PROG%
```

```

2350NEXT II
2360IF Adc%>Oldadc% THEN PROCmaximum
2370IF Adc%>1025 THEN Adc%=Adc%/2:PROCsensdown
2380IF Adc%<200 THEN PROCsensup
2390PROCwrite
2400Stop$=INKEY$(0)
2410IF Stop$<>"" THEN GOTO 3000
2420UNTIL FALSE
2430REM=====
2440DEF PROCmaximum
2450Data%?7=450 MOD 256
2460Data%?8=450 DIV 256
2470Data%?9=50
2480GCOL 0,0
2490CALL Del_marker%
2500Data%?10=Adc% MOD 256
2510Data%?11=Adc% DIV 256
2520Data%?7 =450 MOD 256
2530Data%?8 =450 DIV 256
2540GCOL 0,2
2550CALL Do_marker%
2560Oldadc%=Adc%
2570Flag%=0
2580ENDPROC
2590REM=====
2600DEF PROCsensdown
2610Sen%=Sen%*2:Oldadc%=Oldadc%/2:Sen_level%=Sen_level%-1
2620Flag%=Flag%+1:IF Flag%=1 THEN Flag%=0:GOTO 2710
2630IF Flag%<>0 THEN GOTO 2720
2640Data%?7=450 MOD 256
2650Data%?8=450 DIV 256
2660Data%?9=50
2670Data%?4=Oldadc% MOD 256
2680Data%?5=Oldadc% DIV 256
2690GCOL 0,2
2700CALL Do_marker%
2710IF Flag%=0 THEN FOR I=20 TO 22:PRINT TAB(20,I) "           ":NEXT
I
2720ENDPROC

```

```

2730DEF PROCsensup
2740Sen%=Sen%/2:Oldadc%=Oldadc%*2:Sen_level%=Sen_level%+1
2750IF Flag%=0 THEN PROCupdate
2760Flag%=Flag%-1
2770ENDPROC
2780REM=====
2790DEF PROCwrite
2800PRINT TAB(20,10) "ADC(%) value: ";Adc%/10.0
2810PRINT TAB(20,15) "Sensitivity: ";Sen_level%
2820ENDPROC
2830REM=====
2840DEF PROCupdate
2850Data%?7=450 MOD 256
2860Data%?8=450 DIV 256
2870CALL Del_marker%
2880COLOUR 2
2890PRINT TAB(20,20) "Last maximum in"
2900PRINT TAB(20,21) "Sensitivity: ";Sen_level%-1
2910PRINT TAB(20,22) "ADC(%) value: ";Oldadc%/20.0
2920COLOUR 3
2930ENDPROC
2940DEF PROCerror
2950COLOUR 1
2960SOUND 1,-15,128,5
2970PRINT TAB(20,2) "ERROR!":PRINT TAB(20,4) "Zero input to ADC
":PRINT TAB(20,6) "Press space bar":PRINT TAB(20,7) "to continue":COLOUR
3
2980Err$=GET$:IF Err$<>" " THEN GOTO 2980 ELSE FOR I=2 TO 7:PRINT
TAB(20,I)
"
":NEXT:ENDPROC
2990ENDPROC
3000CLG:CLS:PRINT "SIGNAL PEAKED...":CHAIN"MENU"
3010END

```

Listing of data acquisition and analysis program

```

10REM*****
20REM*
30REM* Author:   A.E. Heath   *
40REM* Date:    10/6/87     *
50REM* Function: Real-time data *
60REM*           aquisition and *
70REM*           analysis of Ruby *
80REM*           R-line spectrum. *
90REM*
100REM*****
110REM
120REM*** Set up arrays and machine
130REM*** code space. Declare and
140REM*** initialise parameters and
150REM*** variables.
160REM
170MODE4
180DIM Y(600): DIM M(9): DIM R_peak(2):DIM Wave(2)
: DIM Temp(2):DIM Amb(2)
190DIM OldD$(20):DIM OldT$(20):DIM R1(20):DIM R2(20)
: DIM Term$(20):DIM OldP(20):DIM AmW(2)
200DIM MC% 400
210OSBYTE = &FFF4
220IRF    = &FE6D
230DRB    = &FE60
240IRQ2V  = &206
250MOS_IRV = &71
260Flag%  = &70
270?Flag% = 0
280Num_ruby%=0
290*FX 16,1
300REM
310REM*** Machine code starts
320REM
330FOR Pass% = 0 TO 3 STEP 3
340P% = MC%
350[ OPT 0
360\
370\Reset the OS at end of scan
380\
390.Reset%
400SEI
410LDA MOS_IRV

```

```
420STA IRQV2
430LDA MOS_IRV+1
440STA IRQV2+1
450LDA #&97
460LDY #&18
470LDX #&6E
480JSR OSBYTE
490CLI
500RTS
510\
520\Initialisation subroutine
530\
540.Set_up%
550SEI \no maskable interrupts
560LDA IRQ2V
570STA MOS_IRV
580LDA IRQ2V+1
590STA MOS_IRV+1
600LDA #Routine MOD 256
610STA IRQ2V
620LDA #Routine DIV 256
630STA IRQ2V+1
640\
650\Initialise User VIA
660\
670LDA #&97
680LDY #&50
690LDX #&6C \Set PCR to high-low
700JSR OSBYTE \transitions on CB(1&2)
710\
720\Enable interrupts for high-low
730\pulse on CB(1&2)
740\
750LDY #&98
760LDX #&6E
770JSR OSBYTE
780CLI \maskable interrupts reenabled
790RTS \return to BASIC
800\
810\-----
820\
830.Routine
840\
850\Interrupt polling routine
```

860\
870TXA
880PHA
890TYA
900PHA
910\Is interrupt caused by scan ?
920\i.e. is bit 7 of IFR set ?
930LDA IRF
940BPL Exit%
950\Is motion flag set ?
960LDA Flag%
970BNE Overrun%
980\Is motion forwards or reverse ?
990LDA IRF
1000AND #&10
1010BEQ Advance%
1020\
1030\-----
1040\
1050\Motion is reverse...
1060LDA #02
1070JMP Store%
1080\
1090.Advance%
1100\Motion is forwards...
1110LDA #01
1120JMP Store%
1130\
1140.Overrun%
1150\Scan is too rapid- flag an error
1160LDA #03
1170\
1180.Store%
1190\Store value in A in Flag%
1200STA Flag%
1210\
1220.Exit%
1230\Restore status quo of OS and
1240\exit from interrupt
1250\
1260\Communicate with DRB to clear
1270\interrut in hardware
1280CMP DRB
1290\

```

1300\Get all registers off stack
1310PLA
1320TAY
1330PLA
1340TAX
1350\
1360\Indirect through OS to continue
1370\interrupt chain
1380JMP (MOS_IRV)
1390\
1400]
1410NEXT Pass%
1420REM
1430REM*** End of machine code
1440REM
1450REM-----
1460CLS
1470READ R_test:Sens%=Z%
1480PROCstart
1490PROCaxis
1500PROCplot
1510PROCpeaks
1520PROCoutput
1530PROCexit
1540END
1550REM-----
1560DEF PROCstart
1570Direc%=0
1580PRINT TAB(12,1) "Ruby R-line":PRINT TAB(3,2)
"High Pressure Data Aquisition"
1590INPUT TAB(0,6) "Scan direction (F/R) [F] ? " Reply$
1600IF Reply$="" OR Reply$="F" THEN Direc%=1 ELSE IF Reply$="R"
THEN Direc%=2
1610IF Direc%=0 THEN 1590
1620PRINT TAB(0,8) "Scan origin read from controller (nm) "
1630INPUT Scan_start
1640IF Scan_start<9000 OR Scan_start>12000 PRINT TAB(0,10)
"***Error Out of range":GOTO 1620
1650PRINT TAB(0,15) "Scan will be over range:"
1660PRINT TAB(0,16) FNform(Scan_start,1);" to ";FNform(Scan_start+60,1)
1670PRINT TAB(0,27) "Press any key to continue or E to exit"
1680Reply$=GET$
1690IF Reply$="E" THEN PROCexit
1700ENDPROC

```

```

1710REM-----
1720DEF PROCaxis
1730CLS
1740MOVE 79,23
1750DRAW 79,1000
1760MOVE 79,23
1770DRAW 1279,23
1780REM Annotate the axes
1790FOR I=200 TO 1000 STEP 200
1800MOVE 49,I
1810DRAW 79,I
1820NEXT I
1830Mve=10-10*(Scan_start/10-INT(Scan_start/10))
1840Mve=79+20*Mve
1850 FOR I = Mve TO Mve+1000 STEP 200
1860MOVE I,3
1870DRAW I,23
1880NEXT I
1890ENDPROC
1900REM-----
1910DEF PROCplot
1920IF Direc%=1 THEN X_counter%=0 ELSE X_counter%=601
1930MOVE 79,23
1940CALL Set_up%
1950REPEAT ?Flag%=0
1960REPEAT UNTIL ?Flag%<>0
1970UNTIL ?Flag%=Direc%
1980REM
1990REPEAT UNTIL ?Flag%<>0 AND ?Flag%=Direc%
2000REM Execute next bit if interrupt is enabled from user VIA
2010*FX 17,1
2020Y_value=ADVAL(1)/Sens%
2030num_pt%=num_pt%+1
2040DN ?Flag% GOTO 2050,2100,2150
2050REM Come here if ADVANCING in scan
2060X_counter%=X_counter%+1
2070Y(X_counter%)=Y_value
2080PLOT 69,(79+X_counter%*2),(23+Y_value)
2090GOTO 2190
2100REM Come here if REVERSING in scan
2110X_counter%=X_counter%-1
2120Y(X_counter%)=Y_value
2130PLOT 69,(79+X_counter%*2),(23+Y_value)
2140GOTO 2190

```

```

2150REM Come here if scan is too fast
2160IF Direc%=1 THEN X_counter%=X_counter%+1 ELSE X_counter%=X_counter%-1
2170Y(X_counter%)=Y_value
2180PRINT "Error!!"
2190REM Reset the flag and check to see if scan completed
2200?Flag%=0
2210IF num_pt%<600 THEN 1990
2220CALL Reset%
2230IF A%<>1 THEN GOTO 2290
2240SOUND 1,-15,97,5
2250SOUND 1,-15,105,5
2260SOUND 1,-15,89,5
2270SOUND 1,-15,41,5
2280SOUND 1,-15,69,10
2290PRINT TAB(4,26) "Press <SB> to continue"
2300PRINT TAB(4,27) "or E to EXIT"
2310Reply$=GET$
2320IF Reply$="E" THEN PROCexit
2330ENDPROC
2340REM-----
2350DEF PROCpeaks
2360FOR I=26TO27:PRINTTAB(4,I)"
":NEXT I:PRINTTAB(4,27)"Processing..."
2370FOR I=5 TO 590
2380Grad1=FNgrad(I)
2390Grad2=FNgrad(I+1)
2400IF Grad1>=0 AND Grad2<0 THEN PROCwidth(I)
2410NEXT I
2420ENDPROC
2430REM-----
2440DEF FNgrad(II)
2450m=0
2460FOR l=1 TO 4
2470m=m+(Y(II+l)-Y(II-l))*l
2480NEXT l
2490m=m/60.0
2500ENDPROC
2510REM-----
2520DEF PROCwidth(Z)
2530LOCAL secder:secder=0.0
2540secder=28*(Y(Z-4)+Y(Z+4))+7*(Y(Z-3)+Y(Z+3))-8
*(Y(Z-2)+Y(Z+2))-17*(Y(Z-1)+Y(Z+1))-20*Y(Z)
2550secder=secder/462
2560IF secder<R_test THEN PROCruby(Z)

```

```

3000INPUT#X,AmW(1),AmW(2)
3010INPUT#X,AmD$
3020INPUT#X,line$
3030IF AmD$<>Dat$ THEN PRINT "*** ERROR: Dates on ambient parameter
and session files are different. Repeat ambient and final pressure
scans."
3040IF AmD$<>Dat$ THEN ENDPROC
3050IF EOF# THEN GOTO 3140
3060num=0
3070REPEAT num=num+1
3080INPUT#X,OldD$(num)
3090INPUT#X,OldT$(num)
3100INPUT#X,R1(num),R2(num)
3110INPUT#X,OldP(num)
3120INPUT#X,Term$(num)
3130UNTIL EOF#
3140CLOSE#X
3150PRINT"Updating session file..."
3160X=OPENOUT("SAVED")
3170PRINT#X,AmW(1),AmW(2)
3180PRINT#X,AmD$
3190PRINT#X,"-----"
3200FOR I=1 TO num
3210PRINT#X,OldD$(I)
3220PRINT#X,OldT$(I)
3230PRINT#X,R1(I),R2(I)
3240PRINT#X,OldP(num)
3250PRINT#X,"*****"
3260NEXT I
3270PRINT#X,date$
3280PRINT#X,title$
3290PRINT#X,R_peak(1),R_peak(2)
3300PRINT#X,Pres
3310PRINT#X,"*****"
3320CLOSE#X
3330ENDPROC
3340DEF FNform(n,dec)
3350n=n*10^dec+0.5
3360=INT(n)/10^dec
3370DATA -0.05

```